

ISSN 1881-7831 Online ISSN 1881-784X

DD & T

Drug Discoveries & Therapeutics

Volume 14, Number 1
February 2020



www.ddtjournal.com

DD & T

Drug Discoveries & Therapeutics



ISSN: 1881-7831
Online ISSN: 1881-784X
CODEN: DDTRBX
Issues/Year: 6
Language: English
Publisher: IACMHR Co., Ltd.

Drug Discoveries & Therapeutics is one of a series of peer-reviewed journals of the International Research and Cooperation Association for Bio & Socio-Sciences Advancement (IRCA-BSSA) Group. It is published bimonthly by the International Advancement Center for Medicine & Health Research Co., Ltd. (IACMHR Co., Ltd.) and supported by the IRCA-BSSA.

Drug Discoveries & Therapeutics publishes contributions in all fields of pharmaceutical and therapeutic research such as medicinal chemistry, pharmacology, pharmaceutical analysis, pharmaceuticals, pharmaceutical administration, and experimental and clinical studies of effects, mechanisms, or uses of various treatments. Studies in drug-related fields such as biology, biochemistry, physiology, microbiology, and immunology are also within the scope of this journal.

Drug Discoveries & Therapeutics publishes Original Articles, Brief Reports, Reviews, Policy Forum articles, Case Reports, News, and Letters on all aspects of the field of pharmaceutical research. All contributions should seek to promote international collaboration in pharmaceutical science.

Editorial Board

Editor-in-Chief:

Kazuhisa SEKIMIZU
Teikyo University, Tokyo, Japan

Co-Editors-in-Chief:

Xishan HAO
Tianjin Medical University, Tianjin, China
Takashi KARAKO
National Center for Global Health and Medicine, Tokyo, Japan
Munehiro NAKATA
Tokai University, Hiratsuka, Japan

Senior Editors:

Guanhua DU
Chinese Academy of Medical Science and Peking Union Medical College, Beijing, China
Hiroshi HAMAMOTO
Teikyo University, Tokyo, Japan
Xiao-Kang LI
National Research Institute for Child Health and Development, Tokyo, Japan
Masahiro MURAKAMI
Osaka Ohtani University, Osaka, Japan
Yutaka ORIHARA
The University of Tokyo, Tokyo, Japan

Tomofumi SANTA
The University of Tokyo, Tokyo, Japan
Hongbin SUN
China Pharmaceutical University, Nanjing, China
Fengshan WANG
Shandong University, Ji'nan, China

Web Editor:

Yu CHEN
The University of Tokyo, Tokyo, Japan

Proofreaders:

Curtis BENTLEY
Roswell, GA, USA
Thomas R. LEBON
Los Angeles, CA, USA

Editorial and Head Office:

Pearl City Koishikawa 603,
2-4-5 Kasuga, Bunkyo-ku,
Tokyo 112-0003, Japan
Tel.: +81-3-5840-9697
Fax: +81-3-5840-9698
E-mail: office@ddtjournal.com

Drug Discoveries & Therapeutics

Editorial and Head Office

Pearl City Koishikawa 603, 2-4-5 Kasuga, Bunkyo-ku,
Tokyo 112-0003, Japan

Tel: +81-3-5840-9697, Fax: +81-3-5840-9698
E-mail: office@ddtjournal.com
URL: www.ddtjournal.com

Editorial Board Members

Alex ALMASAN (Cleveland, OH)	Yongzhou HU (Hangzhou, Zhejiang)	Tohru MIZUSHIMA (Tokyo)	Yuhong XU (Shanghai)
John K. BUOLAMWINI (Memphis, TN)	Yu HUANG (Hong Kong)	Abdulla M. MOLOKHIA (Alexandria)	Bing YAN (Ji'nan, Shandong)
Jianping CAO (Shanghai)	Amrit B. KARMARKAR (Karad, Maharashtra)	Yoshinobu NAKANISHI (Kanazawa, Ishikawa)	Chunyan YAN (Guangzhou Guangdong)
Shousong CAO (Buffalo, NY)	Toshiaki KATADA (Tokyo)	Siripom OKONOGI (Chiang Mai)	Xiao-Long YANG (Chongqing)
Jang-Yang CHANG (Tainan)	Gagan KAUSHAL (Philadelphia, PA)	Weisan PAN (Shenyang, Liaoning)	Yun YEN (Duarte, CA)
Fen-Er CHEN (Shanghai)	Ibrahim S. KHATTAB (Kuwait)	Chan Hum PARK (Eumseong)	Yongmei YIN (Tianjin)
Zhe-Sheng CHEN (Queens, NY)	Shiroh KISHIOKA (Wakayama, Wakayama)	Rakesh P. PATEL (Mehsana, Gujarat)	Yasuko YOKOTA (Tokyo)
Zilin CHEN (Wuhan, Hubei)	Robert Kam-Ming KO (Hong Kong)	Shivanand P. PUTHLI (Mumbai, Maharashtra)	Takako YOKOZAWA (Toyama, Toyama)
Xiaolan CUI (Beijing)	Nobuyuki KOBAYASHI (Nagasaki, Nagasaki)	Shafiqur RAHMAN (Brookings, SD)	Rongmin YU (Guangzhou, Guangdong)
Shaofeng DUAN (Lawrence, KS)	Norihiro KOKUDO (Tokyo, Japan)	Adel SAKR (Cairo)	Tao YU (Qingdao, Shandong)
Mohamed F. EL-MILIGI (6th of October City)	Toshiro KONISHI (Tokyo)	Gary K. SCHWARTZ (New York, NY)	Guangxi ZHAI (Ji'nan, Shandong)
Hao FANG (Ji'nan, Shandong)	Peixiang LAN (Wuhan, Hubei)	Luqing SHANG (Tianjin)	Liangren ZHANG (Beijing)
Marcus L. FORREST (Lawrence, KS)	Chun-Guang LI (Melbourne)	Yuemao SHEN (Ji'nan, Shandong)	Lining ZHANG (Ji'nan, Shandong)
Takeshi FUKUSHIMA (Funabashi, Chiba)	Minyong LI (Ji'nan, Shandong)	Rong SHI (Shanghai)	Na ZHANG (Ji'nan, Shandong)
Harald HAMACHER (Tübingen, Baden-Württemberg)	Xun LI (Ji'nan, Shandong)	Brahma N. SINGH (New York, NY)	Ruiwen ZHANG (Houston, TX)
Kenji HAMASE (Fukuoka, Fukuoka)	Jikai LIU (Wuhan, Hubei)	Tianqiang SONG (Tianjin)	Xiu-Mei ZHANG (Ji'nan, Shandong)
Junqing HAN (Ji'nan, Shandong)	Jing LIU (Beijing)	Sanjay K. SRIVASTAVA (Abilene, TX)	Xuebo ZHANG (Baltimore, MD)
Xiaojiang HAO (Kunming, Yunnan)	Xinyong LIU (Ji'nan, Shandong)	Chandan M. THOMAS (Bradenton, FL)	Yingjie ZHANG (Ji'nan, Shandong)
Kiyoshi HASEGAWA (Tokyo)	Yuxiu LIU (Nanjing, Jiangsu)	Li TONG (Xining, Qinghai)	Yongxiang ZHANG (Beijing)
Waseem HASSAN (Rio de Janeiro)	Hongxiang LOU (Jinan, Shandong)	Murat TURKOGLU (Istanbul)	Jian-hua ZHU (Guangzhou, Guangdong)
Langchong HE (Xi'an, Shaanxi)	Xingyuan MA (Shanghai)	Hui WANG (Shanghai)	
Rodney J. Y. HO (Seattle, WA)	Ken-ichi MAFUNE (Tokyo)	Quanxing WANG (Shanghai)	
Hsing-Pang HSIEH (Zhunan, Miaoli)	Sridhar MANI (Bronx, NY)	Stephen G. WARD (Bath)	

(As of February 2020)

Review

- 1 - 7 **New insights into the molecular basis of lactase non-persistence/persistence: a brief review.**
Raja Amir Hassan Kuchay

Original Article

- 8 - 13 **Polysaccharides of a fermented food, natto, suppress sucrose-induced hyperglycemia in an *in vivo* evaluation system and inhibit glucose uptake by human intestinal cells.**
Yasuhiko Matsumoto, Miki Takahashi, Kazuhisa Sekimizu
- 14 - 20 **Generic selection criteria for safety and patient benefit [IX]: Evaluation of "feeling of use" of sodium hyaluronate eye drops using the Haptic Skill Logger (HapLog[®]) wearable sensor for evaluating haptic behaviors.**
Miho Goto, Mitsuru Nozawa, Yuko Wada, Ken-ichi Shimokawa, Fumiyoshi Ishii
- 21 - 26 **Pulse wave transit time during exercise testing reflects the severity of heart disease in cardiac patients.**
Yuta Takayanagi, Akira Koike, Hiroshi Kubota, Longmei Wu, Isao Nishi, Akira Sato, Kazutaka Aonuma, Yasushi Kawakami, Masaki Ieda
- 27 - 34 **Development of an algorithm using ultrasonography-assisted peripheral intravenous catheter placement for reducing catheter failure.**
Chiho Kanno, Ryoko Murayama, Mari Abe-Doi, Toshiaki Takahashi, Yui Shintani, Junko Nogami, Chieko Komiyama, Hiromi Sanada
- 35 - 41 **Functional role of c-Jun NH₂-terminal kinase-associated leucine zipper protein (JLP) in lysosome localization and autophagy.**
Ryusuke Suzuki, I Ketut Gunarta, Jambaldorj Boldbaatar, Purev Erdenebaatar, Ravdandorj Odongoo, Katsuji Yoshioka

Brief Report

- 42 - 49 **Usefulness of next-generation DNA sequencing for the diagnosis of urinary tract infection.**
Toru Ishihara, Nobuo Watanabe, Shigeaki Inoue, Hiromichi Aoki, Tomoatsu Tsuji, Bunsei Yamamoto, Hidetaka Yanagi, Masayuki Oki, Kirill Kryukov, So Nakagawa, Sadaki Inokuchi, Hideki Ozawa, Tadashi Imanishi
- 50 - 53 **Association of moderately abnormal behavior and administered neuraminidase inhibitors.**
Tamie Sugawara, Yasushi Ohkusa, Kiyosu Taniguchi, Chiaki Miyazaki, Mariko Y. Momoi, Nobuhiko Okabe

Case Report

- 54 - 57** **Efficacy of Chinese prescription Kangen-karyu for patient with metabolic syndrome.**
Tsutomu Kitazawa, Chan Hum Park, Kazuyuki Hiratani, Jae Sue Choi, Takako Yokozawa

Communication

- 58 - 60** **Discovering drugs to treat coronavirus disease 2019 (COVID-19).**
Liyong Dong, Shasha Hu, Jianjun Gao

New insights into the molecular basis of lactase non-persistence/persistence: a brief review

Raja Amir Hassan Kuchay*

Department of Biotechnology, Baba Ghulam Shah Badshah University, Rajouri, J&K, India.

SUMMARY Lactose, a disaccharide and main carbohydrate in milk, requires hydrolysis in the intestinal tract to release its monosaccharides galactose and glucose for use as energy source by enterocytes. This hydrolysis is catalyzed by the enzyme lactase, a β -galactosidase located in the brush border membrane of small intestinal enterocytes. In most mammals, lactase activity declines after the weaning, a condition known as lactase non-persistence (LNP). Lactase persistence (LP) is an autosomal dominant trait enabling the continued production of the enzyme lactase throughout adult life. Non-persistence or persistence of lactase expression into adult life being a polymorphic trait has been attributed to various single nucleotide polymorphisms in the enhancer region surrounding lactase gene (*LCT*). However, latest research has pointed to 'genetic-epigenetic interactions' as key to regulation of lactase expression. LNP and LP DNA haplotypes have demonstrated markedly different epigenetic aging as genetic factors contribute to gradual accumulation of epigenetic changes with age to affect lactase expression. This review will attempt to present an overview of latest insights into molecular basis of LNP/LP including the crucial role of 'genetic-epigenetic interactions' in regulating lactase expression.

Keywords Lactase non-persistence, lactase persistence, genetic-epigenetic interactions

1. Introduction

Lactase (EC 3.2.1.23.62), a bifunctional enzyme having lactase and phlorizin hydrolase activities is an integral glycoprotein of the microvillus membrane of small intestinal enterocytes (1,2). Lactase activity is responsible for hydrolysing the milk sugar lactose to glucose and galactose, phlorizin hydrolase activity is responsible for hydrolysing aryl and alkyl β -glycosides to phlorizin and β -glycosylceramides (3-5). The gene encoding lactase (*LCT*) is about 50 kb, composed of 17 exons, has a one kb promoter region preceding it and maps physically to chromosome 2q21 (6-8). Lactase is synthesized as a pre-pro enzyme having cleavable signal peptide, large pro-part, domains containing phlorizin hydrolase/lactase active sites and a short intracellular domain at the C-terminus (9,10). Processing of lactase to pro and mature form involves cleavage of signal peptide, formation of homodimers and glycosylation in ER/Golgi complex. During intracellular transport, the pro-lactase protein is both N- and O-glycosylated in the ER and the Golgi complex. This glycosylation is necessary for both intracellular transport and enzymatic activity (11,12). Subsequently mature lactase is sorted to the apical membrane of the enterocyte (13,14) (Figure 1).

Lactase is a critical enzyme for neonates that depend on their mother's milk for nourishment. In mammals, the normal course of events for the newborn is to subsist on milk over the first few months of life and then be weaned. Thus, mammals have evolved a developmental pattern of small intestinal gene expression that promotes high level production of lactase early in life, followed by a turn-off of lactase expression around the time of weaning. This is indeed what happens in almost all mammals, including most humans. In the majority of human populations, lactase activity declines after weaning, a condition known as lactase non-persistence (LNP or adult-type hypolactasia) (15). The age of onset of down-regulation is different in different populations (16,17). Lactase persistence (LP) is an autosomal dominant trait enabling the continued production of the enzyme lactase throughout adult life. In general, the frequency of lactase persistence is high in European populations, whereas it is low in the native populations of Australia, America, Africa, and Asia (14).

2. Lactase non-persistence (LNP)

Hypolactasia is a general term for very low activity of lactase in the jejunal mucosa. It may occur due to down-

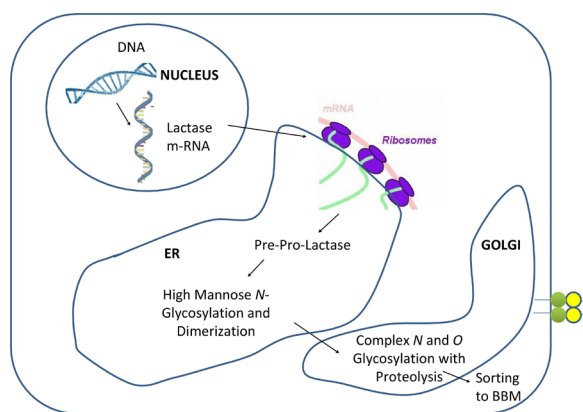


Figure 1. Transport and processing of lactase through ER and Golgi.

regulation of lactase activity after weaning (lactase non-persistence; LNP) or damage to intestinal mucosa leading to secondary lactase deficiency. Total lack of lactase activity from infancy is known as congenital lactase deficiency (CLD). In subjects with hypolactasia, most of lactose remains un-hydrolyzed causing an osmotic load in the small intestine that leads to influx of water into the lumen contributing to rapid intestinal transit (18). LNP is a genetically determined condition. It is the ancient phenotype and is characterized by decline in lactase activity during childhood (19). LNP causes primary lactose malabsorption (19). Secondary lactose malabsorption is caused by other reasons than genetically determined LNP, such as microbial infections, celiac disease or malnutrition that damage the intestinal villi (20). CLD is an autosomal recessive inherited severe gastrointestinal disorder in newborns. CLD manifests as a watery diarrhea during the first days of life of an infant fed with lactose-containing milk making them underweight with symptoms of dehydration and acidosis (21,22).

LNP is an autosomal recessive gastrointestinal condition that is the result of a decline in the activity of lactase in the intestinal lumen after weaning. Down-regulation of lactase is considered as a normal phenomenon among mammals, and symptoms are remarkably milder than experienced in CLD (23). Wang *et al.* (1995) studied the onset of LNP in children aged from 2 months to 11 years (24). Genetically programmed down-regulation of the lactase gene was observed starting from the second year of life, although the extent and onset was not constant (24). They concluded that a developmentally regulated *trans*-acting DNA-binding protein could bind to only one kind of lactase allele and influence transcription and/or mRNA stability (24). Various studies have pointed to a wide ethnic and regional variation in the age of onset of LNP. In majority of Thai children lactase activity decreases by the age of two years, in black populations LNP has been shown to manifest between one to eight years, whereas

in white populations low lactase levels are rarely seen in children less than five years of age (25-27). Among Indian children, the onset of down-regulation of lactase expression and activity is between 3-5 years of age and it is complete between 7-8 years (28). Studies of the Finnish population have shown that LNP can manifest up to 20 years (26). However, data has also confirmed that the majority of Finns developed LNP by age of 10 years (29). In South America, Africa and Asia, over 50% of the population has LNP and in some Asian countries this rate is almost 100% (4).

3. Lactase persistence (LP)

LP is an autosomal dominant trait enabling the continued production of the enzyme lactase throughout adult life (3). LP is common among people of European ancestry, but with the exception of some African, Middle Eastern and Southern Asian groups, is rare or absent elsewhere in the world (30). To explain the highly geographic variations in the prevalence of LP, various researchers have produced some hypotheses to explain these variations focused on some selective factors related to milk supply because it is the only source of lactose, substrate of the lactase enzyme. These hypotheses are: (1) The culture historical hypothesis based on genetic selection and correlates the occurrence of LP with dairy culture (31,32); (2) The calcium absorption hypothesis put forward to explain the prevalence of LP in Northern Europe and based on fact that lactose could enhance absorption of calcium and thus individuals with LP will have less rickets and pelvic deformities resulting in a selection in favour of LP (33); (3) The arid climate hypothesis speculated that in desert climates (Middle and near East) where water and food were scarce, nomadic groups could survive by utilizing milk as a food source, and in particular, as a source of clean, uncontaminated water (34). In a phylogenetic approach, correlation of high lactose digestion frequency was tested with percentage dependence on pastoralism, levels of solar radiation and dry months/year or average rainfall and adjusted for relatedness in the analysis (32). These data revealed that percentage reliance on pastoralism best explained the variation observed between populations and concluded that lactose digestion capacity had most likely evolved as an adaptation to dairying, and that high frequency lactose digestion capacity had not evolved in the absence of milking (32). The co-evolution of genes for LP and milk consumption also becomes one of the most well-known gene-culture models for human evolutionary change (35). Table 1 presents the frequencies of various LP alleles around selected countries/populations of the world [as reviewed by Mattar *et al.* (2012) (36)].

4. Genetic-epigenetic interactions as molecular basis of LNP/LP

Table 1. Frequencies of various LP alleles around selected countries/populations

Country/Population	Allele Type and Frequency (%)				
	<i>LCT</i> -13910C>T	<i>LCT</i> -13915T>G	<i>LCT</i> -14010G>C	<i>LCT</i> -13907C>G	<i>LCT</i> -14009T>G
Finland	58.1	-	-	-	-
Tanzania	-	-	31.9	-	-
Sudan (Afro-Asiatic Beja)	-	-	-	20.6	-
Italy (North-East)	23.7	-	-	-	-
Italy (North-Central)	13.3	-	-	-	-
Italy (Southern)	5.5-8	-	-	-	-
Ethiopia (Amharic)	-	13.2	-	-	-
Sudan (Jaali)	-	14.2	-	-	6.6
Saudi Arabia	-	59.4	-	-	-
Ethiopia (Afar)	-	15	-	20	-
Ethiopia (Somali camel herders)	1.9	5.1	0.5	5.6	1.4
Xhosa (South Africa)	-	-	12.8	-	-
Sardinia	7.2	-	-	-	-
Jordan	-	39.1	-	-	-
Chile (Amerindians)	5.8	-	-	-	-
Xhosa (mixed ancestry)	-	-	8.1	-	-
Ethiopia (Somali camel herders)	-	-	0.5	-	-
Brazil (Caucasian)	24.7	-	-	-	-
Brazil (African origin)	18.3	-	-	-	-
Kenya	-	-	27.6	-	-
Estonia	51.4	-	-	-	-
Canary Islands	36.5	-	-	-	-
Chile (Hispanics)	22	-	-	-	-
Hungary	35.9	-	-	-	-
Russia (Northern)	38.9	-	-	-	-
US (African origin)	9	-	-	-	-
Mali (Fulbe)	37	-	-	-	-

Research on molecular basis of developmental down-regulation of lactase has been going on for a long time but the causes remained elusive. Initially, decreased production of lactase, synthesis of an inactive high molecular weight lactase and defective post-translational modifications were the factors attributed to down regulation of lactase activity after weaning (37-40). However, subsequent research indicated that a genetic polymorphism controlled by an element which acts in *cis* to the lactase gene might be responsible for LNP/LP trait (41,42). Evidence that LNP/LP is controlled by a *cis*-acting regulatory variant upstream of *LCT* came from linkage studies in the Finnish families (43). Total of 52 non-coding variants were identified using sequence analysis of the 47 kb region upstream of *LCT*. Two of the single nucleotide polymorphisms (SNPs), C/T -13910 (rs4988235), in intron 13 and G/A -22018 (rs182549), in intron 9 of *MCM6* gene (minichromosome maintenance 6) upstream of the *LCT* locus showed complete co-segregation with LNP/LP trait (43). Further studies revealed several new sequence variants in very close proximity to -13910*T (44-47), two of which are clearly associated with LP in different parts of East Africa (-13915*G and -14010*C). One of these, -13915*G, was also shown to be associated with high lactase expression in Saudi Arabia (48). A third SNP, -13907*G, revealed much weaker evidence, but was found in several studies and there were several other candidates found in lactase persistent or milk

drinking people (44-47). Positive selection for LP which allows the dietary consumption of animal milk by adult humans without risk of symptoms of lactose intolerance has been attributed to present day frequencies of these alleles (49-52). Population expansion, migration, allele surfing and cultural/environmental processes may also have influenced the distributions of these alleles (49,52).

Transfection studies of promoter-reporter gene constructs, DNA-protein and protein-protein interaction have explored the functional significance of these SNPs in regulating the lactase expression (53,54). It has been proposed that multiple transcription factors and their interactions with *LCT* immediate promoter influence the decline of the lactase enzyme after childhood (54,55). A transcription factor, Oct-1, was identified which bound more strongly to the -13910*T containing motif than to the alternative C allele, providing a possible mechanism for up-regulation of *LCT* expression (55). In addition, binding sites to intestinal transcription factors GATA-6, HNF-4 α , Fox and Cdx-2 were also identified in the -13910 region, providing further support that this region underlies the developmental regulation of lactase expression in human (55). In a recent study on *in-vitro* functional analyses of infrequent nucleotide variants in the lactase enhance, four allelic variants were chosen for *in-vitro* functional tests (56). These include (1) -14009*G (rs869051967), selected because it was strongly associated with digester status (57); (2) -14011*T (rs4988233), although too rare to test for

association, was analyzed as it is located immediately adjacent to the known functional variant -14010^*C (58); (3) -13779^*G (rs527991977) was of interest because it was found to be relatively common in some groups in India including milk drinking Toda and some hunter-gatherers (58); (4) -14028^*C (rs759157971) had previously been found as the only *LCT* enhancer allele identified in the second highest expressing transcript of a homozygous lactase persistent person (45,59). Results indicate a clear effect on promoter activity upregulation as assessed by transfection assays in case of -14009^*G and -14011^*T , but the molecular interactions leading to such effects may be different (56). For -14028^*C variant, the results suggest a clear change in transcription factor binding, but no obvious effect in transfections and -13779^*G variant displays greater effect in transfections but less on transcription factor binding (56). Independent haplotypic backgrounds with different geographic distribution gave rise to each of the four variants (56).

Epigenetics is described as inherited alterations in gene expression or silencing that take place without changes in DNA sequence (60,61). Epigenetic mechanisms are often attributed to transcriptional variation within the same cell type, determining cell identity and affecting genomic functions in response to aging and environmental cues (62-65). DNA methylation is critical for the regulation of gene expression during differentiation in many self-renewing tissues, including the germline and embryonic, hematopoietic, and epidermal stem cells (66,67). Being one of the most rapidly renewing tissues in the human body, cooperation between transcription factors, signaling pathways and epigenetic mechanisms is essential for the tight control of the constant renewal of intestinal tissue (68,69).

Recently, the role DNA methylation in LNP/LP has also been reported (70). It was found that LNP occurs due to DNA variation dependent accumulation of methylation with the age. Research suggests that LNP haplotypes containing the -13910^*C allele accumulates modified cytosine's that silence the regulatory elements in *LCT* rather than the haplotype containing the -13910^*T allele (Figure 2). This genetic dependent epigenetic aging may account for age specific down-regulation and inter-individual variation of lactase activity in different human populations. Therefore, individual genetic landscape sets the epigenetic clock for regulation of lactase expression (70,71). Labrie *et al.* (2016), employing high density tiling microarrays, performed chromosome-wide profiling of DNA modification consisting of methylation and other epigenetic cytosine modifications followed by targeted bisulfite sequencing-based interrogation of the human and mouse lactase genes in intestinal cells and other tissues (70). Results indicated that gradual decline in lactase gene expression following infancy in mammals may be directed by changes in DNA modification

densities at several distinct regulatory elements (70). This was followed by exploration of how genetic factors including C/T -13910 SNP containing haplotypes contributed to the epigenetic aging and could impact age-specific changes in epigenetic marks of *LCT-MCM6* (70). Epigenetically controlled regulatory elements for the lactase gene were validated using RNA interference (RNAi) in human tissue culture and CRISPR-Cas9-induced genetic deletions in the mouse models (70). It was revealed that accumulation of transcriptionally suppressive epigenetic changes on haplotypes carrying the -13910^*C allele led to LNP, while haplotypes containing -13910^*T allele escape from inactivation to facilitate LP (70). 35 CpG sites which clustered into seven distinct regions: *LCT* intron 5, intron 3, intron 2, exon 1, *MCM6* exon 17, exon 16 and intron 13 displayed significant DNA modification differences. Each of the seven regulatory regions had age-related DNA modification changes in the enterocyte samples stratified for C/T -13910 genotypes (70). Individuals with -13910^*C allele of LNP exhibited a 4-fold higher density of modified cytosine's at *MCM6* intron 13-exon 13 compared to the -13910^*T individuals with LP (70). Another study examined transcriptional and epigenetic variation of the *LCT* in enterocytes along the proximal-to-distal axis of the mouse small intestine (72). Aging and environmentally induced changes enabled by divergent epigenetic programming in gene transcription occurring in cells of the same type were reported (72). *MCM6* exon 13-intron 13 site emerged as a key modulator of the age-dependent establishment and maintenance of the *LCT* transcriptional gradient (72). Thus, aging and environmentally induced gradients of *LCT* mRNA have been supported by DNA modification patterns which could potentially affect phenotypic outcome by modifying transcriptional programs within same cell types (72). DNA modifications and chromatin

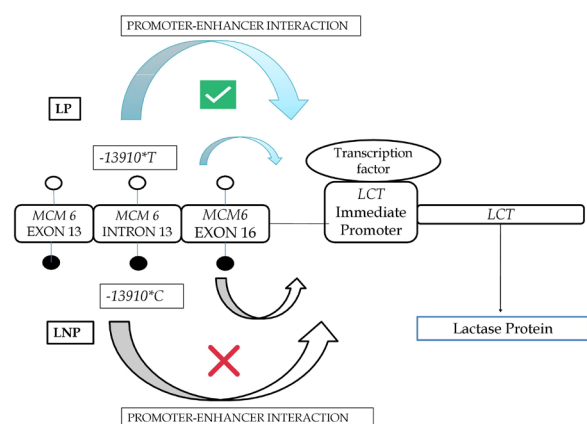


Figure 2. Relationship between lactase expression, promoter enhancer interactions and methylation status of selected regulatory sites where DNA variation dependent accumulation of methylation occurs with the age [As first reported by Labrie *et al.* (2016) and reviewed by Swallow and Troelsen (2016)]. Filled circles represent methylated DNA.

architectural protein CTCF (CCCTC-Binding Factor) may work in tandem with transcription factors to create and maintain age-dependent transcriptional gradients of *LCT* in cells of the same type (72). Furthermore, a recent study identified putative lactase meQTLs (methylation quantitative trait loci), which are differentially methylated between lactase persistent and lactase non-persistent individuals. -13910*T allele in genetically homogenous populations appears to be dominant, leading complete correlation of LP with the presence of the variant allele and tri-modal distribution in lactase enzymatic activities. However, methylation at the *LCT* enhancer and the *LCT* promoter are both affected by the genotype at rs4988235, and appear to be continuously associated with lactase phenotypes in heterogeneous populations (73). DNA methylation, rather than differential regulation of intestinal transcription factors like CDX2, POU2F1, GATA4/6 or HNF1 α , in the enhancer and promoter site of the *LCT* gene was predictive of LNP/LP as indicated by regression (73).

5. Conclusion

Being a multifactorial phenomenon, regulation of lactase expression may involve complex spatial and developmental patterns in the small intestine. New avenues for basic and applied research in genetics of LNP/LP were unraveled with identification of the C/T -13910 and G/A -22018 polymorphisms. However, with recent advances in genomics and increasing role of DNA modifications (like DNA methylation) in tissue development and progression of many common diseases, genetic-epigenetic interactions may be pivotal to uncovering the molecular origin of complex disease (74). In this context, investigation of age-dependent epigenetic changes for disease-associated genetic variants has provided new insights into molecular basis of LNP/LP. Latest research into molecular basis of LNP/LP has made it clear that genetic variation seems to be setting up the stage, either allowing or preventing DNA modification accumulation with age at key regulatory sites (70,72). It would be interesting to further investigate and elaborate how an escape from inactivation is brought about with age-related epigenetic changes. In future, examining DNA methylation profiles of fetuses (with low lactase expression for all haplotypes) and of children (with high lactase expression for all haplotypes) could provide fascinating details into genetics induced epigenetic regulation of lactase expression.

Acknowledgements

We thank Prof. Akhtar Mahmood and Dr. Safrun Mahmood for inspiring us to write this review. We thank reviewers for their time and effort. Author is thankful to lab members (Mr. Yasir and Ms. Sobia) for their timely

inputs. Laboratory of Dr. Raja Amir was supported by UGC Start Up grant, New Delhi India.

References

1. Mantei N, Villa M, Enzler T, Wacker H, Boll W, James P, Hunziker W, Semenza G. Complete primary structure of human and rabbit lactase-phlorizin hydrolase: Implications for biosynthesis, membrane anchoring and evolution of the enzyme. *Embo J*. 1988; 7:2705-2713.
2. Skovbjerg H, Noren O, Sjoström H, Danielsen EM, Enevoldsen BS. Further characterization of intestinal lactase/phlorizin hydrolase. *Biochim Biophys Acta*. 1982; 707:89-97.
3. Swallow DM. Genetics of lactase persistence and lactose intolerance. *Annu Rev Genet*. 2003; 37:197-219.
4. Lomer MC, Parkes GC, Sanderson JD. Review article: Lactose intolerance in clinical practice – myths and realities. *Aliment Pharmacol Ther*. 2008; 27:93-103.
5. Kuchay RA, Mahmood A, Mahmood S. Adult-type hypolactasia: A genetic perspective. *J Pediatr Biochem*. 2012; 2:143-151.
6. Boll W, Wagner P, Mantei N. Structure of the chromosomal gene and cDNAs coding for lactase-phlorizin hydrolase in humans with adult-type hypolactasia or persistence of lactase. *Am J Hum Genet*. 2012; 48:889-902.
7. Kruse TA, Bolund L, Grzeschik KH, Ropers HH, Sjoström H, Noren O, Mantei N, Semenza G. The human lactase-phlorizin hydrolase gene is located on chromosome 2. *FEBS Lett*. 1998; 240:123-126.
8. Harvey CB, Fox MF, Jeggo PA, Mantei N, Povey S, Swallow DM. Regional localization of the lactase-phlorizin hydrolase gene, *LCT*, to chromosome 2q21. *Ann Hum Genet*. 1993; 57:179-185.
9. Arribas JC, Herrero AG, Martin-Lomas M, Canada FJ, He S, Withers SG. Differential mechanism-based labeling and unequivocal activity assignment of the two active sites of intestinal lactase phlorizin hydrolase. *Eur J Biochem*. 2000; 267:6996-7005.
10. Neele AM, Einerhand AW, Dekker J, Bqller HA, Freund JN, Verhave M, Grand RJ, Montgomery RK. Verification of the lactase site of rat lactase-phlorizin hydrolase by site-directed mutagenesis. *Gastroenterology*. 1995; 109:1234-1240.
11. Naim HY, Lentze MJ. Impact of *O*-glycosylation on the function of human intestinal lactase-phlorizin hydrolase. Characterization of glycoforms varying in enzyme activity and localization of *O*-glycoside addition. *J Biol Chem*. 1992; 267:25494-25504.
12. Jacob R, Weiner JR, Stadge S, Naim NY. Additional *N*-glycosylation and its impact on the folding of intestinal lactase phlorizin hydrolase. *J Biol Chem*. 2000; 275:10630-10637.
13. Naim HY, Naim H. Dimerization of lactase-phlorizin hydrolase occurs in the endoplasmic reticulum, involves the putative membrane spanning domain and is required for an efficient transport of the enzyme to the cell surface. *Eur J Cell Biol*. 1996; 70:198-208.
14. Troelsen JT. Adult-type hypolactasia and regulation of lactase expression. *Biochim Biophys Acta*. 2005; 1723:19-32.
15. Wang Y, Harvey CB, Hollox EJ, Phillips AD, Poulter M, Clay P, Walker-Smith JA, Swallow DM. The genetically

- programmed down-regulation of lactase in children. *Gastroenterology*. 1998; 114:1230-1236.
16. Simoons F. Age of onset of lactose malabsorption. *Pediatrics*. 1980; 66:646-648.
 17. Flatz G. Genetics of lactose digestion in humans. *Adv Hum Genet*. 1987; 16:1-77.
 18. Arola H, Tamm A. Metabolism of lactose in the human body. *Scand J Gastroenterol Suppl*. 1994; 202:21-25.
 19. Sahi T. Hypolactasia and lactase persistence. Historical review and the terminology. *Scand J Gastroenterol Suppl*. 1994; 202:1-6.
 20. Nieminen U, Kahri A, Savilahti E, Farkkila MA. Duodenal disaccharidase activities in the follow-up of villous atrophy in coeliac disease. *Scand J Gastroenterol*. 2001; 36:507-510.
 21. Savilahti E, Launiala K, Kuitunen P. Congenital lactase deficiency. A clinical study on 16 patients. *Arch Dis Child*. 1983; 58:246-252.
 22. Jarvela I, Sabri Enattah N, Kokkonen J, Varilo T, Savilahti E, Peltonen L. Assignment of the locus for congenital lactase deficiency to 2q21, in the vicinity of but separate from the lactase-phlorizin hydrolase gene. *Am J Hum Genet*. 1998; 63:1078-1085.
 23. Sahi T. The inheritance of selective adult-type lactose malabsorption. *Scand J Gastroenterol Suppl*. 1974; 30:1-73.
 24. Wang Y, Harvey CB, Pratt WS, Sams VR, Sarner M, Rossi M, Auricchio S, Swallow DM. The lactase persistence/non-persistence polymorphism is controlled by a *cis*-acting element. *Hum Mol Genet*. 1995; 4:657-662.
 25. Keusch GT, Troncale FJ, Miller LH, Promadhat V, Anderson PR. Acquired lactose malabsorption in Thai children. *Pediatrics*. 1969; 43:540-545.
 26. Sahi T, Isokoski M, Jussila J, Launiala K. Lactose malabsorption in Finnish children of school age. *Acta Paediatr Scand*. 1972; 61:11-16.
 27. Welsh JD, Poley JR, Bhatia M, Stevenson DE. Intestinal disaccharidase activities in relation to age, race, and mucosal damage. *Gastroenterology*. 1978; 75:847-855.
 28. Kuchay RA, Thapa BR, Mahmood A, Mahmood S. Effect of C/T -13910 *cis*-acting regulatory variant on expression and activity of lactase in Indian children and its implication for early genetic screening of adult-type hypolactasia. *Clin Chim Acta*. 2011; 412:1924-1930.
 29. Rasinpera H, Enattah NS, Kuokkanen M, Totterman N, Lindahl H, Jarvela I, Kolho KL. Genetic test, which can be used to diagnose adult-type hypolactasia in children. *Gut*. 2004; 53:1571-1576.
 30. Itan Y, Powell A, Beaumont MA, Burger J, Thomas MG. The origins of lactase persistence in Europe. *PLoS Comput Biol*. 2009; 5:e1000491.
 31. McCracken. Lactase deficiency: An example of dietary evolution. *Curr Anthropol*. 1971; 12:479-517.
 32. Holden C, Mace R. Phylogenetic analysis of the evolution of lactose digestion in adults. *Hum Biol*. 1997; 69:605-628.
 33. Flatz G, Rotthauwe HW. Lactose nutrition and natural selection. *Lancet*. 1973; 2:76-77.
 34. Cook GC, Al-Torki, M T. High intestinal lactase concentrations in adult Arabs in Saudi Arabia. *Br Med J*. 1975; 3:135-136.
 35. Ross CT, Richerson PJ. New frontiers in the study of human cultural and genetic evolution. *Curr Opin Genet Dev*. 2014; 29:103-109.
 36. Mattar R, Mazo DFC, Carrilho FJ. Lactose intolerance: Diagnosis, genetic, and clinical factors. *Clin Exp Gastroenterol*. 2012; 5:113-121.
 37. Nsi-Emvo E, Launay JF, Raul F. Is adult type hypolactasia in intestine of mammals related to changes in the intracellular processing of lactase? *Cell Mol Biol*. 1987; 33:335-344.
 38. Lloyd M, Mevissen G, Fischer M, Olsen W, Goodspeed D, Genini M, Boll W, Semenza G, Mantei N. Regulation of intestinal lactase in adult hypolactasia. *J Clin Invest*. 1992; 89:524-529.
 39. Rings EH, De Boer PA, Moorman AF, Van Beers EH, Dekker J, Montgomery RK, Grand RJ, Buller HA. Lactase gene expression during early development of rat small intestine. *Gastroenterology*. 1992; 103:1154-1161.
 40. Rossi M, Maiuri L, Fusco MI, Salvati VM, Fuccio A, Auricchio S, Mantei N, Zecca L, Gloor SM, Semenza G. Lactase persistence versus decline in human adults: Multifactorial events are involved in down-regulation after weaning. *Gastroenterology*. 1997; 112:1506-1514.
 41. Harvey CB, Hollox EJ, Poulter M, Wang Y, Rossi M, Auricchio S, Iqbal TH, Cooper BT, Barton R, Sarner M, Korpela R, Swallow DM. Lactase haplotype frequencies in Caucasians: Association with the lactase persistence/non-persistence polymorphism. *Ann Hum Genet*. 1998; 62:215-223.
 42. Hollox EJ, Poulter M, Zvarik M, Ferak V, Krause A, Jenkins T, Saha N, Kozlov AI, Swallow DM. Lactase haplotype diversity in the Old World. *Am J Hum Genet*. 2001; 68:160-172.
 43. Enattah NS, Sahi T, Savilahti E, Terwilliger JD, Peltonen L, Jarvela I. Identification of a variant associated with adult-type hypolactasia. *Nat Genet*. 2002; 30:233-237.
 44. Ingram CJE, Elamin MF, Mulcare CA, Weale ME, Tarekegn A, Raga TO, Bekele E, Elamin FM, Thomas MG, Bradman N, Swallow DM. A novel polymorphism associated with lactose tolerance in Africa: Multiple causes for lactase persistence? *Hum Genet*. 2007; 120:779-788.
 45. Ingram CJ, Mulcare CA, Itan Y, Thomas MG, Swallow DM. Lactose digestion and the evolutionary genetics of lactase persistence. *Hum Genet*. 2009; 124:579-591.
 46. Tishkoff SA, Reed FA, Ranciaro A, *et al*. Convergent adaptation of human lactase persistence in Africa and Europe. *Nat Genet*. 2007; 39:31-40.
 47. Enattah NS, Jensen TG, Nielsen M, *et al*. Independent introduction of two lactase-persistence alleles into human populations reflects different history of adaptation to milk culture. *Am J Hum Genet*. 2008; 82:57-72.
 48. Imtiaz F, Savilahti E, Sarnesto A, Trabzuni D, Al-Kahtani K, Kagevi I, Rashed MS, Meyer BF, Jarvela I. The T/G 13915 variant upstream of the lactase gene (*LCT*) is the founder allele of lactase persistence in an urban Saudi population. *J Med Genet*. 2007; 44:e89.
 49. Liebert A, Lopez S, Jones BL, Montalva N, Gerbault P, Lau W, Thomas MG, Bradman N, Maniatis N, Swallow DM. World-wide distributions of lactase persistence alleles and the complex effects of recombination and selection. *Hum Genet*. 2017; 136:1445-1453.
 50. Allentoft ME, Sikora M, Sjogren KG, *et al*. Population genomics of bronze age Eurasia. *Nature*. 2015; 522:167-172.
 51. Bersaglieri T, Sabeti PC, Patterson N, Vanderploeg T, Schaffner SF, Drake JA, Rhodes M, Reich DE, Hirschhorn JN. Genetic signatures of strong recent

- positive selection at the lactase gene. *Am J Hum Genet.* 2004; 74:1111-1120.
52. Gerbault P, Moret C, Currat M, Sanchez-Mazas A. Impact of selection and demography on the diffusion of lactase persistence. *PLoS One.* 2009; 4:e6369.
 53. Olds LC, Sibley E. Lactase persistence DNA variant enhances lactase promoter activity *in vitro*: Functional role as a *cis* regulatory element. *Hum Mol Genet.* 2003; 12:2333-2340.
 54. Troelsen JT, Olsen J, Moller J, Sjoström H. An upstream polymorphism associated with lactase persistence has increased enhancer activity. *Gastroenterology.* 2003; 125:1686-1694.
 55. Lewinsky RH, Jensen TG, Moller J, Stensballe A, Olsen J, Troelsen JT. T-13910 DNA variant associated with lactase persistence interacts with Oct-1 and stimulates lactase promoter activity *in vitro*. *Hum Mol Genet.* 2005; 14:3945-3953.
 56. Liebert A, Jones BL, Danielsen ET, Olsen AK, Swallow DM, Troelsen JT. *In vitro* functional analyses of infrequent nucleotide variants in the lactase enhancer reveal different molecular routes to increased lactase promoter activity and lactase persistence. *Ann Hum Genet.* 2016; 80:307-318.
 57. Jones BL, Raga TO, Liebert A, Zmarz P, Bekele E, Danielsen ET, Olsen AK, Bradman N, Troelsen JT, Swallow DM. Diversity of lactase persistence alleles in Ethiopia: Signature of a soft selective sweep. *Am J Hum Genet.* 2013; 93:538-544.
 58. Gallego Romero I, Basu Mallick C, Liebert A, *et al.* Herders of Indian and European cattle share their predominant allele for lactase persistence. *Mol Biol Evol.* 2012; 29:249-260.
 59. Poulter M, Hollox E, Harvey CB, Mulcare C, Peuhkuri K, Kajander K, Sarner M, Korpela R, Swallow DM. The causal element for the lactase persistence/non-persistence polymorphism is located in a 1 Mb region of linkage disequilibrium in Europeans. *Ann Hum Genet.* 2003; 67:298-311.
 60. Jaenisch R, Bird A. Epigenetic regulation of gene expression: How the genome integrates intrinsic and environmental signals. *Nat Genet.* 2003; 33:245-254.
 61. Bird A. Perceptions of epigenetics. *Nature.* 2007; 447:396-398.
 62. Kundaje A, Meuleman W, Ernst J, *et al.* Integrative analysis of 111 reference human epigenomes. *Nature.* 2015; 518:317-330.
 63. Barrero MJ, Boue S, Izpisua Belmonte JC. Epigenetic mechanisms that regulate cell identity. *Cell Stem Cell.* 2010; 7:565-570.
 64. Sheaffer KL, Kim R, Aoki R, Elliott EN, Schug J, Burger L, Schubeler D, Kaestner KH. DNA methylation is required for the control of stem cell differentiation in the small intestine. *Genes Dev.* 2014; 28:652-664.
 65. Benayoun BA, Pollina EA, Brunet A. Epigenetic regulation of ageing: Linking environmental inputs to genomic stability. *Nat Rev Mol Cell Biol.* 2015; 16:593-610.
 66. Sen GL, Reuter JA, Webster DE, Zhu L, Khavari PA. DNMT1 maintains progenitor function in self-renewing somatic tissue. *Nature.* 2010; 463:563-567.
 67. Smith ZD, Meissner A. DNA methylation: Roles in mammalian development. *Nat Rev Genet.* 2013; 14:204-220.
 68. Vermeulen L, Snippert HJ. Stem cell dynamics in homeostasis and cancer of the intestine. *Nat Rev Cancer.* 2014; 14:468-480.
 69. Roostae A, Benoit YD, Boudjadi S, Beaulieu JF. Epigenetics in intestinal epithelial cell renewal. *J Cell Physiol.* 2016; 231:2361-2367.
 70. Labrie V, Buske OJ, Oh E, *et al.* Lactase nonpersistence is directed by DNA-variation-dependent epigenetic aging. *Nat Struct Mol Biol.* 2016; 23:566-573.
 71. Swallow DM, Troelsen JT. Escape from epigenetic silencing of lactase expression is triggered by a single-nucleotide change. *Nat Struct Mol Biol.* 2016; 23:505-507.
 72. Oh E, Jeremian R, Oh G, Groot D, Susic M, Lee K, Foy K, Laird PW, Petronis A, Labrie V. Transcriptional heterogeneity in the lactase gene within cell-type is linked to the epigenome. *Sci Rep.* 2017; 7:41843.
 73. Leseva MN, Grand RJ, Klett H, Boerries M, Busch H, Binder AM, Michels KB. Differences in DNA methylation and functional expression in lactase persistent and non-persistent individuals. *Sci Rep.* 2018; 8:5649.
 74. Jin Z, Liu Y. DNA methylation in human diseases. *Gene Dis.* 2018; 5:1-8.
- Received October 18, 2019; Revised February 12, 2020; Accepted February 19, 2020
- *Address correspondence to:*
 Dr. Raja Amir Hassan, Assistant Professor, Department of Biotechnology, Baba Ghulam Shah Badshah University, Rajouri, J&K, 185234, India.
 E-mail: kuchay_bgsbu@yahoo.com
- Released online in J-STAGE as advance publication February 26, 2020.

Polysaccharides of a fermented food, natto, suppress sucrose-induced hyperglycemia in an *in vivo* evaluation system and inhibit glucose uptake by human intestinal cells

Yasuhiko Matsumoto^{1,2}, Miki Takahashi^{2,3}, Kazuhisa Sekimizu^{2,3,*}

¹ Department of Microbiology, Meiji Pharmaceutical University, Tokyo, Japan;

² Teikyo University Institute of Medical Mycology, Tokyo, Japan;

³ Genome Pharmaceuticals Institute Co., Ltd., Tokyo, Japan.

SUMMARY Natto is a well-known traditional Japanese food produced by fermenting soybeans with *Bacillus subtilis* var *natto*. Here we found that the water-soluble viscous fraction of natto inhibits sucrose- or glucose-induced hyperglycemia in silkworms. The water-soluble viscous fraction treated with DNase I, RNase A, and proteinase K, followed by phenol extraction also suppressed sucrose-induced hyperglycemia in silkworms. The enzyme-treated polysaccharide fraction of natto inhibits glucose uptake by Caco-2 cells, human intestinal epithelial cells. These findings suggest that the polysaccharide components of natto selected on the basis of their suppressive effects on sucrose-induced hyperglycemia in silkworms inhibit glucose uptake by human intestinal cells.

Keywords Glucose uptake, natto, polysaccharide, silkworm, sucrose-induced hyperglycemia

1. Introduction

Sucrose intake causes a rapid increase in blood glucose levels, a main factor in the development of diabetes. Suppression of the rapid postprandial increase in blood glucose is considered to be useful toward preventing the onset of diabetes, and the development of a food with such an effect is highly desired. For this purpose, mammalian experimental systems have been applied to evaluate increases in blood glucose levels and assessment of substances that may suppress these increases. These types of experiments, however, require a large number of mammals, which is problematic not only in terms of cost, but also from the view of animal welfare. To overcome these problems, we propose the use of silkworms as a model animal (1-3). We previously reported that silkworms ingesting a sucrose-containing diet exhibit an increase in blood glucose levels and that acarbose and voglibose, which are α -glucosidase inhibitors, inhibit the blood glucose-increasing effect of sucrose ingestion (4). Furthermore, we identified a lactic acid bacterial strain, *Enterococcus faecalis* YM0831, that suppresses sucrose-induced hyperglycemia in silkworms as well as sucrose-induced hyperglycemia in humans (5). On the basis of these findings, we consider that the silkworm evaluation system could be useful for screening substances that suppress sucrose-induced hyperglycemia in humans.

Caco-2 cells are cultured cells derived from human colon adenocarcinoma used for evaluating the glucose absorption process in human intestinal epithelial cells (6,7). Thus, we used Caco-2 cells to evaluate the effect of substances that suppress sucrose-induced hyperglycemia in silkworms on a human cell type.

Polysaccharides derived from bacteria have diverse structures and physiologic activities (8-10). Polysaccharides produced by soil bacteria, such as *Rhizobium altiplani*, *Cupriavidus* sp., *Paenibacillus polymyxa*, *Pantoea eucalypti*, *Variovorax boronicumulans*, and *Xanthomonas cynarae*, inhibit sucrose-induced hyperglycemia in silkworms (11). Therefore, we hypothesized that polysaccharides secreted by other types of bacteria could suppress postprandial hyperglycemia.

Natto is a traditional Japanese food produced by fermenting soybean with *Bacillus subtilis* var *natto*. *Bacillus subtilis* var *natto* grows on the surface of soybeans and produces various viscous polysaccharides. Natto has preventive effects on lifestyle-related diseases, and suppresses postprandial hyperglycemia (12,13). The active compounds in natto, however, have remained unknown. In this study, we examined whether the polysaccharides extracted from natto suppress sucrose-induced hyperglycemia in silkworms. Furthermore, we investigated whether the natto-derived polysaccharides identified in a

silkworm evaluation system to inhibit sucrose-induced hyperglycemia also inhibit glucose uptake by human intestinal Caco-2 cells.

2. Materials and Methods

2.1. Preparation of the water-soluble viscous fraction and enzyme-treated polysaccharide fraction of natto

The preparation scheme for the water-soluble viscous fraction and enzyme-treated polysaccharide fraction of natto is shown in Figure 1. Water was added to commercially available natto, and the mixture was thoroughly stirred. The soybeans were removed from the mixture and a water extract fraction was obtained. Two volumes of ethanol were added to the water extract fraction, and a filamentous precipitate was collected by centrifugation to obtain a water-soluble viscous fraction. Enzymatic treatment of the water-soluble viscous fraction was performed as described previously (11). The water-soluble viscous fraction was treated with DNase I (1,000 U/mL; Promega) and RNase A (10 µg/mL; NIPPON GENE CO., LTD.) for 24 h at 37°C, and then incubated overnight at 37°C with proteinase K (100 µg/mL). An equal volume of phenol:chloroform:isoamyl alcohol (50:49:1) was added to the fraction, and the samples were vigorously shaken. The upper layer fraction was collected after centrifugation, followed by the addition of two volumes of ethanol to the upper layer fraction. The precipitate was collected by centrifugation and dried to

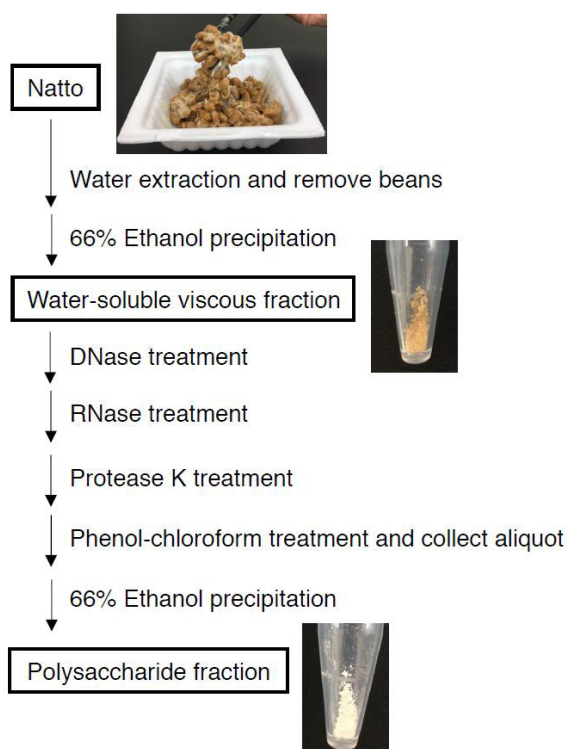


Figure 1. Preparation scheme of the water-soluble viscous fraction and the enzyme-treated polysaccharide fraction of natto.

obtain an enzyme-treated polysaccharide fraction.

2.2. Measurement of sugar, DNA, RNA, and protein

The amounts of sugars, DNA, RNA, and proteins in the enzyme-treated polysaccharide fraction were determined using the phenol-sulfuric acid method, the fluorescent-based Qubit assay for DNA and RNA, and the Bradford assay, respectively, according to a previous report (11).

2.3. Sucrose or glucose tolerance tests of silkworms

Silkworms were reared as described previously (14,15). Silkworm sucrose or glucose tolerance tests were conducted according to the previously reported method (4). A diet containing 10% (w/w) sucrose or glucose was prepared by mixing an artificial diet (Silkmate 2S: Nihon Nosan Co., Ltd., Kanagawa, Japan) and D-sucrose or D-glucose. Test samples were mixed with the diet containing 10% (w/w) sucrose or glucose. A sucrose diet with or without polysaccharide samples was fed to 5th-instar silkworm larvae for 1 h, and then the silkworm hemolymph was collected by cutting the first proleg and glucose concentrations were measured with a glucometer (Accu-Chek, Roche).

2.4. Glucose uptake assay in Caco-2 cells

Glucose uptake by Caco-2 cells was determined by the previously described method (5). Caco-2 cells were obtained from American Type Cell Collection (ATCC, Manassas, VA, USA) and cultured in Dulbecco's Modified Eagle Medium (DMEM, Gibco, NY, USA) containing 10% fetal bovine serum (Gibco) and 1% penicillin/streptomycin (Gibco) at 37°C with 5% CO₂ in air. Caco-2 cells were cultured in a monolayer in a 96-well plate (Tissue culture test plate 96F: TPP, Switzerland). The cells were incubated for an additional 24 h in serum-free DMEM. Subsequently, the cells were washed with Na buffer [10 mM HEPES (pH 7.4), 140 mM NaCl, 20 mg/mL bovine serum albumin] and incubated in Na buffer for 15 min. After incubation, the cells were incubated in Na buffer with 50 µM 2-deoxy-2-[(7-nitro-2, 1, 3-benzoxadiazol-4-yl)amino]-D-glucose (2-NBDG; Cayman Chemical, MI, USA) for 10 min and then washed twice with ice-cold phosphate buffered saline (PBS) to remove the 2-NBDG. Fluorescence of the cells containing 2-NBDG was detected by fluorescence microscopy (IX73: Olympus, Tokyo, Japan) and calculated by Image J ver. 1.43u (National Institutes of Health, USA).

2.5. Chemicals

Acarbose was purchased from LKT Laboratories, Inc. (St. Paul, MN, USA). Voglibose was kindly provided by the Takeda Pharmaceutical Company (Osaka, Japan).

2.5. Statistical analysis

All experiments were performed at least twice. The significance of differences was calculated using a two-tailed Student's *t*-test at the significance level of $\alpha = 0.05$.

3. Results

3.1. Suppressive effect of a water-soluble viscous fraction obtained from natto on sucrose-induced hyperglycemia in silkworms

We prepared a water-soluble viscous fraction from four commercially available types of natto and examined the suppressive effects on sucrose-induced hyperglycemia in silkworms. The water-soluble viscous fraction obtained from natto (#4) significantly suppressed sucrose-induced hyperglycemia in silkworms (Figure 2). The water-soluble viscous fraction obtained from natto #4 suppressed sucrose-induced hyperglycemia in silkworms in a dose-dependent manner (Figure 3A). Indigestible dextrin is a typical water-soluble dietary fiber, the solution of which is viscous (16). Indigestible dextrin lowers postprandial hyperglycemia in rats (16). Indigestible dextrin (200 mg/g diet), however, did not suppress sucrose-induced hyperglycemia in silkworms (Figure 3B). These findings suggest that the viscous components of natto have suppressive activity on sucrose-induced hyperglycemia in silkworms and that the suppressive activity is greater than that of indigestible dextrin.

3.2. Suppressive effect of a natto polysaccharide fraction on sucrose-induced hyperglycemia in silkworms

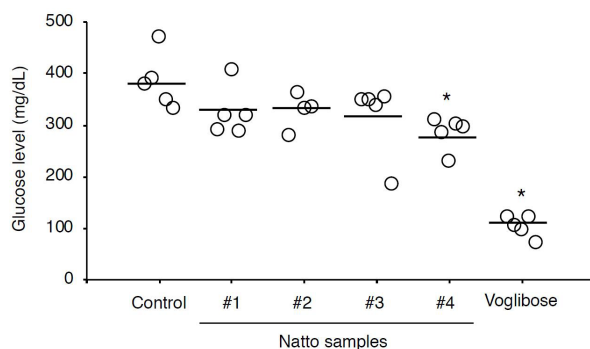


Figure 2. Inhibitory effects of water-soluble viscous fractions of natto on sucrose-induced hyperglycemia in silkworms. A water-soluble viscous fraction (50 mg/g diet) prepared from four commercially available types of natto, and voglibose (40 mg/g diet) were mixed with a 10% sucrose-containing diet. Silkworms were fed a diet containing 10% (w/w) sucrose with or without commercially available natto #1-4 (50 mg/g diet) and acarbose (40 mg/g diet) for 1 h. Glucose levels in the silkworm hemolymph were measured ($n = 4-5$ /group). Bars indicate the mean value of each sample. Statistically significant differences between the control and experimental groups were evaluated using Student's *t*-test. *: $p < 0.05$.

The water-soluble viscous fraction obtained from natto was treated with DNase, RNase, proteinase K, and phenol to obtain an enzyme-treated polysaccharide fraction. The enzyme-treated polysaccharide fraction contained (per gram dry weight) 32% sugar, and less than 1% DNA, RNA, and protein (Table 1). Addition of the enzyme-treated polysaccharide fraction to a sucrose-containing diet suppressed sucrose-induced hyperglycemia in silkworms, similarly to the water-soluble viscous fraction (Figure 4). This finding suggests that the natto-derived polysaccharides suppress sucrose-induced hyperglycemia.

3.3. Suppressive effect of a water-soluble viscous fraction obtained from natto on glucose-induced hyperglycemia in silkworms

Sucrose in the intestinal tract is cleaved into glucose and fructose by α -glucosidase and is absorbed into the intestinal cells (4). Acarbose and voglibose,

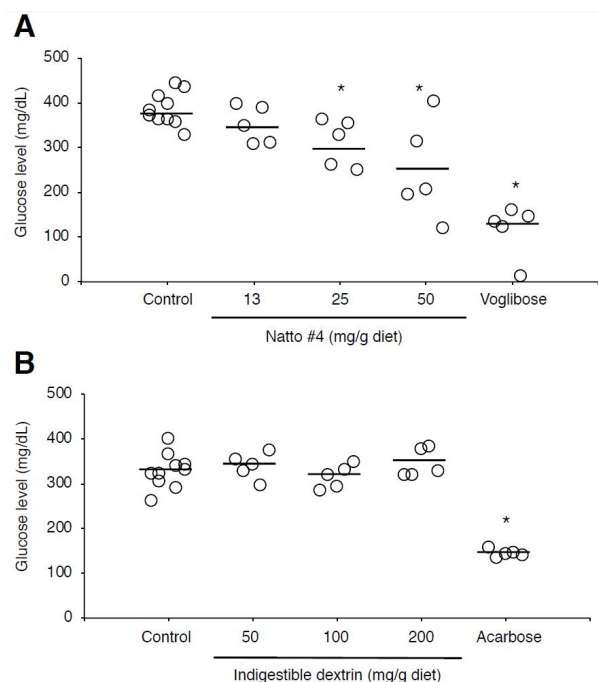


Figure 3. Dose-dependent inhibitory effects of a water-soluble viscous fraction obtained from natto on sucrose-induced hyperglycemia in silkworms. (A) Dose-dependent inhibitory effects of a water-soluble viscous fraction obtained from natto #4 on sucrose-induced hyperglycemia in silkworms. Silkworms were fed a diet containing 10% (w/w) sucrose with or without the water-soluble viscous fraction obtained from natto #4 (13, 25, 50 mg/g diet) and voglibose (40 mg/g diet) for 1 h. Glucose levels in the silkworm hemolymph were measured ($n = 5-10$ /group). Bars indicate the mean value of each sample. Statistically significant differences between the control and experimental groups were evaluated using Student's *t*-test. *: $p < 0.05$. (B) Dose-dependent inhibitory effects of indigestible dextrin on sucrose-induced hyperglycemia in silkworms. Silkworms were fed a diet containing 10% (w/w) sucrose with or without indigestible dextrin (50, 100, 200 mg/g diet) and acarbose (40 mg/g diet) for 1 h. Glucose levels in the silkworm hemolymph were measured ($n = 5-10$ /group). Bars indicate the mean value of each sample. Statistically significant differences between the control and experimental groups were evaluated using Student's *t*-test. *: $p < 0.05$.

Table 1. Amounts of sugar, DNA, RNA, and protein in Natto #4 enzyme-treated fraction

Fraction	Sugar (mg/g)	DNA (mg/g)	RNA (mg/g)	Protein (mg/g)
Enzyme-treated polysaccharide sample	320	0.04	0.3	3.4

The amounts of sugars, DNA, RNA, and proteins in the enzyme-treated polysaccharide fraction were determined by the phenol-sulfuric acid method, the fluorescent-based Qubit assay for DNA and RNA, and Bradford assay, respectively. The amounts of sugars, DNA, RNA, and proteins in 1 g of dry weight of the enzyme-treated fraction are shown.

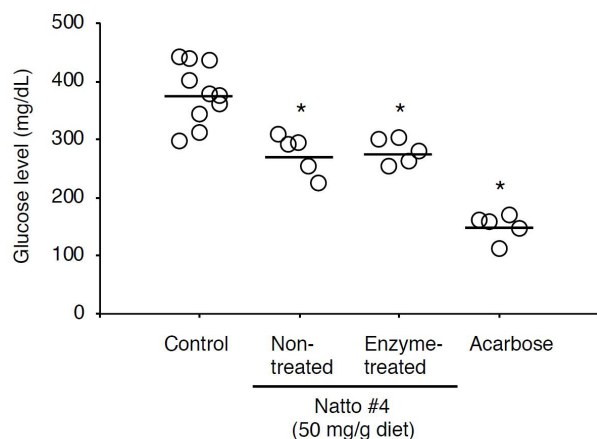


Figure 4. Inhibitory effects of the polysaccharide fraction of natto on sucrose-induced hyperglycemia in silkworms. A water-soluble viscous fraction obtained from natto #4 was treated with DNase, RNase, proteinase K, and phenol to obtain an enzyme-treated polysaccharide fraction (Enzyme-treated natto #4). The water-soluble viscous fraction (Non-treated natto #4, 50 mg/g diet) prepared from natto #4, an enzyme-treated polysaccharide fraction (Enzyme-treated natto #4, 50 mg/g diet), and acarbose (40 mg/g diet) were mixed with a 10% sucrose containing diet. Silkworms were fed a diet containing 10% (w/w) sucrose with or without the water-soluble viscous fraction (Non-treated natto #4, 50 mg/g diet), the enzyme-treated polysaccharide fraction (Enzyme-treated natto #4, 50 mg/g diet), or acarbose (40 mg/g diet) for 1 h. Glucose levels in the silkworm hemolymph were measured ($n = 5-10/\text{group}$). Bars indicate the mean value of each sample. Statistically significant differences between the control and experimental groups were evaluated using Student's t -test. *: $p < 0.05$.

α -glucosidase inhibitors, inhibit sucrose-induced hyperglycemia, but do not suppress glucose-induced hyperglycemia (4). *E. faecalis* YM0831, which has inhibitory activity against glucose transport in the isolated silkworm intestine suppresses both sucrose- and glucose-induced hyperglycemia in silkworms (5). In the present study, addition of the water-soluble viscous fraction obtained from natto to the diet suppressed sucrose- and glucose-induced hyperglycemia in silkworms (Figure 5). These findings suggest that the water-soluble viscous fraction obtained from natto inhibits the transport of glucose in the intestine, similar to *E. faecalis* YM0831.

3.4. Inhibitory effect of a natto polysaccharide fraction on glucose uptake by Caco-2 cells

E. faecalis YM0831 inhibits glucose uptake by Caco-2 cells derived from human colon adenocarcinoma

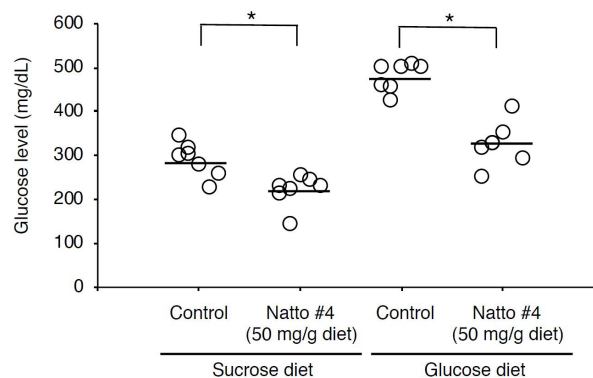


Figure 5. Inhibitory effects of the water-soluble viscous fraction of natto on glucose-induced hyperglycemia in silkworms. The water-soluble viscous fraction (50 mg/g diet) prepared from four commercially available types of natto was mixed with 10% sucrose- or glucose-containing diet, respectively. Silkworms were fed a diet containing 10% (w/w) sucrose or glucose with or without the water-soluble viscous fractions (50 mg/g diet) for 1 h. Glucose levels in the silkworm hemolymph were measured ($n = 6-7/\text{group}$). Bars indicate the mean value of each sample. Statistically significant differences between control and experimental groups were evaluated using the Student's t -test. *: $p < 0.05$.

(5). Here we found that addition of the enzyme-treated polysaccharide fraction of natto inhibited glucose uptake by Caco-2 cells (Figure 6). On the other hand, even when indigestible dextrin was added, glucose uptake by Caco-2 cells was not inhibited (Figure 6). These findings suggest that the enzyme-treated polysaccharide fraction of natto has high activity to inhibit glucose uptake by intestinal tract cells compared with indigestible dextrin.

4. Discussion

In this study, we found that a natto-derived, water-soluble viscous fraction and its enzyme-treated polysaccharide fraction suppressed sucrose-induced hyperglycemia in silkworms and inhibited glucose uptake by human intestinal cells. The polysaccharides obtained from natto are expected to inhibit glucose uptake by intestinal cells in human individuals and suppress postprandial hyperglycemia.

Although ingestion of natto was previously reported to suppress hyperglycemia, its active substances were not identified (12, 13). Natto contains viscous substances such as poly- γ -glutamic acid and levan, a polysaccharide (17). Poly- γ -glutamic acid is used as a base material for an insulin drug delivery system (18). There are no reports that polyglutamic acid has

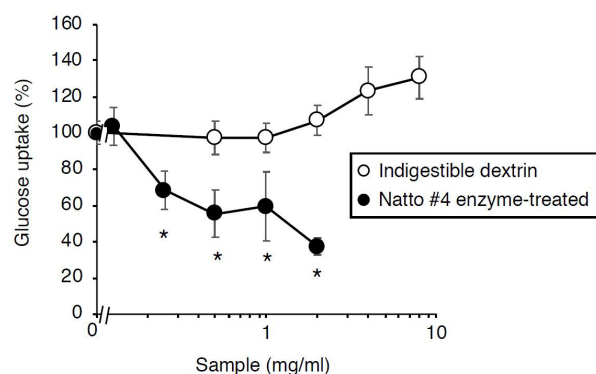


Figure 6. Inhibitory effect of natto-derived polysaccharide fraction on glucose uptake by human intestinal cell, Caco-2 cells. Various concentrations of enzyme-treated polysaccharide fraction (Enzyme-treated natto #4) and indigestible dextrin were added to the uptake system of 2-NBDG in Caco-2 cells and fluorescence uptake by the Caco-2 cells was measured. $n = 3/\text{group}$. Statistically significant differences between the control and experimental groups were evaluated using Student's t -test. *: $p < 0.05$.

blood glucose-suppressing activity following sucrose intake. Levan has various functions, such as moisture retention, and is used for food additives, cosmetics, and drug development (19). Research suggests, however, that administration of levan derived from natto does not have a blood glucose-suppressive effect in normal rats or diabetic rats treated with streptozotocin, and does not improve symptoms of diabetes (20). Therefore, this report is the first to demonstrate that natto-derived viscous components suppress the increase in blood glucose after sucrose ingestion. Our results suggest that the viscous component of natto suppresses postprandial hyperglycemia by inhibiting glucose uptake in intestinal tract cells. The molecular structure and mechanism of action of the polysaccharides in natto that inhibit glucose uptake in human intestinal cells require further clarification.

Experiments using the silkworm evaluation system revealed that the viscous component of natto has a suppressive effect against sucrose- and glucose-induced hyperglycemia. Silkworms are useful for large-scale *in vivo* evaluation because they are inexpensive and can be reared in large groups (21-27). We reported the discovery of several active substances that suppress postprandial hyperglycemia using the silkworm evaluation system (4,11,28). The inhibitory effects of each of the four natto products we examined on sucrose-induced hyperglycemia in silkworms differed. Therefore, we will next search for a highly active natto using the silkworm evaluation system. We propose that the silkworm evaluation system is useful for developing functional fermented foods.

In the present study, we found that natto-derived polysaccharides identified by an *in vivo* evaluation system using silkworms inhibited glucose uptake by human intestinal cells. The development of more functional natto using the silkworm evaluation system

and verification of the effectiveness of natto for humans are future challenges.

Acknowledgements

We thank Kana Hashimoto and Mari Maeda (Genome Pharmaceuticals Institute Co., Ltd., Tokyo, Japan) for their technical assistance in rearing the silkworms. The project was supported by JSPS KAKENHI grant number JP15H05783 (Scientific Research (S) to K.S.) and JSPS KAKENHI grant number JP17K08288 (Scientific Research (C) to Y.M.). The project was also supported by the Supporting Industry Program of the Ministry of Economy, Trade and Industry and Genome Pharmaceuticals Institute Co., Ltd. (Tokyo, Japan). The authors declare no conflicts of interest.

References

1. Matsumoto Y, Sumiya E, Sugita T, Sekimizu K. An invertebrate hyperglycemic model for the identification of anti-diabetic drugs. *PloS one*. 2011; 6:e18292.
2. Matsumoto Y, Sekimizu K. Evaluation of anti-diabetic drugs by using silkworm, *Bombyx mori*. *Drug Discov Ther*. 2016; 10:19-23.
3. Matsumoto Y, Ishii M, Hayashi Y, Miyazaki S, Sugita T, Sumiya E, Sekimizu K. Diabetic silkworms for evaluation of therapeutically effective drugs against type II diabetes. *Sci Rep*. 2015; 5:10722.
4. Matsumoto Y, Ishii M, Sekimizu K. An *in vivo* invertebrate evaluation system for identifying substances that suppress sucrose-induced postprandial hyperglycemia. *Sci Rep*. 2016; 6:26354.
5. Matsumoto Y, Ishii M, Hasegawa S, Sekimizu K. *Enterococcus faecalis* YM0831 suppresses sucrose-induced hyperglycemia in a silkworm model and in humans. *Commun Biol*. 2019; 2:157.
6. Andrade N, Silva C, Martel F. The effect of oxidative stress upon intestinal sugar transport: an *in vitro* study using human intestinal epithelial (Caco-2) cells. *Toxicol Res (Camb)*. 2018; 7:1236-1246.
7. Schreck K, Melzig MF. Intestinal saturated long-chain fatty acid, glucose and fructose transporters and their inhibition by natural plant extracts in Caco-2 cells. *Molecules*. 2018; 23.
8. Rehm BH. Bacterial polymers: biosynthesis, modifications and applications. *Nat Rev Microbiol*. 2010; 8:578-592.
9. Nwodo UU, Green E, Okoh AI. Bacterial exopolysaccharides: functionality and prospects. *Int J Mol Sci*. 2012; 13:14002-14015.
10. Freitas F, Alves VD, Reis MA. Advances in bacterial exopolysaccharides: from production to biotechnological applications. *Trends Biotechnol*. 2011; 29:388-398.
11. Ishii M, Matsumoto Y, Sekimizu K. Bacterial polysaccharides inhibit sucrose-induced hyperglycemia in silkworms. *Drug Discov Ther*. 2018; 12:185-188.
12. Weng Y, Yao J, Sparks S, Wang KY. Nattokinase: an oral antithrombotic agent for the prevention of cardiovascular disease. *Int J Mol Sci*. 2017; 18. doi: 10.3390/ijms18030523.
13. Schallmeyer M, Singh A, Ward OP. Developments in the use of *Bacillus* species for industrial production. *Can J*

- Microbiol. 2004; 50:1-17.
14. Kaito C, Akimitsu N, Watanabe H, Sekimizu K. Silkworm larvae as an animal model of bacterial infection pathogenic to humans. *Microb Pathog.* 2002; 32:183-190.
 15. Kurokawa K, Kaito C, Sekimizu K. Two-component signaling in the virulence of *Staphylococcus aureus*: a silkworm larvae-pathogenic agent infection model of virulence. *Methods Enzymol.* 2007; 422:233-244.
 16. Wakabayashi S, Kishimoto Y, Matsuoka A. Effects of indigestible dextrin on glucose tolerance in rats. *J Endocrinol.* 1995; 144:533-538.
 17. Oner ET, Hernandez L, Combie J. Review of Levan polysaccharide: From a century of past experiences to future prospects. *Biotechnol Adv.* 2016; 34:827-844.
 18. Khalil IR, Burns AT, Radecka I, Kowalczyk M, Khalaf T, Adamus G, Johnston B, Khechara MP. Bacterial-derived polymer poly-γ-glutamic acid (γ-PGA)-based micro/nanoparticles as a delivery system for antimicrobials and other biomedical applications. *Int J Mol Sci.* 2017; 18. doi: 10.3390/ijms18020313.
 19. Srikanth R, Reddy CH, Siddartha G, Ramaiah MJ, Uppuluri KB. Review on production, characterization and applications of microbial levan. *Carbohydr Polym.* 2015; 120:102-114.
 20. de Melo FC, Zaia CT, Celligoi MA. Levan from *Bacillus subtilis* Natto: its effects in normal and in streptozotocin-diabetic rats. *Braz J Microbiol.* 2012; 43:1613-1619.
 21. Nwibo DD, Hamamoto H, Matsumoto Y, Kaito C, Sekimizu K. Current use of silkworm larvae (*Bombyx mori*) as an animal model in pharmaco-medical research. *Drug Discov Ther.* 2015; 9:133-135.
 22. Panthee S, Paudel A, Hamamoto H, Sekimizu K. Advantages of the silkworm as an animal model for developing novel antimicrobial agents. *Front Microbiol.* 2017; 8:373.
 23. Paudel A, Panthee S, Urai M, Hamamoto H, Ohwada T, Sekimizu K. Pharmacokinetic parameters explain the therapeutic activity of antimicrobial agents in a silkworm infection model. *Sci Rep.* 2018; 8:1578.
 24. Matsumoto Y, Ishii M, Shimizu K, Kawamoto S, Sekimizu K. A silkworm infection model to evaluate antifungal drugs for cryptococcosis. *Med Mycol J.* 2017; 58:E131-E137.
 25. Ishii M, Matsumoto Y, Nakamura I, Sekimizu K. Silkworm fungal infection model for identification of virulence genes in pathogenic fungus and screening of novel antifungal drugs. *Drug Discov Ther.* 2017; 11:1-5.
 26. Meng X, Zhu F, Chen K. Silkworm: a promising model organism in life science. *J Insect Sci.* 2017; 17. doi: 10.1093/jisesa/iex064.
 27. Matsumoto Y, Sekimizu K. Silkworm as an experimental animal for research on fungal infections. *Microbiol Immunol.* 2019; 63:41-50.
 28. Ishii M, Matsumoto Y, Sekimizu K. Inhibitory effects of alpha-cyclodextrin and its derivative against sucrose-induced hyperglycemia in an *in vivo* evaluation system. *Drug Discov Ther.* 2018; 12:122-125.

Received January 9, 2020; Accepted February 15, 2020

*Address correspondence to:

Dr. Kazuhisa Sekimizu, Teikyo University Institute of Medical Mycology, 359 Otsuka, Hachioji, Tokyo, 192-0395, Japan.
E-mail: sekimizu@main.teikyo-u.ac.jp

Generic selection criteria for safety and patient benefit [IX]: Evaluation of "feeling of use" of sodium hyaluronate eye drops using the Haptic Skill Logger (HapLog[®]) wearable sensor for evaluating haptic behaviors

Miho Goto¹, Mitsuru Nozawa¹, Yuko Wada², Ken-ichi Shimokawa³, Fumiyoshi Ishii^{2,*}

¹ Triad Japan Co. Ltd., Kanagawa, Japan;

² Department of Self-medication and Health Care Sciences, Meiji Pharmaceutical University, Tokyo, Japan;

³ Department of Pharmaceutical Sciences, Meiji Pharmaceutical University, Tokyo, Japan.

SUMMARY We compared the pharmaceutical properties, such as surface tension, drop volume, nozzle inner diameter, and force to push the drug product out of the container (squeeze force), of purified sodium hyaluronate eye drops preparations of one brand-name (Hyalein) and 11 generic drugs used for treatment of keratoconjunctiva epithelial disorders, and examined product selection based on the needs of the patient. The surface tension of Nissen (51.0 dyn/cm) and Nitten (52.3 dyn/cm) was significantly lower than that of Hyalein (62.8 dyn/cm), whereas Nitten PF (69.5 dyn/cm) was significantly higher than Hyalein. The drop volume of Tearbalance (42.4 mg), Nissen (43.7 mg), and Nitten (42.7 mg) was significantly lower than that of Hyalein (50.4 mg). We compared the squeeze force using a wearable touch sensor (Haptic Skill Logger: HapLog[®]) and digital force gauge (DF). The squeeze force of HapLog[®] showed values of about 1.7- to 3.5-fold higher than that of DF. Moreover, the squeeze force of Eyecare (34.0 N), Kyorin (35.4 N), and Nitten PF (44.3 N) by HapLog[®] was significantly higher than that of Hyalein (10.5 N). In contrast, the squeeze force of Kyorin (20.8 N) and Nitten PF (25.0 N) by DF was significantly higher than that of Hyalein (12.2 N). Two questionnaire surveys on the feeling of instillation of eye drops revealed a strong negative correlation between feeling of use and squeeze force.

Keywords HapLog[®], Digital force gauge, Ophthalmic liquids/solutions, Sodium hyaluronate ophthalmic solution

1. Introduction

In recent years, Japan has been actively promoting the use of generic drugs (GE) from the viewpoint of optimizing or reducing medical expenses (1). Based on a document by the Ministry of Health, Labor and Welfare, "Changes to generic drugs listed in prescriptions" (March 5, 2012 Health Department Director General, Health Department 0305 No. 12), when a brand name is written on the drug listed in the prescription (*i.e.* brand name prescription drug), the changing and dispensing to a generic drug with a different content or similar alternative dosage form without prior confirmation by the prescribing physician is allowed (2). To reduce medical costs (3,4), the choice and selection of generic drugs are important to the pharmacist who is responsible for dispensing to the patient.

There are various types of eye drop containers, and the ease of eye drop use (*i.e.* ease of extrusion or

instillation) differs depending on the container used as well as the properties of the contents (for example, viscosity) (5). If the container is too hard, it may be difficult for elderly people or people with weak finger strength to use; in contrast, if it is too soft, an excessive amount may be instilled at once. Such problems may lead to poor compliance.

To date, one study has investigated the squeeze force required to instill a drop of ophthalmic solution using a digital force gauge (DF) (5). However, in the method of measuring squeeze force, all are different from the use of dropping an eye drop container with a finger, the container was fixed from both sides with a hemispherical urethane spherical compression jig, and the force (squeeze force) against which one was pressed with a digital force gauge was measured (6).

Therefore, using the Haptic Skill Logger (HapLog[®]), a wearable contact force sensor that allows the measurement of squeeze force by pushing the eye

drop container directly with fingers (7), we report the evaluation of various measurements, surface tension, nozzle inner diameter and drop volume from the container, and squeeze force, and "feeling of use".

2. Materials and Methods

2.1. Materials

Ethical pharmaceutical eye drops containing purified sodium hyaluronate ophthalmic solution (one brand-name "Hyalein[®] Ophthalmic Solution 0.1%" and 11 generic products) were used in this study. The product name, abbreviated name, class, company name, and lot number of these products are listed in Table 1. In addition, all products are currently available on the market and registered with the Pharmaceutical and Medical Devices Agency (PMDA) (8). All the reagents used were of analytical grade.

2.2. Measurement of surface tension

The surface tension of each preparation was measured according to a previous study (6). Briefly, the ophthalmic solutions taken from each formulation were measured at $25 \pm 1^\circ\text{C}$ using a tension meter method with a Du Noüy type surface tension meter (Rigo Co., Ltd., Tokyo, Japan). Each drug was measured 6 times and the average value was calculated.

2.3. Measurement of drop weight

The drop weight of each preparation was measured according to a previous study (6). Briefly, the weight obtained by instilling one drop from each preparation was measured 6 times using an analytical balance XSE204 (Mettler Toledo Co. Ltd., Tokyo, Japan) at $25 \pm 1^\circ\text{C}$, and the average value was calculated.

2.4. Measurement of nozzle inner diameter

The inner diameter of the ophthalmic container was

measured 6 times using a digital caliper type 19974 (Shinwa Rules Co., Ltd., Niigata, Japan) and the average value was calculated.

2.5. Measurement of squeeze force required to instill a drop of ophthalmic solution using DF

The measurement of the weight obtained by instilling one drop from each formulation and the measurement of the squeeze force required to instill one drop of eye drop were performed according to a previous study (6). Each preparation was set in a holder to which a DF (ZP-50N; Imada Co., Aichi, Japan) was attached, and the handle was slowly turned to form a hemispherical urethane spherical compression jig (Imada Co., Aichi, Japan). The eye drop container was sandwiched from both sides, and the force applied at the moment when a drop was instilled was doubled to obtain a squeeze force. The doubling of the force was applied at the moment of drop instillation because the force on one side of the container, which is sandwiched from both sides, is displayed in DF measurement; therefore, we assumed that the same force was also applied from the other side. Each formulation was measured 6 times and the average value was calculated.

2.6. Measurement of squeeze force using HapLog[®]

The squeeze force of each drug product was measured using HapLog[®] according to a previous study (9). After full explanation of the purpose of this survey to the subjects (8 individuals), the RAND function of Excel was used to randomize the 12 types of eye drop containers. Then, a wearable touch sensor HapLog[®] (Tec Gihan Co., Ltd., Kyoto, Japan), as a tactile sensibility evaluation tool, was used to measure the pressure change applied to the fingertips for each drop, which were in a randomized order. For the measurement method using HapLog[®], touch sensors were attached to the dominant thumb and index finger, and the center of the eye drop container was grasped using the thumb and index finger; the total force (thumb + index finger)

Table 1. Eye drop products used in this study

Product name	Abbreviated name	Company name	Lot numbers
Hyalein [®] Ophthalmic Solution 0.1%	Hyalein	Santen Pharmaceutical Co., Ltd.	1HT6404
Eyecare [®] Ophthalmic Solution 0.1%	Eyecare	Kaken Pharmaceutical Co., Ltd.	E55320
Tearbalance [®] Ophthalmic Solution 0.1%	Tearbalance	Senju Pharmaceutical Co., Ltd.	H564
Hyalonsan [®] Ophthalmic Solution 0.1%	Hyalonsan	Toa Pharmaceutical Co., Ltd.	A47AK
Hyaluronate Na Ophthalmic Solution 0.1% "Kyorin"	Kyorin	Kyorin Rimedio Co., Ltd.	94AA
Sodium Hyaluronate Ophthalmic Solution 0.1% "Nissin"	Nissin	Nissin Pharmaceutical Co., Ltd.	311131
Hyaluronate Na Ophthalmic Solution 0.1% "Pfizer"	Pfizer	Pfizer Japan Inc.	MA02
Hyaluronate Na Ophthalmic Solution 0.1% "Wakamoto"	Wakamoto	Wakamoto Co., Ltd.	5470
Sodium Hyaluronate Ophthalmic Solution 0.1% "TS"	TS	Teika Pharmaceutical Co., Ltd.	KE05
Sodium Hyaluronate Ophthalmic Solution 0.1% "Towa"	Towa	Towa Pharmaceutical Co., Ltd.	A001A
Sodium Hyaluronate Ophthalmic Solution 0.1% "Nitten"	Nitten	Nitten Pharmaceutical Co., Ltd.	L1738C
Sodium Hyaluronate PF Ophthalmic Solution 0.1% "Nitten"	Nitten PF	Nitten Pharmaceutical Co., Ltd.	GF96

required to instill a drop was recorded as the squeeze force (N). The measurements began with the eye drops placed on a laboratory bench. The dominant hand with a tactile sensor was used to hold the eye drop container, and the other hand carried a transparent petri dish. After instilling a drop of the drug solution onto the petri dish, the eye dropper was returned to the experimental table. This operation was measured 10 times for each eye drop container. From the HapLog[®] measurement data, the average maximum squeeze force applied to the fingertip (average maximum pressure), the average time required from the start of pressurization to the drip (average drip time), and the average value of the total squeeze force were analyzed. This was calculated for each person and the total average was also calculated. However, among 10 repeated measurements, the first 3 were deemed as practice, and only 6 measurement replicates (measurements 4 to 9) were utilized for calculation of average. Although these can generate free touch feeling of the fingertips and allow simultaneous evaluation of wearer's finger contact force and touch feeling, calibration was performed for each wearer because individual differences due to the wearing methods and finger sizes cause an error in contact force measurement (7).

2.7. Statistical analysis

For each measured parameter, the values were compared using Dunnett's multiple comparison test or Pearson's correlation coefficient test (10). A *p*-value under 0.05 or 0.01 was regarded as significant.

2.8. Questionnaire survey using a 6-point scale

Immediately after the measurements for each eye drop, a questionnaire survey was conducted regarding the individual's feeling about the container (*i.e.* the ease of eye drop use), which was evaluated on a 6-point scale (Table 2).

Table 2. Questionnaire survey on the feeling of applying various eye drops

Point score	Products symbol (A - L)
Very difficult	1
Difficult	2
Slightly difficult	3
Slightly easy	4
Easy	5
Very easy	6

Questionnaire survey. We would like to ask you about your feeling when using one drop of a range of eye drops (A to L). When discharging or instilling one drop products (A to L), please circle the number showing the feeling of use. Difficult to apply represents that it is difficult to discharge or instill a single drop (it requires a pressing force, it takes time to take out). Easy to apply represents it is easy to instill a single drop, and the drop comes out smoothly. If the eye drop is easy to apply, but it is difficult to instill only one drop and you get two drops, then please circle the number with a double circle.

2.9. Questionnaire survey using a continuous scale of absolute values

A questionnaire survey using a continuous scale of absolute values for ease of eye drop use or instillation was conducted (Figure 1). In the evaluation, the ease of eye drop instillation was expressed in the range of 0 to 72 mm and the difficulty of instillation in the range of 0 to -72 mm. The responses to the questionnaire were evaluated by quantifying the measurement of the position marked with a circle on the scale with the distance (mm) from point 0.

3. Results

3.1. Measurement of surface tension

The surface tension of each formulation used in this experiment was measured. The results are shown in Figure 2. The surface tension of Hyalein was 62.8 dyn/cm, whereas that of ranged from 51.0 to 69.5 dyn/cm (Figure 2). In particular, Nissin (51.0 dyn/cm) and Nitten (52.3 dyn/cm) had significantly lower surface tension. In contrast, Hyalonsan (67.1 dyn/cm) and Nitten PF (69.5 dyn/cm) had significantly higher values.

3.2. Measurement of drop weight

The drop weight from each eye drop container used in this experiment was measured (Figure 3). The drop weight of Hyalein was 50.4 mg, whereas that of the generic drugs ranged from 42.4 to 52.2 mg (Figure 3). In particular, Tearbalance (42.2 mg), Nissin (43.7 mg),

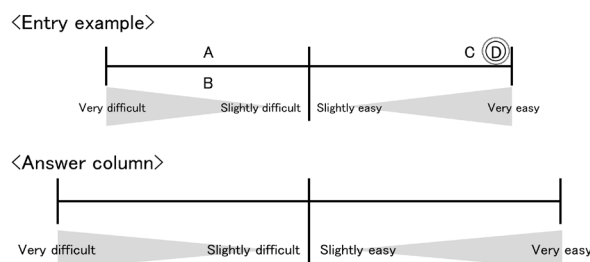


Figure 1. Questionnaire survey on the feeling of using various eye drops (Continuous scale). We would like to ask you about your feeling when using one drop of a range of eye drops (A to L). In the scale below, the left side of the center is somewhat hard to instill/discharge a drop, the right side is somewhat easy to instill; the closer to the left end, the more difficult to instill; the closer to the right end, the more easily to instill. When instilling one drop of each of the eye drops (A to L), enter the product code in the position of the feeling of use that fits the scale below. Difficult to apply indicates that it is difficult to instill one drop (requires a pressing force, takes time to instill, *etc.*). Easy to apply indicates that it is easy to instill one drop, and one drop comes out smoothly. If it is easy to instill, but difficult to take out only one drop and you get 2 drops, please circle the number with a double circle. Entry example: A and B are both relatively difficult to instill, C is very easy to instill, D is even more easy to instill, but two drops are instilled.

and Nitten (42.7 mg) had significantly lower values.

3.3. Measurement of nozzle inner diameter

The nozzle inner diameter of each eye drop container used in this experiment was measured (Figure 4, bar graph). The nozzle inner diameter of Hyalein was 1.69 mm, whereas that of the generic drugs ranged from 0.95 to 2.03 mm (Figure 4). In particular, Tearbalance (1.06 mm), Wakamoto (1.18 mm), and Nitten PF (0.95 mm) had significantly lower values, whereas Kyorin (2.03 mm) had a significantly higher nozzle inner diameter.

3.4. Measurement of eye drop container thickness

The thickness of each eye drop container used in this experiment was measured (Figure 4, line graph). The thickness of Hyalein was 0.84 mm, whereas that of the generic drugs ranged from 0.45 to 1.18 mm (Figure 4). In particular, thickness of Eyecare (0.57 mm), Kyorin (0.53 mm), Pfizer (0.49 mm), Wakamoto (0.45 mm), TS (0.52 mm), Towa (0.46 mm) and Nitten (0.64 mm) were significantly lower. In contrast, thickness of Tearbalance (1.18 mm) and Hyalonsan (1.15 mm) were significantly higher.

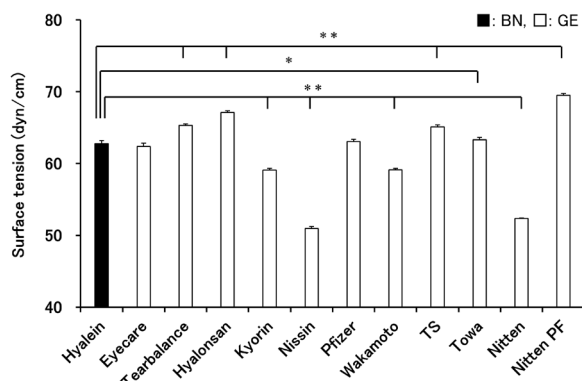


Figure 2. Surface tension measurement of various eye drops preparations ($n = 6$). BN: brand-name drug, GE: generic drug, * $p < 0.05$, ** $p < 0.01$ (vs Hyalein, Dunnett-test)

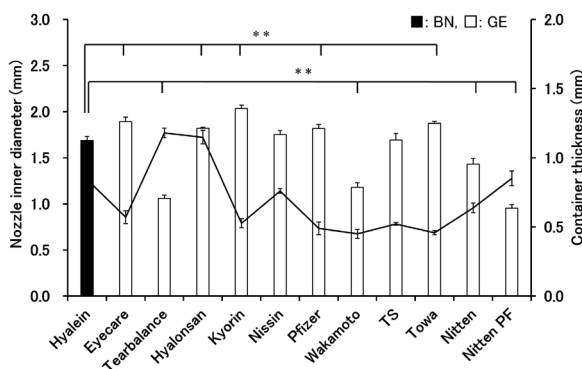


Figure 4. Nozzle inner diameter (Bar graph) and container thickness (line graph) measurement of various eye drops preparations ($n = 6$). BN: brand-name drug, GE: generic drug, ** $p < 0.01$ (vs Hyalein, Dunnett-test).

3.5. Measurement of squeeze force with HapLog® and DF

The results of the average maximum squeeze force of 12 eye drops using HapLog® and DF are shown in Figure 5. For measurements using HapLog®, the average squeeze force for Hyalein was 10.5 N, whereas that for the generic drugs ranged from 14.7 to 44.3 N (Figure 5). In particular, Eyecare (34.0 N), Kyorin (35.4 N), and Nitten PF (44.3 N) showed significantly higher values. In contrast, for DF measurements, the average squeeze force for Hyalein was 12.2 N, and that of the generic drugs ranged from 8.2 to 25.0 N. In particular, Kyorin (20.8 N) and Nitten PF (25.0 N) showed significantly higher values.

3.6. Questionnaire using a 6-point scale of the "feeling of use" of various eye drops

The relationship between the ratings and the squeeze force measured using HapLog® is shown in Figure 6. Hyalein was rated 6.0 points because it was very easy to instill, whereas the evaluation of the generic drugs ranged from 1.4 to 5.5 points. In particular, Kyorin (2.3 points) and Nitten PF (1.4 points) had significantly

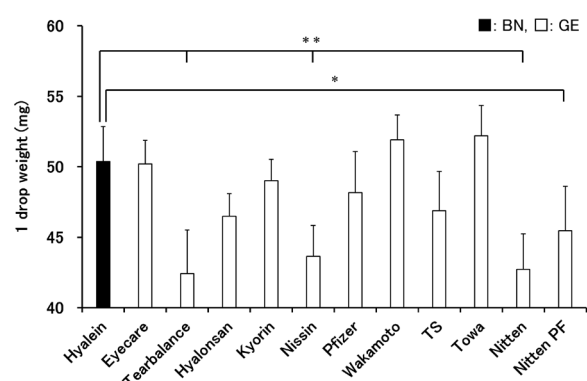


Figure 3. One drop weight measurement of various eye drops preparations ($n = 6$). BN: brand-name drug, GE: generic drug, * $p < 0.05$, ** $p < 0.01$ (vs Hyalein, Dunnett-test)

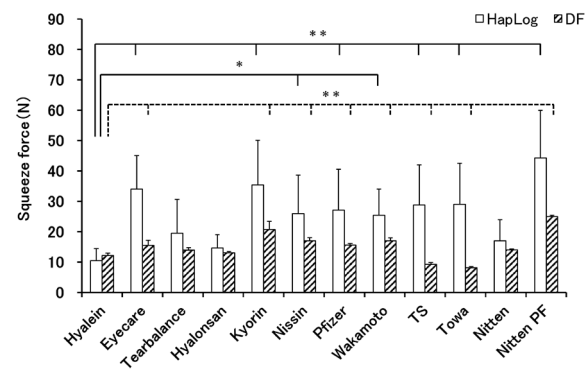


Figure 5. Squeeze force of various eye drops measured using HapLog® and DF ($n = 6$). DF: digital force gauge, * $p < 0.05$, ** $p < 0.01$ (vs Hyalein, Dunnett-test)

lower ratings for ease of instillation. The correlation coefficient was calculated from the approximate curve and showed a strong negative correlation ($y = -0.1357x + 7.6511$, $R^2 = 0.8937$).

3.7. Questionnaire survey using a continuous scale of the "feeling of use" of various eye drops

The relationship between the scale and squeeze force measured using HapLog[®] is shown in Figure 7. Hyalein was evaluated at 66.8 mm, whereas the evaluation of the generic drugs ranged from -68.4 mm to 66.1 mm. In particular, Kyorin (-35.3 mm) and Nitten PF (-68.4 mm) were significantly underrated. The correlation coefficient was calculated from the approximate curve and showed a strong negative correlation ($y = -3.9804x + 120.77$, $R^2 = 0.9095$).

4. Discussion

Kawashima studied the difference in drop volume of various eye drops, and suggested that drop volume may be influenced by the characteristics of eye drops, the shape of eye drop container, and the application technique of eye drops (11). The characteristics of

ophthalmic solutions are determined by the liquidity of the ophthalmic solution, surface tension, and viscosity, and the amount of drops varies with the product, even if an ophthalmic container with the same shape is used. Kawashima also found that eye drops with high surface tension have a large drop volume, whereas drops with low surface tension have a small drop volume (11). Consistent with this, we found that the surface tension of Hyalein (1.69 mm) and Nissin (1.75 mm), which have similar nozzle inner diameters, was 62.8 dyn/cm and 51.0 dyn/cm, respectively, and the drop volume was 50.4 mg and 43.7 mg, respectively (Figures 2-4).

Furthermore, Wada *et al.* reported that surfactants, such as benzalkonium chloride, affect the surface tension of eye drops and that surface tension decreases in a concentration-dependent manner (6). Among the preparations used in the present study, Hyalein (62.8 dyn/cm), Nissin (51.0 dyn/cm), and Wakamoto (59.1 dyn/cm) contain the cationic surfactant benzalkonium chloride. In addition, the ophthalmic solution Nitten (52.3 dyn/cm) contains polysorbate 80, a nonionic surfactant. Nissin, Wakamoto, and Nitten showed significantly low surface tension values, but Hyalein did not show low values despite containing benzalkonium chloride (Figure 2). This is attributed to the addition of the benzalkonium chloride preservative, propylene glycol, which has antibacterial activity (12). Therefore, the concentration of benzalkonium chloride may be lower than in other products. Also, Nagai *et al.* reported that benzalkonium chloride causes strong corneal epithelial damage and that polysorbate 80 has a delayed corneal epithelial wound healing effect (13). Based on this, products other than benzalkonium chloride-containing preparations (Hyalein, Nissin and Wakamoto) and polysorbate 80-containing preparations (Nitten) may be appropriate for long-term use in patients.

Yoshikawa and Yamada reported no significant correlation between drop volume and bottle hardness for various glaucoma eye drops (14). Therefore, we investigated the association between drop volume and nozzle diameter. The amounts in one drop of Tearbalance (42.2 mg), Nissin (43.7 mg), Nitten (42.7 mg), and Nitten PF (45.5 mg) were significantly lower than that of Hyalein (50.4 mg) (Figure 3). In addition, the nozzle diameter of Hyalin (1.69 mm), Tearbalance (1.06 mm), Wakamoto (1.18 mm), Nissin (1.43 mm), and Nitten PF (0.95 mm) were significantly low. Therefore, for most formulations, excluding Wakamoto (nozzle diameter 1.18 mm, drop volume 51.9 mg), the nozzle diameter and the drop volume were correlated (Figures 3 and 4).

The hardness and squeeze characteristics of each eye drop container are important not only in terms of ease of use, but also in terms of economy. Murakami *et al.* reported that the shape of the eye drop container, the material of the main body, and the hardness of the

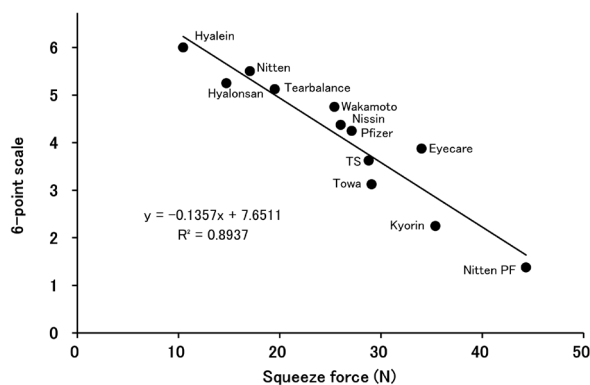


Figure 6. Correlation between 6-point scale and squeeze force of various eye drops measured using Haplog[®] ($n = 8$).

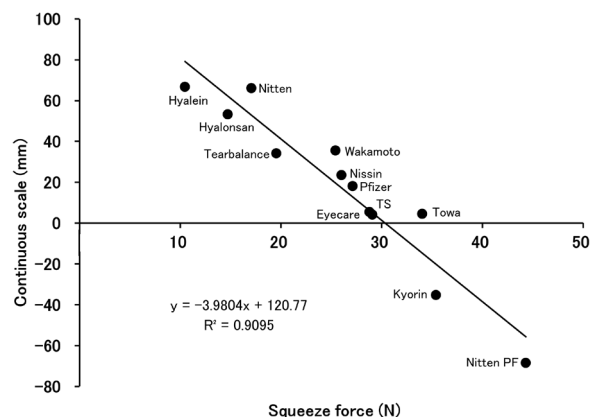


Figure 7. Correlation between continuous scale and squeeze force of various eye drops measured using Haplog[®] ($n = 8$).

container can influence the squeeze characteristics (15). Similarly, the squeeze force was reported to be affected by the material and hardness of the container, whereas the drop volume is affected by the surface tension of the eye drops and the opening diameter of the nozzle tip of the container (16). In addition, Wada *et al.* found a strong negative correlation between the squeeze characteristic of eye drops and subjective ease of extrusion (6). We found that the average maximum squeeze force of each of the eye drops using HapLog[®] and DF was 10.5 N and 12.2 N for Hyalein, respectively, whereas Eyecare (34.0 N and 15.5 N), Kyorin (35.4 N and 20.8 N), TS (28.8 N and 9.3 N), Towa (29.1 N and 8.2 N), and Nitten PF (44.3 N and 25.0 N) showed 1.7- to 3.5-fold differences between HapLog[®] and DF. These differences may be due to the difference in the measurement method; HapLog[®] was sandwiched between the surfaces of the fingers, whereas the eye drop container was sandwiched by "points" using the DF with hemispherical urethane spherical compression jig. Moreover, the products that require high squeeze power to instill eye drops may be considered undesirable, and Kyorin and Nitten PF showed high squeeze force values. Nitten PF is a formulation that does not contain any preservative, and is available in a special eye drop container that drops a chemical solution through a membrane filter in order to prevent bacterial contamination. The drug solution may be more resistant when passing through the membrane filter compared with the hardness of the container (17), and may be the reason behind the high squeeze force value of Nitten PF. Therefore, when changing from other products to Nitten PF, it is necessary to inform the patient that the drug solution is more difficult to instill from the container due to absence of preservatives; in general, it is important to accurately convey the characteristics of each product to the patient.

Hyodo *et al.* investigated differences in the squeeze force required for eye drops and the time required for instillation of glaucoma eye drops, and found that the average maximum squeeze force and average drip time affected the usability of eye drops (18,19). Additionally, Doi *et al.* reported that Azorga[®] combination ophthalmic suspension (Novartis Pharma Co., Ltd., Tokyo, Japan) affects the subjective ease of use (*i.e.* feeling of use) of eye drops (20). Therefore, we conducted a questionnaire survey on the "feeling of use" of 12 types of eye drops using HapLog[®], and found a negative correlation with the 6-point scale and the continuous scale ($R^2 = 0.8937$ and 0.9095 , Pearson's correlation coefficient -0.945359 and -0.953684 , respectively). Furthermore, the results of both scales were almost equivalent: Hyalein (6.0 and 66.8, respectively) > Nitten (5.5 and 66.1) > Hyalonsan (5.3 and 53.3) > Tearbalance (5.1 and 34.1) > Wakamoto (4.8 and 35.6) > Nissin (4.4 and 23.5) > Pfizer (4.3 and 18.1) > Eyecare (3.9 and 5.4) > TS (3.6 and 4.1) \approx Towa (3.1 and 4.5) > Kyorin (2.3 and -35.3) > Nitten (1.4 and -68.4). In particular, the evaluations for Kyorin

(2.3 and -35.3) and Nitten PF (1.4 and -68.4) were significantly lower than that for Hyalein (6.0 and 66.8) (Figures 6 and 7). As the 6-point scale and continuous scale yielded comparable results, the squeeze force was inversely correlated with the "feeling of use" (ease of eye drops) regarding the "usability" of each preparation. Furthermore, for patients using Hyalein, it seems that generic drugs (such as Nitten, Hyalonsan and Tearbalance) with similar "feelings of use" may be recommended without any sense of incongruity.

In our study, we confirmed that the squeeze force required for instillation varies depending on the container and the patient. In addition, in regards to instillation, a greater force of the finger was required when instilling with HapLog[®] compared with DF. Currently, there are a wide variety of eye drops available in the market; if the pharmacist understands the "usage" differences between the brand name and the generic products, they may be able to make appropriate eye drop recommendations that meet the needs of patients that are taking medication.

Acknowledgements

The authors wish to thank Ms. Misaki Ishida for providing technical assistance during the experimentation. The authors also wish to thank the Frontier Science Business Division of Shiseido Co., Ltd. (Tokyo, Japan) for supplying HapLog[®].

References

1. Ministry of Health, Labour and Welfare, about promoting the use of generic drugs, <https://www.mhlw.go.jp/seisaku/2012/03/01.html> (accessed January 9, 2020).
2. Ministry of Health, Labour and Welfare, about the change to the generic medicine of the medicine listed in the prescription (March 5, 2012 Hoken 0305 No. 12). <https://www.mhlw.go.jp/bunya/iryohoken/iryohoken15/dl/tuuchi1-4.pdf#search=%27%E4%B8%80%E8%88%AC%E5%90%8D%E5%87%A6%E6%96%B9%E6%8E%A8%E9%80%B2+%E5%8E%9A%E7%94%9F%E5%8A%B4%E5%83%8D%E7%9C%81%27> (accessed January 9, 2020).
3. Nakajima M, Wada Y, Shimokawa K, Ishii F. Comparative study of medical expenses between generic and switch OTC drugs: Ophthalmic solution containing sodium cromoglicate. *Jpn J Commun Pharm.* 2016; 4:23-33. (in Japanese)
4. Sugawara H, Shimamori Y, Yoshimachi S, Gotou T, Hayase Y. Comparative study of medical cost about generic drugs use promotion of eye drops. *Jpn J Drug Inform.* 2012; 14:62-68. (in Japanese)
5. Kuramoto M, Higami T, Takahashi Y, Higaki A, Yamashita N, Gouda S, Adachi A, Muro C, Hashimoto H, Hamaguchi T, Kadobayashi M. Study on the usability of ophthalmic solutions (I): The variation in squeezing force and drop volume. *J Jpn Soc Pharm Health Sci.* 2004; 30:13-19. (in Japanese)
6. Wada Y, Nozawa M, Goto M, Shimokawa K, Ishii F. Generic selection criteria for safety and patient benefit

- [III] Comparing the pharmaceutical properties and patient usability of original and generic ophthalmic solutions containing timolol maleate. *J Jpn Soc Pharm Health Sci.* 2015; 41:394-403. (in Japanese)
7. Nakatani M, Kawazoe T. Haptic Skill Logger (HapLog): The wearable sensor for evaluating haptic behaviors. *J Robotics Soc Jpn.* 2012; 30:499-501. (in Japanese)
 8. Pharmaceuticals and Medical Devices Agency (PMDA) (Tokyo, Japan). <https://www.pmda.go.jp/> (accessed January 9, 2020).
 9. Nozawa M, Goto M, Wada Y, Kumazawa M, Shimokawa K, Ishii F. Generic selection criteria for safety and patient benefit [VII]: Comparing the physicochemical and pharmaceutical properties of brand-name and generic terbinafine hydrochloride cream. *Drug Discov Ther.* 2018; 12:16-20.
 10. Yanai H. 4 Steps Excel Statistics (4rd Edition), OMS Publishing, Saitama Japan 2015. (in Japanese)
 11. Kawashima Y. Eye drop container and 1 drop volume. *Recipe plus.* 2019; 17:72. (in Japanese)
 12. Nagai N, Ito Y, Okamoto N, Shimomura Y. An in vitro evaluation for corneal damages after instillation of eye drops using rat debrided corneal epithelium: changes in corneal damage of benzalkonium chloride by addition of thickening agent. *Yakugaku Zasshi.* 2012; 132:837-843. (in Japanese)
 13. Nagai N, Murao T, Ito Y, Okamoto N. Effect of polysorbate 80 and ethylenediaminetetraacetic acid (EDTA) instillation on corneal wound healing in rat debrided corneal epithelium. *J Eye.* 2010; 27:1299-1302. (in Japanese)
 14. Yoshikawa K, Yamada H. Drop volume, rigidity and required squeezing force of glaucoma ophthalmic solution containers. *Clin Ophthalmol.* 2002; 56:1587-1593. (in Japanese)
 15. Murakami M, Ohta C, Yasuda M, Amano M. Comparative evaluation of the pharmaceutical properties of original and generic betamethasone ophthalmic solution. *Jpn J Drug Inform.* 2019; 20:227-231. (in Japanese)
 16. Ochiai A, Iida K, Kato Y, Danjo K. Design of an eye drop container for glaucoma eye drops considering, its usability by patients: evaluation of factors affecting squeezing strength and drop volume. *J Pharm Sci Tech.* 2012; 72:312-317. (in Japanese)
 17. Nitten Pharmaceutical Co., Ltd. Home page, About PF eye drops, <https://www.nitten-eye.co.jp/documents/pf/> (accessed January 9, 2020).
 18. Hyodo R, Hayashi Y, Mizoue S, Kawasaki S, Yoshikawa K, Ohashi Y. Glaucoma eyedrop usability evaluation by tactile pressure sensor. *J Eye.* 2010; 27:99-104. (in Japanese)
 19. Hyodo R, Hayashi Y, Mizoue S, Miyata K, Kamao T, Yoshikawa K, Ohashi Y. Effect of squeezing pressure and dropping time on eyedrop container usability. *J Eye.* 2011; 28:1050-1054. (in Japanese)
 20. Doi N, Maida C, Takahashi E, Ide M, Miyamoto E, Akiyama S. Influences of eye drop containers on the subjective usability of a high-viscosity eye drop suspension (Azorga® combination ophthalmic suspension). *J Jpn Soc Pharm Health Sci.* 2018; 44:380-392. (in Japanese)

Received January 14, 2020; Revised February 19, 2020;
Accepted February 22, 2020

*Address correspondence to:

Fumiyoshi Ishiii, Department of Self-medication and Health Care Sciences, Meiji Pharmaceutical University, 2-522-1, Noshio, Kiyose, Tokyo 204-8588, Japan
E-mail: fishii@my-pharm.ac.jp

Pulse wave transit time during exercise testing reflects the severity of heart disease in cardiac patients

Yuta Takayanagi¹, Akira Koike^{2,3,*}, Hiroshi Kubota⁴, Longmei Wu³, Isao Nishi⁵, Akira Sato³, Kazutaka Aonuma³, Yasushi Kawakami¹, Masaki Ieda³

¹ Department of Clinical Laboratory, University of Tsukuba Hospital, Tsukuba, Japan;

² Medical Science, Faculty of Medicine, University of Tsukuba, Tsukuba, Japan;

³ Department of Cardiology, Faculty of Medicine, University of Tsukuba, Tsukuba, Japan;

⁴ Master's Program in Medical Sciences, Graduate School of Comprehensive Human Sciences, University of Tsukuba, Tsukuba, Japan;

⁵ Department of Cardiology, Kamisu Clinical Education and Training Center, University of Tsukuba, Kamisu, Japan.

SUMMARY The pulse wave transit time (PWTT) is easily measured as the time from the R wave of an electrocardiogram to the arrival of the pulse wave measured by an oxygen saturation monitor at the earlobe. We investigated whether the change of PWTT during exercise testing reflects cardiopulmonary function. Eighty-nine cardiac patients who underwent cardiopulmonary exercise testing (CPX) were enrolled. We analyzed the change of PWTT during exercise and the relationship between the shortening of the PWTT and CPX parameters. PWTT was significantly shortened from rest to peak exercise (204.6 ± 33.6 vs. 145.6 ± 26.4 msec, $p < 0.001$) in all of the subjects. The patients with heart failure had significantly higher PWTT at peak exercise than the patients without heart failure (152.7 ± 27.1 vs. 140.4 ± 24.8 msec, $p = 0.031$). The shortening of PWTT from rest to peak exercise showed significant positive correlations with the peak O₂ uptake (VO₂) ($r = 0.56$, $p < 0.001$), anaerobic threshold ($r = 0.40$, $p = 0.016$), and % increase of systolic blood pressure during exercise ($r = 0.75$, $p < 0.001$), and a negative correlation with the slope of the increase in ventilation versus the increase in CO₂ output (VE-VCO₂ slope) ($r = -0.42$, $p = 0.010$) in the patients with heart failure. PWTT was shortened during exercise as the exercise intensity increased. In the patients with heart failure, the shortening of PWTT from rest to peak exercise was smaller in those with lower exercise capacity and those with higher VE-VCO₂ slope, an established index known to reflect the severity of heart failure.

Keywords Pulse wave transit time, exercise testing, cardiopulmonary function

1. Introduction

The pulse wave transit time (PWTT) is the time from the electrocardiogram R wave to the arrival of the pulse wave measured by an oxygen saturation monitor at the earlobe. PWTT is thought to be at least partly related to cardiovascular function, as it has been reported to shorten when the blood pressure rises (1,2). As a parameter that can be easily and continuously measured, PWTT has the potential to serve as a useful clinical tool for identifying changes in cardiovascular function, especially during exercise. Little is known, however, about the change of PWTT during exercise or the relation of that change to cardiopulmonary function.

Cardiopulmonary exercise testing (CPX) is one of the most useful clinical tools for evaluating the

severity of disease and the limitations of physical activities in cardiac patients (3). Among the parameters obtained from CPX, the peak oxygen uptake (VO₂) noninvasively reflects maximal cardiac output during exercise and is accordingly considered a strong prognostic factor and gold standard for selecting patients for cardiac transplantation (4,5). The slope of the increase in ventilation (VE) versus the increase in CO₂ output (VCO₂) during exercise (VE-VCO₂ slope) is another important parameter for evaluating the severity of heart failure (6).

In the present study we compared PWTT at rest, at anaerobic threshold (AT), and at peak exercise between patients with and without heart failure. We also evaluated the relation of the change of PWTT during exercise with the established CPX indices.

2. Methods

2.1. Study subjects

This is the retrospective study. The subjects for this study were 103 consecutive cardiac patients who underwent CPX for evaluation of exercise capacity and/or severity of cardiac disease at the University of Tsukuba Hospital between March 2017 and April 2018. Fourteen of the subjects were excluded because the PWTT at peak exercise could not be measured. In total, 89 subjects were selected (Table 1). The etiologies of heart disease in the cardiac patients were valvular heart disease in 28 patients, congenital heart disease in 25, coronary artery disease in 19, idiopathic dilated cardiomyopathy in 6, arrhythmia in 5, and other cardiac disease in 6. Thirty-eight of the patients had heart failure categorized as New York Heart Association class II or III. The protocol was approved by the Institutional Review Board of the University of Tsukuba Hospital. All of the subjects gave their informed consent to perform CPX.

2.2. Exercise testing and respiratory gas analysis

An incremental symptom limited exercise test was performed using an upright, electromagnetically braked cycle ergometer (Strength Ergo 8; Mitsubishi Electric Engineering Co., Ltd., Tokyo, Japan). The exercise test began with 4 minutes of rest on the ergometer followed by 4 minutes of warm-up at 0 or 20 W at 50 rpm. The load was then increased by 1 W every 6 seconds (10 W/min).

VO_2 , VCO_2 , and VE were measured throughout the test using an Aeromonitor AE-300s (Minato Medical Science, Osaka, Japan). The Aeromonitor AE-300s consists of a microcomputer, a hot wire flowmeter, and a gas analyzer composed of a sampling tube, filter, suction pump, infrared CO_2 analyzer, and O_2 analyzer equipped with a paramagnetic oxygen cell. The VO_2 and VCO_2 were calculated breath-by-breath based on the mathematical analysis described by Beaver *et al.* (7). The time alignment between the concentration and flow was performed based on the time delays of the O_2 and CO_2 analyzers (the flow delay from the sampling site to the analyzer plus the response time of the analyzer) (8). Before the parameters from the respiratory gas analysis were calculated, the breath-by-breath data were interpolated to give second-by-second values. These second-by-second values were then calculated as successive 3-second averages, and the averages were translated into a 5-point moving average.

The peak VO_2 was calculated as the average of the values obtained during the last 15 seconds of incremental exercise. The percentage of peak VO_2 was calculated by dividing the measured peak VO_2 by the predicted peak VO_2 . The predicted peak VO_2 was determined on

the basis of a normal Japanese population (9). The VE- VCO_2 slope during incremental exercise was calculated from the start of incremental exercise to the respiratory compensation point by least-squares linear regression, as previously described (5). The AT was determined by V-slope analysis (10). The ratio of the increase in VO_2 to the increase in the work rate ($\Delta\text{VO}_2/\Delta\text{WR}$) was calculated by least-squares linear regression from the data recorded from 30 seconds after the start of incremental exercise to 30 seconds before the end of exercise (5).

2.3. Analysis of the PWTT

Figure 1 demonstrates the measurement of PWTT. PWTT was measured using an electrocardiograph (STS 2100; NIHON KOHDEN, Tokyo, Japan) and oxygen saturation monitor attached to the earlobe. PWTT was defined as the interval from the R wave of the electrocardiogram to the arrival of the pulse wave measured by an oxygen saturation monitor at the earlobe. PWTT was continuously measured from rest to the end of the exercise test as the average of the previous 64 beats, and sampled every 15 seconds. The shortening of PWTT was expressed as a percentage of the decrease in PWTT at peak exercise versus that at rest.

2.4. Statistical analysis

Data are presented as the mean \pm S.D. Intergroup differences for variables were compared by the unpaired *t* test or the Fisher's exact test where appropriate. The linear regression analysis was used to correlate the measured variables. All analyses were performed using SPSS version 22.0 software (SPSS Inc., Chicago, Illinois). A *p* value < 0.05 was considered statistically significant for all comparisons.

3. Results

The cardiopulmonary parameters of the study patients are shown in Table 2. The patients with heart failure had significantly higher brain natriuretic peptide than the patients without heart failure. In the comparison of CPX parameters between the two groups, the patients with heart failure had significantly lower values of peak VO_2 (16.5 ± 4.3 vs. 22.7 ± 4.3 mL/min/kg, $p < 0.001$), AT (12.5 ± 2.6 vs. 15.4 ± 3.1 mL/min/kg, $p < 0.001$), and $\Delta\text{VO}_2/\Delta\text{WR}$ (9.1 ± 2.0 vs. 10.4 ± 1.4 mL/min/W, $p = 0.002$), and a significantly higher value of VE- VCO_2 slope (34.6 ± 5.8 vs. 29.8 ± 4.2 , $p < 0.001$).

Figure 2 shows the PWTT at rest, AT, and peak exercise in the study patients. When analyzed in the whole study population, PWTT was significantly shortened from rest to AT (204.6 ± 33.6 vs. 169.5 ± 31.4 msec, $p < 0.001$), and from AT to peak ($169.5 \pm$

Table 1. Clinical characteristics of the study patients

Characteristics	All Patients (n = 89)	Patients with HF (n = 38)	Patients without HF (n = 51)	p value
Male/Female	45/44	18/20	27/24	0.380
Age (years)	53.3 ± 21.9	59.8 ± 21.1	48.4 ± 21.4	0.014
Height (cm)	160.2 ± 8.3	159.1 ± 7.9	161.1 ± 8.6	0.460
Weight (kg)	59.9 ± 11.6	59.8 ± 11.8	60.0 ± 11.7	0.909
BMI (kg/m ²)	23.2 ± 3.6	23.6 ± 4.1	23.0 ± 3.2	0.774
Etiology				
Valvular disease	28 (31.5)	8 (21.1)	20 (39.2)	0.105
Congenital heart disease	25 (28.1)	7 (18.4)	18 (35.3)	0.098
Coronary artery disease	19 (21.3)	12 (31.6)	7 (13.7)	0.066
Idiopathic dilated cardiomyopathy	6 (6.7)	6 (15.8)	0	0.005
Arrhythmia	5 (5.6)	0	5 (9.8)	0.069
Other cardiac disease	6 (6.7)	5 (13.2)	1 (2.0)	0.080
Complication				
Hypertension	44 (49.4)	23 (60.5)	21 (41.2)	0.088
Hyperlipidemia	30 (33.7)	16 (42.1)	14 (27.5)	0.177
Diabetes	25 (28.1)	16 (42.1)	9 (17.6)	0.017
Smokers	22 (24.7)	13 (34.2)	9 (17.6)	0.087
Chronic kidney disease	9 (10.1)	8 (21.1)	1 (2.0)	0.004
Creatinine	0.81 ± 0.25	0.90 ± 0.31	0.73 ± 0.15	0.006
Non-HDL cholesterol	130.3 ± 36.2	130.5 ± 36.1	130.0 ± 37.1	0.412
Rhythm				
Sinus	84 (94.4)	34 (89.5)	50 (98.0)	0.159
Atrial fibrillation	2 (2.2)	2 (5.3)	0	0.180
Pacing	3 (3.4)	2 (5.3)	1 (2.0)	0.573
Medication				
β-blockers	36 (40.4)	26 (68.4)	10 (19.6)	< 0.001
ACEI/ARB	41 (46.1)	25 (65.8)	16 (31.4)	0.001
Diuretics	30 (33.7)	22 (57.9)	8 (15.7)	< 0.001
Ca-channel blockers	23 (25.8)	16 (42.1)	7 (13.7)	0.003

Data are presented as the mean ± S.D. or No. (%) of patients unless otherwise indicated. HF, Heart failure; ACEI, Angiotensin converting enzyme inhibitor; ARB, Angiotensin receptor blocker.

Table 2. Cardiopulmonary parameters of the study patients

Characteristics	All Patients (n = 89)	Patients with HF (n = 38)	Patients without HF (n = 51)	p value
At rest				
BNP (pg/mL)	96.0 ± 132.8	145.0 ± 178.2	57.4 ± 59.1	0.006
LVEF (%)	62.3 ± 10.5	59.9 ± 10.6	64.1 ± 10.2	0.074
LVDd (mm)	46.6 ± 7.0	47.8 ± 6.4	45.8 ± 7.3	0.176
LVDs (mm)	31.0 ± 7.1	32.6 ± 7.3	30.0 ± 6.8	0.103
Heart rate (beats/min)	75.5 ± 13.0	74.9 ± 15.1	75.9 ± 11.4	0.723
Systolic blood pressure (mmHg)	133.9 ± 24.7	138.8 ± 30.0	130.3 ± 19.4	0.107
Diastolic blood pressure (mmHg)	76.0 ± 12.9	73.8 ± 12.7	77.7 ± 12.9	0.150
At Peak Exercise				
Work rate (W)	86.0 ± 32.2	69.8 ± 26.4	98.0 ± 31.0	< 0.001
Heart rate (beats/min)	135.6 ± 27.0	123.4 ± 27.1	144.6 ± 23.2	< 0.001
Systolic blood pressure (mmHg)	181.2 ± 33.8	170.2 ± 34.4	189.3 ± 31.3	0.008
Diastolic blood pressure (mmHg)	88.8 ± 16.4	83.7 ± 16.2	92.6 ± 15.7	0.011
R	1.14 ± 0.13	1.11 ± 0.14	1.15 ± 0.12	0.126
Peak VO ₂ (mL/min/kg)	20.0 ± 5.3	16.5 ± 4.3	22.7 ± 4.3	< 0.001
Peak VO ₂ (%)	78.2 ± 19.3	64.7 ± 14.6	88.3 ± 15.9	< 0.001
VE-VCO ₂ slope	31.8 ± 5.4	34.6 ± 5.8	29.8 ± 4.2	< 0.001
AT (mL/min/kg)	14.2 ± 3.2	12.5 ± 2.6	15.4 ± 3.1	< 0.001
ΔVO ₂ /ΔWR (mL/min/W)	9.8 ± 1.8	9.1 ± 2.0	10.4 ± 1.4	0.002
PWTT				
Rest (ms)	204.6 ± 33.6	202.9 ± 37.4	205.8 ± 30.8	0.687
AT (ms)	169.5 ± 31.4	171.7 ± 34.4	167.7 ± 29.0	0.570
Peak (ms)	145.6 ± 26.4	152.7 ± 27.1	140.4 ± 24.8	0.031
Shortening of PWTT (%)	28.3 ± 10.1	23.8 ± 11.2	31.6 ± 7.8	< 0.001

Data are presented as the mean ± S.D. or No. (%) of patients unless otherwise indicated. BNP, brain natriuretic peptide; LVDd, left ventricular diastolic dimension; LVDs, left ventricular systolic dimension; LVEF, left ventricular ejection fraction; R, gas exchange ratio; VO₂, O₂ uptake; VE, minute ventilation; VCO₂, CO₂ output; AT, anaerobic threshold.

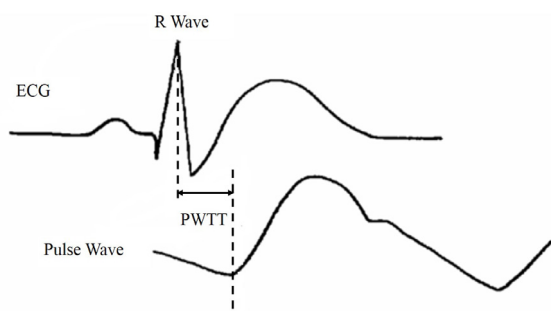


Figure 1. The pulse wave transit time (PWTT) was calculated as the interval from the R wave of the electrocardiogram (ECG) to the arrival of the pulse wave measured by an oxygen saturation monitor at the earlobe.

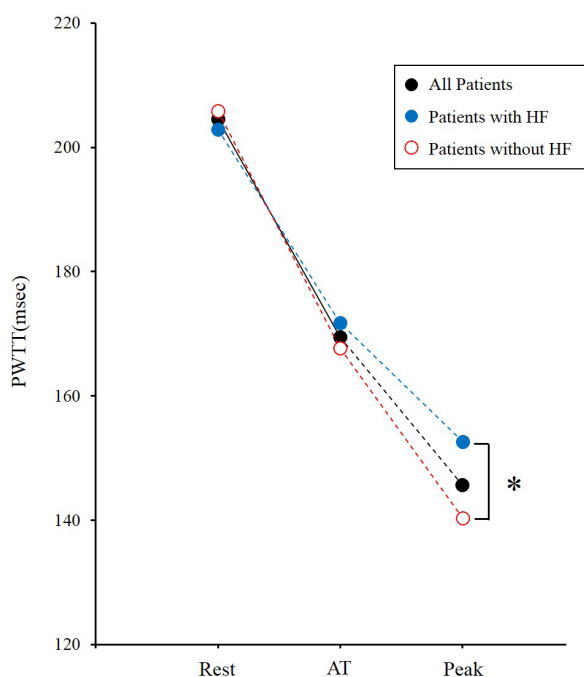


Figure 2. Comparisons of the pulse wave transit time (PWTT) at rest, anaerobic threshold (AT), and peak exercise among the study patients. * $p < 0.05$ compared between the patients with heart failure (HF) and patients without HF.

31.4 vs. 145.6 ± 26.4 msec, $p < 0.001$). There were no significant differences in PWTT at rest or in AT between the patients with and without heart failure. The patients with heart failure, however, had significantly higher PWTT at peak exercise (152.7 ± 27.1 vs. 140.4 ± 24.8 msec, $p = 0.031$). The degree to which PWTT was shortened from rest to peak exercise was significantly lower in the patients with heart failure than in the patients without heart failure (23.8 ± 11.2 vs. $31.6 \pm 7.8\%$, $p < 0.001$).

Figure 3 shows the correlations between the CPX indices and the shortening of the PWTT from rest to peak exercise in the patients with heart failure. The shortening of the PWTT showed significant positive correlations with the peak VO_2 ($r = 0.56$, $p < 0.001$) and AT ($r = 0.40$, $p = 0.016$), and a negative correlation

with the VE-VCO_2 slope ($r = -0.42$, $p < 0.010$). The shortening of PWTT showed a significant positive correlation with the % increase in systolic blood pressure ($r = 0.75$, $p < 0.001$).

4. Discussion

The PWTT was significantly shortened as the exercise intensity increased in the cardiac patients enrolled in this study. The patients with heart failure had significantly higher PWTT at peak exercise than the patients without heart failure. The shortening of PWTT from rest to peak exercise showed positive correlations with the peak VO_2 , AT, and % increase in systolic blood pressure, and a negative correlation with the VE-VCO_2 slope, indicating a lesser degree of shortening of PWTT in patients with lower exercise capacity and/or lower cardiopulmonary function during exercise.

4.1. Parameters obtained from CPX

The peak VO_2 generally reflects the maximal cardiac output during exercise. The peak VO_2 has been used as the main parameter of exercise capacity. The AT represents the highest level of VO_2 that a subject can perform without developing sustained lactic acidosis. The lower AT in cardiac patients signifies that the exercise-induced lactic acidosis occurs at a lower intensity of exercise (11,12). The $\Delta\text{VO}_2/\Delta\text{WR}$ is mainly determined by the rate of the increase in cardiac output during incremental exercise. In normal subjects, the $\Delta\text{VO}_2/\Delta\text{WR}$ is approximately 10 mL/min/W, and a lower $\Delta\text{VO}_2/\Delta\text{WR}$ implies impaired response of cardiac output during exercise (13). The VE-VCO_2 slope ranges approximately from 24 to 34 in normal subjects. The steeper VE-VCO_2 slope in heart failure patients mainly reflects high V/Q mismatch caused by reduced pulmonary blood flow (14). In the present study we found that the shortening of PWTT during exercise was lower in subjects with more advanced cardiopulmonary dysfunction, as reflected in a lower peak VO_2 , lower AT, lower $\Delta\text{VO}_2/\Delta\text{WR}$, and higher VE-VCO_2 slope.

4.2. Mechanisms of the shortening of PWTT during exercise

The oxygen demand in skeletal muscle during exercise becomes higher with increasing exercise intensity. In response, the blood pressure, heart rate, and cardiac output rise to meet the increased oxygen demand in skeletal muscle. PWTT, the time of the pulse wave from the heart to the periphery, can therefore be expected to shorten in step with the increasing cardiac output as the exercise intensity increases.

There was no significant difference in PWTT at rest between patients with and without heart failure in the present study. However, PWTT at peak exercise

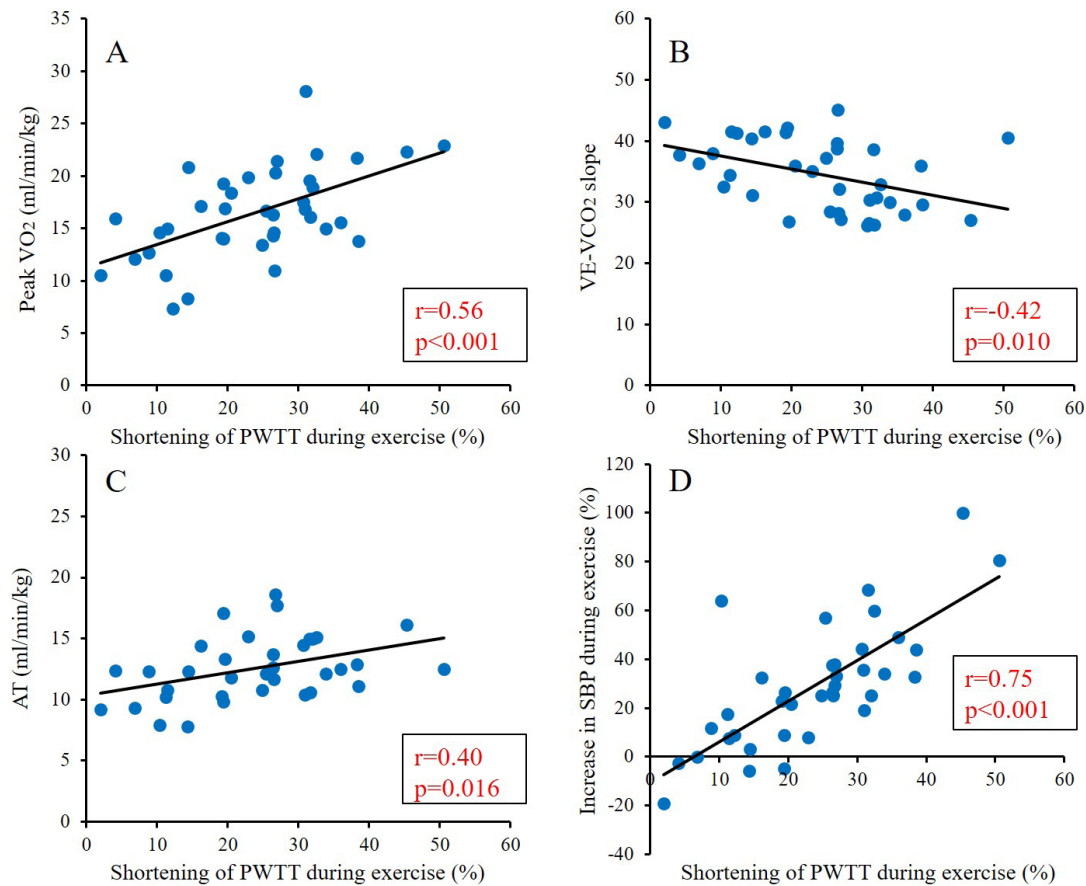


Figure 3. Peak O_2 uptake (VO_2) (panel A), slope of the increase in ventilation versus the increase in CO_2 output (VE- VCO_2 slope) (panel B), anaerobic threshold (AT) (panel C), and % increase in systolic blood pressure (SBP) during exercise (panel D) plotted against the shortening of the pulse wave transit time (PWTT) in the patients with heart failure.

was significantly higher, and the degree of shortening of PWTT during exercise was significantly lower, in the heart failure patients. The shortening of PWTT during exercise was positively correlated with the increase in systolic blood pressure during exercise. Therefore, we assume that the lesser degree of PWTT shortening in the heart failure patients was caused by the limited increase in cardiac output during exercise, as systolic blood pressure partly reflects cardiac output. An impaired increase in cardiac output during exercise can be attributed to factors such as the appearance of myocardial ischemia or a worsening of valvular disease. Increased afterload resulting from excessive activity of the sympathetic nervous system or impaired production of the nitric oxide due to the vascular endothelial dysfunction in cardiac patients must also impair cardiac contractility, thereby influencing cardiac output during exercise.

To our knowledge, the present study is the first report which evaluated the change of PWTT during exercise and its relation with the parameters reflecting cardiopulmonary function during exercise. Standard noninvasive technologies estimating cardiac output have major limitations with regard to the applicability during routine clinical care (15). Very recently, Sano *et al.* (16) found that the change in PWTT predicts

fluid responsiveness in mechanically ventilated anesthetized dogs given a fluid challenge. Suzuki *et al.* (17) also reported the usefulness of estimating cardiac output by PWTT at resting condition in patients after cardiovascular surgeries. Based on the findings of the recent reports and our study, monitoring of PWTT during exercise testing would provide noninvasive, and continuous estimate of cardiac output during exercise.

4.3. Limitations

PWTT during the whole period from rest to peak exercise could not be obtained in 13.6 % of the patients investigated in this study. The PWTT values were missing most often near the point of peak exercise, probably as consequence of noise in the electrocardiogram caused by body movement or failure of the adhesive used to attach the oxygen saturation monitor to the earlobe. In the present study, 2 patients with atrial fibrillation and 3 patients with a pacemaker were included. Although the PWTT could be clearly recorded in these subjects, there is the possibility that the PWTT measurement might be influenced by the presence of atrial fibrillation or pacemakers. The small number of patients in the study precluded any subgroup analysis to consider parameters such as heart

failure with reduced or preserved EF or the cardiac disease etiology. The patients with heart failure were more frequently prescribed medications that may have influenced the circulatory response, such as antihypertensive drugs and beta-blockers. The effects of these medications might be the reason for the higher exercise PWTT in the heart failure group compared to the non-heart failure group. Therefore, the consideration to choose a research design that can exclude the effects of these medications would have been desirable.

4.4. Future directions

Monitoring of PWTT during exercise testing might be useful as a noninvasive estimate of cardiac output during exercise. Further study in a larger population of cardiac patients will be needed to establish the clinical significance of PWTT during exercise.

4.5. Conclusions

PWTT was shortened during exercise as the exercise intensity increased. In the patients with heart failure, the shortening of PWTT from rest to peak exercise was smaller in those with lower exercise capacity and those with higher VE-VCO₂ slope, an established index known to reflect the severity of heart failure.

Acknowledgements

We thank for the support and encouragement from Department of Clinical Laboratory, University of Tsukuba Hospital.

References

1. Wippermann CF, Schranz D, Huth RG. Evaluation of the pulse wave arrival time as a marker for blood pressure changes in critically ill infants and children. *J Clin Monit.* 1995; 11:324-328.
2. Ochiai R, Takeda J, Hosaka H, Sugo Y, Tanaka R, Soma T. The relationship between modified pulse wave transit time and cardiovascular changes in isoflurane anesthetized dogs. *J Clin Monit Comput.* 1999; 15:493-501.
3. Balady GJ, Arena R, Sietsema K, *et al.* Clinician's guide to cardiopulmonary exercise testing in adults: A scientific statement from the American Heart Association. *Circulation.* 2010; 122:191-225.
4. Mancini DM, Eisen H, Kussmaul W, Mull R, Edmunds LH, Wilson JR. Value of peak exercise oxygen consumption for optimal timing of cardiac transplantation in ambulatory patients with heart failure. *Circulation.* 1991; 83:778-786
5. Koike A, Itoh H, Kato M, Sawada H, Aizawa T, Fu LT, Watanabe H. Prognostic power of ventilatory responses during submaximal exercise in patients with chronic heart disease. *Chest.* 2002; 121:1581-1588.
6. Chua TP, Ponikowski P, Harrington D, Anker SD, Webb-Peploe K, Clark AL, Poole-Wilson PA, Coats AJ. Clinical correlates and prognostic significance of the ventilatory response to exercise in chronic heart failure. *J Am Coll Cardiol.* 1997; 29:1585-1590.
7. Beaver WL, Wasserman K, Whipp BJ. On-line computer analysis and breath-by-breath graphical display of exercise function tests. *J Appl Physiol.* 1973; 34:128-132.
8. Sue DY, Hansen JE, Blais M, Wasserman K. Measurement and analysis of gas exchange during exercise using a programmable calculator. *J Appl Physiol.* 1980; 49:456-461.
9. Itoh H, Koike A, Taniguchi K, Marumo F. Severity and pathophysiology of heart failure on the basis of anaerobic threshold (AT) and related parameters. *Jpn Circ J.* 1989; 53:146-154.
10. Wasserman K. New concepts in assessing cardiovascular function. *Circulation.* 1988; 78:1060-1071.
11. Matsumura N, Nishijima H, Kojima S, Hashimoto F, Minami M, Yasuda H. Determination of anaerobic threshold for assessment of functional state in patients with chronic heart failure. *Circulation.* 1983; 68:360-367.
12. Koike A, Hiroe M, Adachi H, Yajima T, Nogami A, Ito H, Takamoto T, Taniguchi K, Marumo F. Anaerobic metabolism as an indicator of aerobic function during exercise in cardiac patients. *J Am Coll Cardiol.* 1992; 20:120-126.
13. Cohen-Solal A, Chabernaude JM, Gourgon R. Comparison of oxygen uptake during bicycle exercise in patients with chronic heart failure and in normal subjects. *J Am Coll Cardiol.* 1990; 16:80-85.
14. Metra M, Dei Cas L, Panina G, Visioli O. Exercise hyperventilation in chronic congestive heart failure, and its relation to functional capacity and hemodynamics. *Am J Cardiol.* 1992; 70:622-628.
15. Saugel B, Cecconi M, Hajjar LA. Noninvasive Cardiac Output Monitoring in Cardiothoracic Surgery Patients: Available Methods and Future Directions. *J Cardiothorac Vasc Anesth.* 2019; 33:1742-1752.
16. Sano H, Fujiyama M, Wightman P, Cave NJ, Gieseg MA, Johnson CB, Chambers P. Investigation of percentage changes in pulse wave transit time induced by mini-fluid challenges to predict fluid responsiveness in ventilated dogs. *J Vet Emerg Crit Care (San Antonio).* 2019; 29:391-398.
17. Suzuki T, Suzuki Y, Okuda J, Minoshima R, Misonoo Y, Ueda T, Kato J, Nagata H, Yamada T, Morisaki H. Cardiac output and stroke volume variation measured by the pulse wave transit time method: a comparison with an arterial pressure-based cardiac output system. *J Clin Monit Comput.* 2019; 33:385-392.

Received October 24, 2019; Revised December 24, 2019; Accepted February 3, 2020

*Address correspondence to:

Dr. Akira Koike, Faculty of Medicine, University of Tsukuba, 1-1-1, Tennodai, Tsukuba, Ibaraki 305-8575, Japan.
E-mail: koike@md.tsukuba.ac.jp

Released online in J-STAGE as advance publication February 17, 2020.

Development of an algorithm using ultrasonography-assisted peripheral intravenous catheter placement for reducing catheter failure

Chiho Kanno¹, Ryoko Murayama^{2,3}, Mari Abe-Doi², Toshiaki Takahashi⁴, Yui Shintani¹, Junko Nogami⁵, Chieko Komiyama⁵, Hiromi Sanada^{1,3,*}

¹Department of Gerontological Nursing/Wound Care Management, Graduate School of Medicine, The University of Tokyo, Tokyo, Japan;

²Department of Advanced Nursing Technology, Graduate School of Medicine, The University of Tokyo, Tokyo, Japan;

³Global Nursing Research Centre, Graduate School of Medicine, The University of Tokyo, Tokyo, Japan;

⁴Department of Life Support Technology (Molten), Graduate School of Medicine, The University of Tokyo, Tokyo, Japan;

⁵The University of Tokyo Hospital, Tokyo, Japan.

SUMMARY Up to 50% peripheral intravenous catheters (PIVs) are removed prematurely because of failures. Catheter failure (CF) leads to replacement and is a great concern for patients and medical staff. It is known that visualization of catheters and vessels with ultrasonography (US) during placement prevents CF. However, US is not a common technique for general nurses. In order to standardize US-assisted PIV placement techniques, an algorithm is needed. This study aimed to develop an algorithm using US-assisted PIV placement to reduce CF rate. Furthermore, to evaluate the effectiveness of the algorithm, CF rates were compared before and after intervention. A pretest-posttest study was performed. The intervention was PIV placement by 23 nurses undergoing training sessions for the algorithm. Intention to treat, per protocol analyses were applied. Logistic regression analysis was used for factor analysis. The CF rate in the pre-intervention group 35.2% (19/54) did not significantly differ from post-intervention group 33.6% (48/143) ($p = 0.831$), yet significantly differ from complete algorithm-use group 8.7% (2/23; $p = 0.017$). In factor analysis, compliance to the algorithm was significantly correlated with CF ($p = 0.032$). The compliance rate was low 16.1% (23/143). Algorithm compliance reduced CF by confirming appropriate catheter tip position from the insertion to the securement phase. This algorithm effectively reduced CF, however, the compliance rate was unacceptable. In order to increase the compliance rate, modified algorithm and new visualizing technology is required.

Keywords Algorithm, incidence, intention to treat analysis, per protocol analysis, rate of compliance

1. Introduction

Peripheral intravenous catheters (PIVs) are used in > 60% of hospital inpatients (1). Approximately 30-50% of PIVs require removal due to complications prior to the completion of infusion therapy; this phenomenon is called catheter failure (CF) (2). CF is defined as "PIV that has been removed due to the signs and symptoms of catheter failure, but not for other reasons such as accidental dislodgement" (3). Catheter replacement can lead to distress and discomfort, substantially increasing clinical staff workloads and medical costs (4). CF is a serious problem for patients who undergo infusion therapy and clinical staff; thus, it should be prevented.

CF is affected by patient, chemical, and mechanical factors. Patient factors include age, female sex,

diabetes, cancer, infection, steroids, bedridden status, and malnutrition (3,5-8). Chemical factors include antibiotic use and hyperosmolar infusion (9,10). Infusion therapy standards of practice recommend the selection of a midline catheter or peripherally inserted central catheter depending on infusion therapy duration to reduce chemical effect.11 Mechanical factors are related to vessel wall irritation and include using too large a catheter for the vasculature, multiple punctures of the same site, and use of a stiff catheter (5,12,13).

Our previous study confirmed the efficacy of a care bundle which was focused on the above mechanical factors related to CF. The care bundle included the use of polyurethane material catheters, selection of a vessel with a diameter of approximately 3.3 times the diameter of the catheter, and adjustment of the catheter

tip position to prevent vessel wall irritation, using ultrasound guidance to confirm catheter tip position within the vessel. The study using the above care bundle revealed low incidence rate of CF, which was 11% in the intervention group versus 30% in the control group (14). This suggested that reducing mechanical irritation prevented CF substantially. Ultrasonography (US) operation was provided by one trained research nurse in that study. However, in current clinical settings, use of US is not a common technique for general nurses. The acquisition of new skills should be standardized; therefore, in the present study, we focused on developing an algorithm to standardize the teaching of US-assisted PIV placement skills.

Algorithms apply evidence to specific behaviors and rules to promote effective and appropriate medical care (15). Conventional algorithms for US-guided PIV insertion were developed to increase the insertion success rate in patients with difficult intravenous access (16,17). However, none of the previous algorithms prevents the incidence of CF. The algorithm developed for the present study, which enables clinical nurses to confirm the appropriateness of the catheter position from the insertion to the securement phase, might be required to decrease the incidence of CF.

The present study aimed to develop an algorithm that enables general nurses to acquire the US-assisted PIV placement skills to prevent CF. Furthermore, to evaluate the effectiveness of the algorithm, CF rates were compared before and after intervention.

2. Methods

2.1. Algorithm

The algorithm was developed to avoid mechanical stimulation and decrease the incidence of CF. The first step of the algorithm development process is verbalizing an outline of US-assisted PIV placement: infusion therapy (situation), patient (subject), catheter placement under US guidance (procedure), and tracking of adverse events and correspondence. The second step systematizing each of the above outline items. The final step is creating graphical representations of the items. Eventually, we developed the algorithm.

A literature review was conducted using MEDLINE and the Japan Medical Abstracts Society to identify evidence of the US-guided PIV placement technique.

The developed algorithm consisted of four additional points to landmark insertion technique as follows: 1. Appropriate blood vessel: The clinical nurses succeed in selecting the vessel whose diameter was approximately 3.3 times the diameter of the catheter and storing the US images. 2. Appropriate insertion: The clinical nurses succeed in performing US-guided insertion when the target blood vessel was not palpable or visible with a tourniquet. 3. Needle in the blood

vessel: The clinical nurses need to verify that the needle is inside the blood vessel and adjust its position, as necessary. 4. Appropriate catheter tip position: The clinical nurses succeed in securing the catheter without any extra compression to the vessel wall and storing the US images (Figure 1).

We developed a training session for applying the algorithm. It is necessary for nurses to acquire the principle and basic knowledge of US, probe techniques, and US image interpretation. To acquire these knowledge and skills, workbook, e-learning, training lectures, and training practice were provided. After that, we confirmed that each of the nurses could use the algorithm in the objective structured clinical examination. During the training period, we provided the simulator and US devices to allow the nurses to practice at any time.

The algorithm and training session were developed under the supervision of an expert in fundamental nursing, an educator of nurse-designated procedures, and two certified dialysis nurses.

2.2. Study design and setting

This study was a pretest-posttest study and was undertaken in a surgical ward, in which the average daily number of PIV placement was high, at a large tertiary metropolitan hospital had 1228 beds in Tokyo, Japan

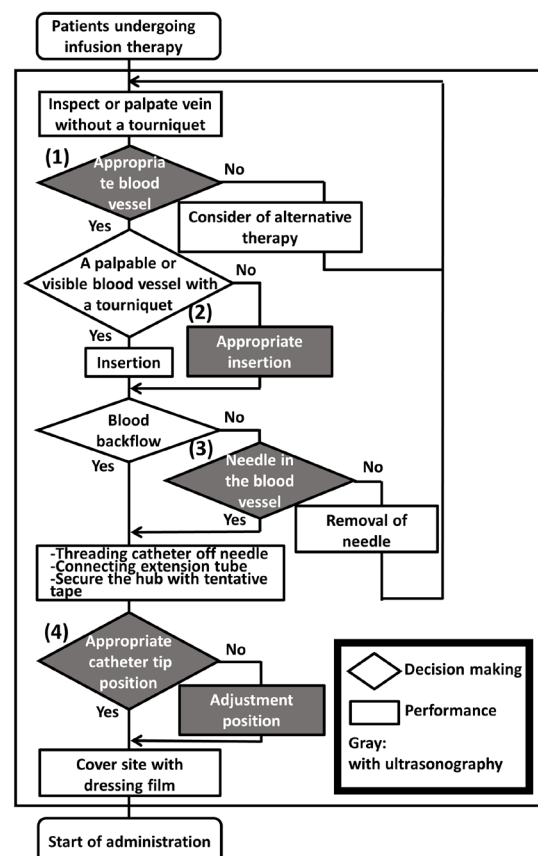


Figure 1. The algorithm using ultrasound-assisted peripheral intravenous catheter placement for reducing catheter failure.

between May 2018 and November 2018.

2.3. Participants

Nurses with > 1 year of experience with PIV placement in adults were eligible to enroll in the training session. Nurses without at least 6 months of continuous experience placing PIV in adults when this study started were excluded. Patients who underwent PIV therapy and had permission from their physician and nurses to participate were eligible to enroll. Patients who were < 20 years of age were excluded. Only PIVs which were inserted by nurses who had undergone the training on the algorithm for US-assisted PIV placement were analyzed.

2.4. Intervention

The intervention was PIV placement using the algorithm of the US-assisted PIV placement by the nurses who underwent the training session. This study included a 4-week pre-intervention period, a 4-week training period, a 10-week habituation period, and a 10-week post-intervention period. The tablet-type US device (SonoSite iViz, FUJIFILM SonoSite Inc., Bothell, US) equipped with liner-array transducers (6.4 MHz) was used to visualize the vessels and catheters.

2.5. Outcomes

The primary outcome was the cumulative incidence rate of CF, calculated as $\{[\text{incidence of CF}]/[\text{total PIVs}]\} \times 100$ (%), and the incidence rate of CF, calculated as $\{[\text{incidence of CF}]/[\text{total PIVs days}]\} \times 1,000$ (CF per 1000 catheter days). The incidence of CF was judged and recorded by the clinical nurse.

The secondary outcome was compliance to the algorithm. Compliance was assessed in accordance with 1. and 4. of the algorithm by one researcher as follows: the first point was 1. Appropriate blood vessel: We confirmed the blood vessels on the obtained images met the accomplishment threshold; and 4. Appropriate catheter tip position: We confirmed the positions on the obtained images met the accomplishment threshold.

2.6. Variables

Nurse characteristics (pre-intervention). We collected the following data about the nurses using a questionnaire: sex, age, years of experience, number of PIV insertions per week, experience level (beginner: < 100; intermediate: 100-800; expert: > 800) (18), experience with US-guided PIV placement, and academic background.

Patient and catheter characteristics (pre- and post-intervention). We collected the following data from the patients' medical records:

1) Patient factors: age, sex, body mass index (BMI),

presence or absence of organ cancer and/or diabetes, oral medicine (antimicrobials, steroids, anticoagulants, and antiplatelets), ambulatory status (KANGODO III and IV), blood examination (C-reactive protein [mg/dL], albumin [g/dL], and platelet [$10^4/\mu\text{L}$]).

2) Medication factors: infusion (hyperosmolality, antibiotic, lipid emulsion, anticoagulant). We collected the following data with observing PIV placement at the bedside.

3) Mechanical factors: material of PIV (Teflon: Surshield Surflo II, Terumo Corporation, Tokyo, Japan; polyurethane: Surflo V3 Plus, Terumo Corporation), PIV lock period, insertion site (forearm, upper arm, hand, cubital fossa), and first-attempt success rate.

2.7. Sample size

Sample sizes were calculated for a comparison test of two proportions: A sample size of 51 PIVs per group conferred 80% power and a two-sided p value of 0.05, to detect an effect size of 25% in the CF rates between the pre- and post-intervention groups. The effect size was determined according to a previous study (17). The number of nurses who would undergo the algorithm training and could perform the insertion were unknown prior to the commencement of the study. For that reason, we doubled our intended sample size, for a total of 102 PIVs. Furthermore, we expected attrition rates of 70%; thus, 140 PIVs was the final calculated sample size.

2.8. Statistical analyses

We performed both the intention to treat (ITT) analysis and per protocol (PP) analysis. Pre- and post-intervention groups were compared in the ITT analysis. For the PP analysis, we compared the pre-intervention group and the complete algorithm-use group. The complete algorithm-use group accomplished both 1. and 4. in the algorithm.

In the univariate model, Fisher's exact test or the chi-square test was used to examine the categorical data, while Student's t test or the Mann-Whitney U test was selected to examine continuous data. The incidence rates of CF per 1000 PIV days were tested with Log-rank test. Logistic regression was used to calculate odds ratios (ORs) and 95% confidence intervals (CIs) after controlling simultaneously for potential confounders of CF. The final multivariate model was built with the variables at p values of < 0.15 and were tested for multicollinearity. The covariates were simultaneously introduced in accordance with a previous study or empirically selected if correlation was indicated.

The statistical analysis was performed using IBM SPSS Statistics ver. 23 (SPSS Inc., Chicago, IL, USA) and EZR (Saitama Medical Center, Jichi Medical University, Saitama, Japan). P values < 0.05 were considered statistically significant.

2.9. Ethical considerations

This study received approval from the Research Ethics Committee of the Faculty of Medicine, The University of Tokyo (No. 11832-(3)). The participants were informed about the study aim and processes, and written informed consent was obtained from each participant. The participants were free to withdraw consent and discontinue participating at any time.

3. Results

3.1. Participant flow

Twenty-five nurses were recruited as participants. Two nurses withdrew consent; thus, 23 nurses were analyzed. Ninety one percent were female. The mean age and nursing experience year were 26 years (interquartile range (IQR), 24-28) and four years (IQR, 2-6) respectively. The mean number of PIV placement per week was 2 (IQR, 1-3). Half of the participants had

intermediate-level experience. None had experience in US-guided PIV placement.

In the pre-intervention group, 54 PIVs were analyzed. In the post-intervention group, 143 PIVs were inserted by clinical nurses who completed algorithm training; these were analyzed as the post-intervention group (Figure 2).

3.2. Incidence of CF and algorithm compliance

3.2.1. Intention-to-treat analysis

The incidence of CF rate as the primary outcome was 35.2% (19/54) in the pre-intervention and 33.6% (48/143) in the post-intervention group. There was no significant intergroup difference in CF ($p = 0.831$). The incidence of CF from the intention-to-treat analysis was 99.9 per 1,000 PIV days compared with 146.7 per 1,000 PIV days in the pre-intervention group ($p = 0.214$; Table 1).

There were significant differences in patient characteristics, catheter usage, and catheter characteristics,

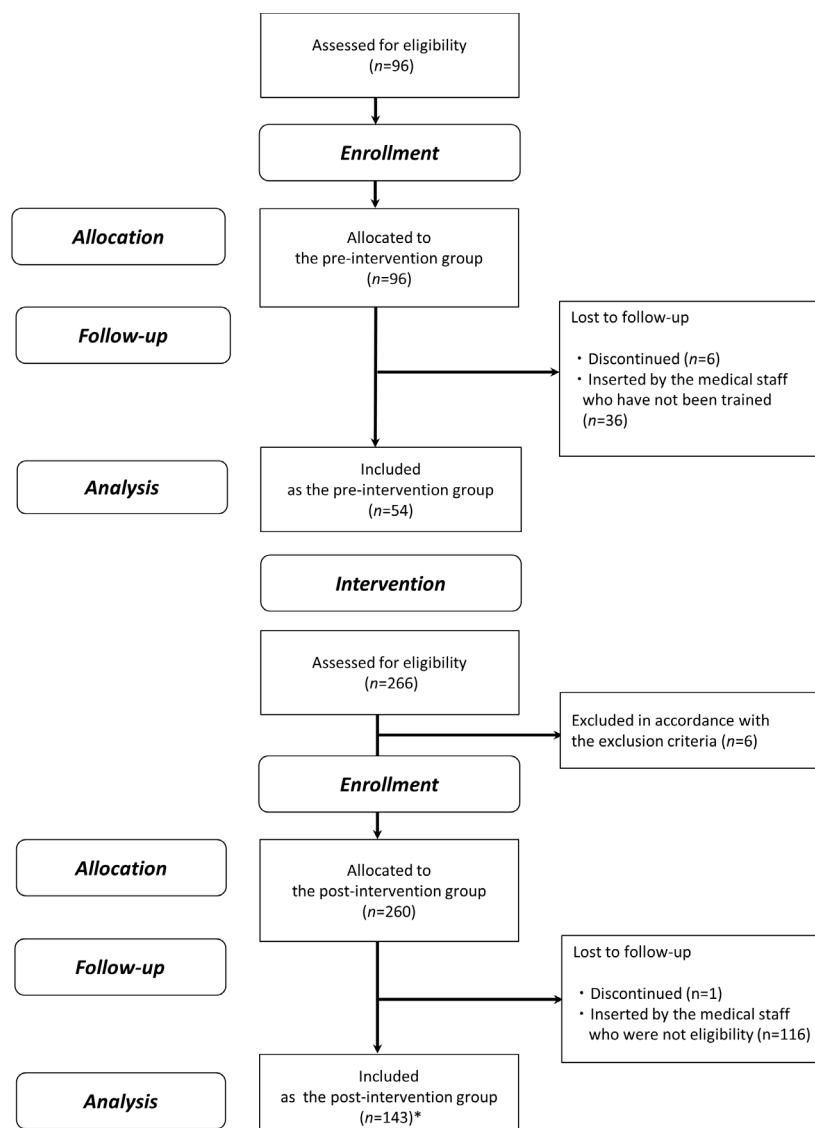


Figure 2. Catheter flowchart after the recruitment.

as follows: BMI ($p = 0.014$), organ cancer ($p = 0.003$), platelet count ($p = 0.025$), multiple entry in each group ($p = 0.034$), infusion, lipid emulsion ($p = 0.019$), experience level ($p < 0.001$), and polyurethane catheter ($p < 0.001$; Table 2).

3.2.2. Per-protocol analysis

There were two groups in the PP analysis set as follows: pre-intervention group and complete algorithm-use group. The incidence of CF rate as the primary outcome was 35.2% (19/54) in the pre-

intervention group and 8.7% (2/23) in complete algorithm-use group. The intergroup difference was significant ($p = 0.017$). The incidence of CF in the per-protocol analysis was 24.4 per 1,000 days compared with 146.7 per 1,000 days in the pre-intervention group ($p = 0.010$; Table 1).

There were significant differences in patient and catheter characteristics between the pre-intervention group and complete algorithm-use group as follows: BMI ($p = 0.043$), organ cancer ($p = 0.015$), oral medicine, steroids ($p = 0.022$), albumin ($p = 0.017$), infusion of antibiotics ($p = 0.024$), infusion of lipid

Table 1. Incidence of catheter failure in intention-to-treat and per-protocol analyses

Items	Catheter failure	p Value ^a	Per 1000 catheter days	p Value ^b
Pre-intervention ($n = 54$)	19 (35.2%)	0.831	146.7	0.214
Post-intervention ($n = 143$)	48 (33.6%)		99.9	
Pre-intervention ($n = 54$)	19 (35.2%)	0.017*	146.7	0.010*
Complete algorithm-use in post-intervention ($n = 23$)	2 (8.7%)		24.4	

^aPearson's chi-square test, ^bLog-rank test; * $p < 0.05$.

Table 2. Patients and catheters characteristics in the intention-to-treat and per protocol analyses

Items	Pre-intervention	Post-intervention		Complete algorithm-use in post-intervention	
Characteristics	($n = 54$)	($n = 143$)	p Value [†]	($n = 23$)	p Value ^{††}
Patient factor					
Male	35 (65%)	98 (69%)	0.619	16 (70%)	0.687
Age, median (IQR)	68 (60-78)	70 (66-77)	0.135	69 (57-75)	0.872
BMI, median (IQR)	21 (18-23)	23 (20-26)	0.014*	24 (3.4) ^d	0.043*
Diabetes	12 (22%)	43 (30%)	0.273	4 (17%)	0.442
Organ cancer	35 (65%)	59 (41%)	0.003*	8 (35%)	0.015*
Oral medicine					
Antimicrobials	12 (22%)	24 (17%)	0.378	2 (8.7%)	0.138
Steroids	2 (3.7%)	19 (13%)	0.052	5 (22%)	0.022*
Anticoagulants and antiplatelets	12 (22%)	49 (34%)	0.103	10 (44%)	0.059
Ambulatory status (KANGODO III and IV)	34 (63%)	109 (76%)	0.063	19 (80%)	0.088
Blood examination					
C-reactive protein [mg/dL], median (IQR)	1.5 (0.2-4.0)	3.1 (0.2-4.7)	0.574	0.5 (0.1-2.6)	0.476
Albumin [g/dL], median (IQR)	3.2 (0.6) ^d	3.3 (0.6) ^{a,d}	0.945	3.6 (0.6) ^{c,d}	0.017*
Platelets [$10^4/\mu\text{L}$], median (IQR)	22 (18-28)	25 (19-32)	0.025*	19 (17-30)	0.798
Multiple entry in each group	17 (32%)	69 (48%)	0.034*	4 (26%)	0.204
Chemical factor					
Infusion					
Hyperosmolality	20 (37%)	36 (25%)	0.100	4 (17%)	0.088
Antimicrobials	18 (33%)	46 (32%)	0.876	2 (8.7%)	0.024*
Lipid emulsion	0	12 (8.4%)	0.019*	3 (13%)	0.024*
Anticoagulants	7 (13%)	28 (20%)	0.278	9 (39%)	0.015*
Technical factor					
Experience level			0.096		0.403
Beginner [<100 catheters]	5 (9.3%)	12 (8.4%)		2 (8.7%)	
Intermediate [$100-800$ catheters]	20 (37%)	77 (54%)		9 (39%)	
Expert [>800 catheters]	29 (54%)	54 (38%)		12 (52%)	
First attempt success	36 (67%)	91 (67%) ^b	0.974	17 (74%)	0.530
Mechanical factor					
Insertion in the forearm	50 (93%)	132 (97%) ^b	0.162	23 (100%)	0.234
Polyurethane catheter	0	80 (57%) ^b	$< 0.001^*$	17 (74%)	$< 0.001^*$
Catheter lock period, median (IQR)	10 (0-11)	18 (0-14)	0.482	0 (0-19)	0.346

t test or Mann-Whitney U test, Pearson chi-square test or Fisher's exact test; IQR = interquartile range; ^a $n = 142$. ^b $n = 136$. ^c $n = 22$. ^dmean (SD); * $p < 0.05$; [†]Between pre-intervention and post-intervention; ^{††}Between pre-intervention and complete algorithm-use in post-intervention.

emulsion ($p = 0.024$), infusion of anticoagulants ($p = 0.015$), experience level ($p < 0.001$), and polyurethane catheter ($p < 0.001$; Table 2).

The compliance rate as the secondary outcome was 16.1% (23/143).

3.2.3. Factor analysis for the relationship between CF and Compliance to the algorithm

Several variates of patient and catheter characteristics showed significant differences in the both ITT and PP analysis sets, thus, we adjusted these variates to determine the factor of CF.

There were significant differences in patient and catheter characteristics between the complete algorithm-use group and the other groups (54 PIVs in the pre-intervention group and 120 PIVs except those in the post-intervention algorithm-compliant group) as follows: albumin ($p = 0.003$), infusion of antibiotics ($p = 0.010$), infusion of anticoagulants ($p = 0.008$), and polyurethane catheter ($p = 0.001$; Table 3). The interaction was confirmed among the variates at p values of < 0.15 in the univariate model. The variates were used to assess for

correlations with other variates (at $\rho > 0.4$ and $p < 0.050$), and covariates were selected for the multivariate model. Ultimately, polyurethane catheter, age, sex, infusion of antibiotics, infusion of anticoagulants, undergoing training session, and compliance to the algorithm were introduced to the logistic regression model to calculate ORs and 95% CIs. In this analysis model, compliance to the algorithm and infusion of anticoagulants were significantly correlated with CF (OR, 0.19; 95% CI, 0.04-0.87; $p = 0.032$ and OR, 0.24; 95% CI, 0.80-0.74; $p = 0.013$, respectively; Table 4).

3.3. Harm

No patients reported any adverse events; thus, this algorithm had acceptable safety in the clinical setting.

4. Discussion

This is the first study in which a US-assisted PIV algorithm demonstrated a decrease in the incidence rate of CF. The defining characteristic of our originally developed algorithm was that it used US for adjustment

Table 3. Patients and catheters characteristics with high compliance

Characteristic	Complete algorithm-use in post-intervention ($n = 23$)	Pre- and post-intervention expect 23 (complete) ($n = 174$)	p Value
Patient factor			
Male	38 (32%)	117 (67%)	0.823
Age, median (IQR)	69 (57-75)	71 (64-78)	0.205
BMI, median (IQR)	24 (21-27)	22 (20-25)	0.055
Diabetes	4 (17%)	51 (29%)	0.231
Organ cancer	8 (35%)	86 (50%)	0.186
Oral medicine			
Antimicrobials	2 (8.7%)	34 (20%)	0.164
Steroids	5 (22%)	16 (9.2%)	0.078
Anticoagulants and antiplatelets	10 (44%)	51 (29%)	0.167
Ambulatory status [KANGODO III and IV]	19 (80%)	124 (71%)	0.252
Blood examination			
C-reactive protein [mg/dL], median (IQR)	0.5 (0.1-2.6)	1.3 (0.2-4.7)	0.196
Albumin [g/dL], median (IQR)	3.8 (3.3-3.9) ^a	3.1 (2.8-3.6)	0.003*
Platelets [$10^4/\mu\text{L}$], median (IQR)	19 (17-30)	25 (20-31)	0.178
Multiple entry in each group	6 (26%)	79 (45%)	0.079
Chemical factor			
Infusion			
Hyperosmolality	4 (17%)	52 (30%)	0.212
Antimicrobials	2 (8.7%)	62 (36%)	0.010*
Lipid emulsion	3 (13%)	9 (5%)	0.151
Anticoagulants	9 (39%)	26 (15%)	0.008*
Technical factor			
Experience level			0.953
Beginner [< 100 catheters]	2 (8.7%)	13 (7.5%)	
Intermediate [100–800 catheters]	9 (39%)	88 (51%)	
Expert [> 800 catheters]	12 (52%)	73 (42%)	
First attempt success	17 (74%)	110 (66%) ^b	
Mechanical factor			
Insertion in the forearm	23 (100%)	159 (95%)	0.349
Polyurethane catheter	17 (74%)	63 (37%)	0.001*
Catheter lock period, median (IQR)	0 (0-13)	0 (0-12)	0.441

Pearson's chi-square test or Fisher's exact test, Mann-Whitney U test; ^a $n = 22$; ^b $n = 167$; * $p < 0.05$.

Table 4. Risk factors associated with catheter failure

Items	OR	95% CI	p Value
Polyurethane catheter	1.26	0.59-2.66	0.552
Age	1.00	0.99-1.03	0.798
Sex	0.99	0.51-1.92	0.974
Infusion; antimicrobials	1.07	0.55-2.05	0.852
Infusion; anticoagulants	0.24	0.08-0.74	0.013*
Undergoing training session	1.04	0.46-2.33	0.933
Compliance to the algorithm	0.19	0.04-0.87	0.032*

Logistic regression; OR = odds ratio; CI = confidence interval; * $p < 0.05$; Hosmer-Lemeshow test $p = 0.942$.

and confirmation of the catheter tip position after insertion, not just during the puncture phase. The incidence rate of CF decreased from 35.2% (19/54) to 8.7% (2/23) in cases where ensured compliance to the algorithm. In factor analysis, compliance to the algorithm were significantly correlated with CF. Nevertheless, the compliance rate was unacceptably low, which is considered a future issue.

CF was significantly associated with compliance to the algorithm. The main purpose of compliance to the algorithm was to avoid irritation to the vessel wall. Injury to the vessel wall is the one of the factors which leads to thrombosis (19). In fact, our factor analysis indicated that compliance to the algorithm and anticoagulants infusion contributed to CF.

Our previous study confirmed that thrombus with subcutaneous edema was related to the incidence of CF (20). Therefore, we determined that the compliance to the algorithm worked effectively to inhibit thrombus formation and to reduce the incidence of CF, although it was not found to be signify, which worked more effectively, 1. Appropriate blood vessel or 4. Appropriate catheter tip position, and whether 2. Appropriate insertion and 3. Needle in the blood vessel worked effectively or not.

Even though nurses participated in the training for using algorithm and had sufficient skills for US-assisted PIV placement certified by objective structured clinical examination, compliance to the algorithm was quiet low, at 23/143 (16.1%).

One of the reasons for the low compliance rate, nurses did not have enough time to use the algorithm. The US technique requires additional time on the conventional method of the PIV placement. The setting of this study was a surgical unit at a large tertiary metropolitan affiliated hospital, and consequently, nurses might have been too busy to implement the algorithm.

The other reason that may be considered is that manipulation of the probe and interpretation of the US images are difficult (21). These difficulties might lead to the low compliance rate. The technique of creating images of the both catheters and vessels at the same time was considered of the hardest point. We need to improve the visualization technology or device performance in order to enable all the nurses to acquire the techniques

related to both probe manipulation and interpretation of the US images. Moreover, artificial intelligence technology and high number of inputs with images of the both catheters and vessels might support nurses' interpretation of the US images of the position of the catheter tip within the vessel.

There were several limitations in this study. Firstly, owing to the characteristics of the pretest-posttest study, maturation must be considered as a potential confounding factor. There was a possibility of overestimating the reduction in the incidence of CF due to the maturation of vein catheterization skills. Secondly, there is a problem of device performance. In clinical settings with restricted space, tablet-type US devices are convenient and easy to carry. On the other hand, the image resolution of the tablet-type devices is lower than the stand-type devices. The difficulty of interpretation of the US images due to the low resolution potentially affected the compliance rate. Thirdly, the setting of this study is one large tertiary metropolitan affiliated hospital, hence, we need to be careful to extrapolate our results to home care or health facilities for recuperation.

In conclusion, we developed an algorithm to standardize US-assisted PIV placement for the purpose of decreasing the incidence of CF, from the insertion phase to the securement phase. There was no significant difference in the CF rate between pre- and post-intervention group. On the other hand, there was significant difference between pre- and complete algorithm-use group. The algorithm can reduce the incidence of CF significantly. However, the algorithm compliance rate was low (16.1%). In order to increase the compliance rate, modified algorithm and new visualizing technology is required.

Conflict of Interest

Ryoko Murayama Mari Abe-Doi belong to the laboratory supported by Terumo Co. Toshiaki Takahashi belongs to the laboratory supported by Molten Co. Chiho Kanno, Yui shintani, Junko Nogami, Chieko Komiyama and Hiromi Sanada have no conflict of interest.

Acknowledgements

The authors wish to thank all patients and medical staff who collaborated and helped us, especially Ms. Noriko Hirai (Chief nurse).

References

- Alexandrou E, Ray-Barruel G, Carr PJ, Frost S, Inwood S, Higgins N, Lin F, Alberto L, Mermel L, Rickard CM. International prevalence of the use of peripheral intravenous catheters. *J Hosp Med.* 2015; 10:530-533.
- Helm RE, Klausner JD, Klemperer JD, Flint LM, Huang E.

- Accepted but unacceptable: peripheral IV catheter failure. *J Infus Nurs.* 2015; 38:189-203.
3. Murayama R, Uchida M, Oe M, Takahashi T, Oya M, Komiyama C, Sanada H. Patient risk factors for developing sign- and symptom-related peripheral intravenous catheter failure: a retrospective study. *J Jpn WOCM.* 2015; 19:394-402.
 4. Rickard CM, Webster J, Wallis MC, Marsh N, McGrail MR, French V, Foster L, Gallagher P, Gowardman JR, Zhang L, McClymont A, Whitby M. Routine versus clinically indicated replacement of peripheral intravenous catheters: a randomised controlled equivalence trial. *The Lancet.* 2012; 380:1066-1074.
 5. Wallis MC, McGrail M, Webster J, Marsh N, Gowardman J, Playford G, Richard CM. Risk factors for peripheral intravenous catheter failure: a multivariate analysis of data from a randomized controlled trial. *Infect Control Hosp Epidemiol.* 2014; 35:63-68.
 6. Reunes S, Rombaut V, Vogelaers D, Brusselaers N, Lizy C, Cankurtaran M, Labeau S, Petrovic M, Blot S. Risk factors and mortality for nosocomial bloodstream infections in elderly patients. *Eur J Intern Med.* 2011; 22:e39-44.
 7. Nassaji-Zavareh M, Ghorbani R. Peripheral intravenous catheter-related phlebitis and related risk factors. *Singapore Med J.* 2007; 48:733-736.
 8. Hadaway L. Infiltration and extravasation. *Am J Nurs.* 2007; 107:64-72.
 9. Timmer J, Schipper H. Peripheral venous nutrition: the equal relevance of volume load and osmolarity in relation to phlebitis. *Clin Nutr.* 1991; 10:71-75.
 10. Monreal M, Quilez F, Rey-Joly C, Boderiguez S, Sopena N, Niera C, Roca J. Infusion phlebitis in patients with acute pneumonia: a prospective study. *Chest.* 1999; 115:1576-1580.
 11. Gorski L, Hadaway L, Hagle M, McGoldrick M, Orr M, Doellman D. Infusion therapy standards of practice (Alexander M, ed.). Infusion Nursing Society, Norwood, USA, 2016; pp. 95.
 12. Uslusoy E, Mete S. Predisposing factors to phlebitis in patients with peripheral intravenous catheters: a descriptive study. *J Am Acad Nurse Pract.* 2008; 20:172-180.
 13. Karadag A, Gorgulu S. Effect of two different short peripheral catheter materials on phlebitis development. *J Intraven Nurs.* 2000; 23:158-166.
 14. Takahashi T, Ryoko M, Mari Abe-Doi, Maki Miyahara-Kaneko, Chiho K, Miwa N, Mariko M, Chieko K, Hiromi S. Preventing peripheral intravenous catheter failure by reducing mechanical irritation. *Sci Rep.* 2020; 1550.
 15. Gaddis G, Greenwald P, Huckson S. Toward improved implementation of evidence-based clinical algorithms: clinical practice guidelines, clinical decision rules, and clinical pathways. *Acad Emerg Med.* 2007; 14:1015-1022.
 16. Anderson J, Greenwell A, Louderback J, Polivka BJ, Behr JH. Comparison of Outcomes of Extended Dwell/Midline Peripheral Intravenous Catheters and Peripherally Inserted Central Catheters in Children. *J Assoc Vasc Access.* 2016; 21:158-164.
 17. Duran-Gehring P, Bryant L, Reynolds JA, Aldridge P, Kalynych CJ, Guirgis FW. Ultrasound-Guided Peripheral Intravenous Catheter Training Results in Physician-Level Success for Emergency Department Technicians. *J Ultrasound Med.* 2016; 35:2343-2352.
 18. Rippey J CR, Carr PJ, Cooke M, Higgins N, Rickard CM. Predicting and preventing peripheral intravenous cannula insertion failure in the emergency department: Clinician 'gestalt' wins again. *Emerg Med Australas.* 2016; 28:658-665.
 19. Anning S. The historical aspects of venous thrombosis. *Med Hist.* 1957; 1:28-37.
 20. Takahashi T, Murayama R, Oe M, Nakagami G, Tanabe H, Yabunaka K, Arai R, Komiyama C, Uchida M, Sanada H. Is Thrombus With Subcutaneous Edema Detected by Ultrasonography Related to Short Peripheral Catheter Failure? A Prospective Observational Study. *J Infus Nurs.* 2017; 40:313-322.
 21. Panebianco NL, Fredette JM, Szyld D, Sagalyn EB, Pines JM, Dean AJ. What you see (sonographically) is what you get: vein and patient characteristics associated with successful ultrasound-guided peripheral intravenous placement in patients with difficult access. *Acad Emerg Med.* 2009; 16:1298-1303.

Received December 24, 2019; Revised February 16, 2020; Accepted February 23, 2020

*Address correspondence to:

Dr. Hiromi Sanada, Department of Gerontological Nursing/Wound Care Management, Graduate School of Medicine, The University of Tokyo, 7-3-1 Hongo, Bunkyo-ku, Tokyo, 113-0033, Japan.

E-mail: hsanada-ky@umin.ac.jp

Functional role of c-Jun NH₂-terminal kinase-associated leucine zipper protein (JLP) in lysosome localization and autophagy

Ryusuke Suzuki, I Ketut Gunarta, Jambaldorj Boldbaatar, Purev Erdenebaatar, Ravidandorj Odongoo, Katsuji Yoshioka*

Division of Molecular Cell Signaling, Cancer Research Institute, Kanazawa University, Kanazawa, Japan.

SUMMARY Lysosomes are involved in many cellular functions, and in turn lysosomal dysfunction underlies a variety of diseases, including cancer and neurodegenerative diseases. Lysosomes are distributed broadly in the cytoplasm and can move throughout the cell in kinesin- and dynein-dependent manners. Although many mechanisms of lysosomal transport have been reported, how lysosomal transport is regulated has yet to be fully elucidated. In this study we analyzed c-Jun NH₂-terminal kinase-associated leucine zipper protein (JLP), an adaptor of kinesin and dynein motor proteins, and found that lysosomes were localized toward the cell periphery in *JLP* knockdown cells, leading to the impairment of autophagosome-lysosome fusion. Furthermore, we performed rescue experiments using wild-type JLP and its various deletion mutants. The results indicated that JLP may regulate lysosome localization and autophagy through interaction of JLP with kinesin-1 heavy chain, but not with dynactin p150^{Glued} or lysosomal transmembrane protein 55b. Our findings provide new insights into the mechanisms of lysosomal trafficking regulation. This study contributes to the understanding of how lysosomes exert their multiple functions, potentially leading to the identification of molecular targets for diseases caused by lysosomal dysfunction.

Keywords dynein, kinesin, lysosomal transport

1. Introduction

Lysosomes are well-known to be terminal, degradative organelles. However, increasing evidence indicates that lysosomes contribute to many other cellular processes, such as antigen presentation, apoptosis, and metabolic signaling (1). Similarly, lysosomal dysfunction underlies a variety of diseases, including cancer, lysosomal storage, and neurodegenerative diseases (1-3). Lysosomes are distributed broadly throughout the cytoplasm and can move toward the microtubule plus-ends and minus-ends, as mediated by kinesin and dynein motors, respectively (1,2). Previous studies have reported many mechanisms of lysosomal transport. In both the kinesin- and dynein-dependent transport of lysosomes, the small GTPase Rab7 has been shown to play important roles in recruiting the motor proteins to the lysosomes (1,2). In addition, Willett *et al.* (4) recently proposed that the lysosomal transmembrane protein 55b (TMEM55B) participates in the regulation of dynein-dependent transport of lysosomes through interaction with the motor adaptor c-Jun NH₂-terminal kinase-associated leucine zipper protein (JLP).

JLP (also known as SPAG9 or JIP4) was first identified as a scaffold protein in the mammalian mitogen-activated protein kinase (MAPK) signaling pathway (5,6), and subsequently was found to also function as an adaptor protein that links cargoes to kinesin and/or dynein motors (7-9). Recent studies have shown that JLP is a multifunctional protein involved in axonal transport, cytokinesis, and oxidative stress-induced cell death (10-14). In this study, we explored the role of JLP in lysosome localization and autophagy, and propose a novel, TMEM55B-independent mechanism of intracellular lysosomal trafficking.

2. Materials and Methods

2.1. Cell culture and reagents

U87, HeLa, HT1080, and HEK293T cells were cultured in Dulbecco's Modified Eagle Medium (DMEM) (Wako, Tokyo, Japan) as described previously (13,14). Amino acid-free DMEM was obtained from Wako.

2.2. Plasmids and viral vector preparation

The pLVTH lentivirus plasmid vectors for two short hairpin RNAs (shRNAs) against human JLP, shJLP#1 and shJLP#2, as well as for scramble shRNA (shScr), were described previously (14). The JLP deletion mutants, including those that lacking the dynactin p150^{Glued}-binding domain (DBD), C-terminal and N-terminal half regions of JLP [amino acid residues 371-490, 657-1,321, and 1-646 of human JLP, respectively (RefSeq accession number NP_00112400)] were generated using overlapping PCR as described by Ito *et al.* (15). The JLP deletion mutants were expressed as hemagglutinin (HA)-tagged proteins using the pCL20c-CMV lentivirus plasmid vector (16). The pCL20c-CMV expression vectors for tandem fluorescent-tagged LC3, HA-tagged wild-type JLP, and JLP mutants lacking MAPK-binding domain (MBD) or kinesin-1 heavy chain (KHC)-binding domain (KBD) were previously described (10,14). To express the HA-JLP proteins at suboptimal levels in cells, a 405-bp deletion was made in the CMV promoter/enhancer region based on Morita *et al.* (17), referred to as CMV Δ 2. However, in some experiments, the original CMV promoter/enhancer was used (see Figure 3 legend). Flag-tagged, truncated TMEM55B [amino acid residues 2-207 (RefSeq accession number NP_653169)], containing a large cytosolic N-terminal domain (CD) of human TMEM55B, was expressed using the pCL20c-CMV vector. All PCR products were verified by sequencing. Lentiviral vectors were produced as previously described (16).

2.3. Immunoprecipitation and western blot analysis

To analyze protein-protein interactions, immunoprecipitation-western blot analysis was performed as previously described (18). Briefly, after transient co-expression of HA-tagged and Flag-tagged proteins, cells were lysed in lysis buffer (50 mM Tris-HCl pH 7.4, 150 mM NaCl, 1% Nonidet P40, 0.25% sodium deoxycholate, 1 mM EDTA) containing Protease Inhibitor Cocktail (Sigma-Aldrich, St. Louis, MO, USA), immunoprecipitated with anti-HA antibody beads (Wako), and analyzed by western blotting using a horseradish peroxidase-conjugated anti-Flag antibody (Sigma-Aldrich). Total cell lysates were prepared and analyzed by western blotting as described previously (16), using anti-actin (1:2,000; A6050; Sigma-Aldrich), anti-p150^{Glued} (1:1,000; 610474; BD Biosciences, San Jose, CA, USA), anti-LC3 (1:2000; MBL, Nagoya, Japan), and anti-JLP (0.25 μ g/mL (13)) primary antibodies.

2.4. Immunocytochemistry, fluorescence, and quantification

Immunocytochemistry was carried out as previously described (16), using anti-HA (1:100; 11867423001, Sigma-Aldrich) and anti-LAMP-1 (1:300; H4A3, Developmental Studies Hybridoma Bank, Iowa City,

IA, USA) primary antibodies. The secondary antibodies were Alexa Fluor 568- and 647-conjugated goat, anti-mouse IgG (both 1:500; Thermo Fisher Scientific, Waltham, MA, USA). Fluorescent images were captured using confocal laser scanning microscopes [(LSM510 META, Carl Zeiss, Oberkochen, Germany, Figures 1-4 and Figure S1, <http://www.ddtjournal.com/action/getSupplementalData.php?ID=53>); (TCS SP8; Leica, Wetzlar, Germany, Figure 5); and (BZ-9000, Keyence, Osaka, Japan, Figure S2, <http://www.ddtjournal.com/action/getSupplementalData.php?ID=53>)]. Quantitative analyses of lysosome distribution in Figures 1-4 and colocalization in Figure 5 were performed essentially as described by Willett *et al.* (4) and Michelet *et al.* (19), respectively.

2.5. Statistical analysis

Significance was determined using a two-tailed, unpaired Student's *t*-test. Values of $p < 0.05$ were considered to be statistically significant.

3. Results

3.1. JLP knockdown results in altered lysosome localization

We first examined whether JLP is involved in lysosome localization. To this end, we generated JLP knockdown cells using two lentiviral shRNAs against JLP (shJLP#1 and shJLP#2). As shown in Figure 1A, highly reduced levels of JLP protein were observed in U87 and HeLa cells expressing shJLP#1 or shJLP#2, as compared to their respective parent cells and control cells expressing shScr. We then performed immunostaining with an antibody against LAMP-1, a lysosome marker, and observed an altered distribution of lysosomes in the JLP knockdown cells. Lysosomes were dispersed toward the cell periphery in the JLP knockdown cells, as compared to parent and control shScr-expressing cells (Figures 1B and 1C). A similar result was obtained when we analyzed HT1080 cells in a similar manner (Figure S1, <http://www.ddtjournal.com/action/getSupplementalData.php?ID=53>). These results strongly suggest that JLP plays a role in lysosome localization, and that JLP knockdown causes lysosome distribution to the cell periphery.

3.2. JLP is involved in lysosome localization independently from its interaction with dynactin p150^{Glued}

As lysosomes are known to move along microtubules toward the centrosome *via* the dynein motor (1,2), we hypothesized that the altered lysosomal distribution is due to an impairment of retrograde transport of lysosomes in JLP knockdown cells. To test this hypothesis, we performed rescue experiments wherein cells were

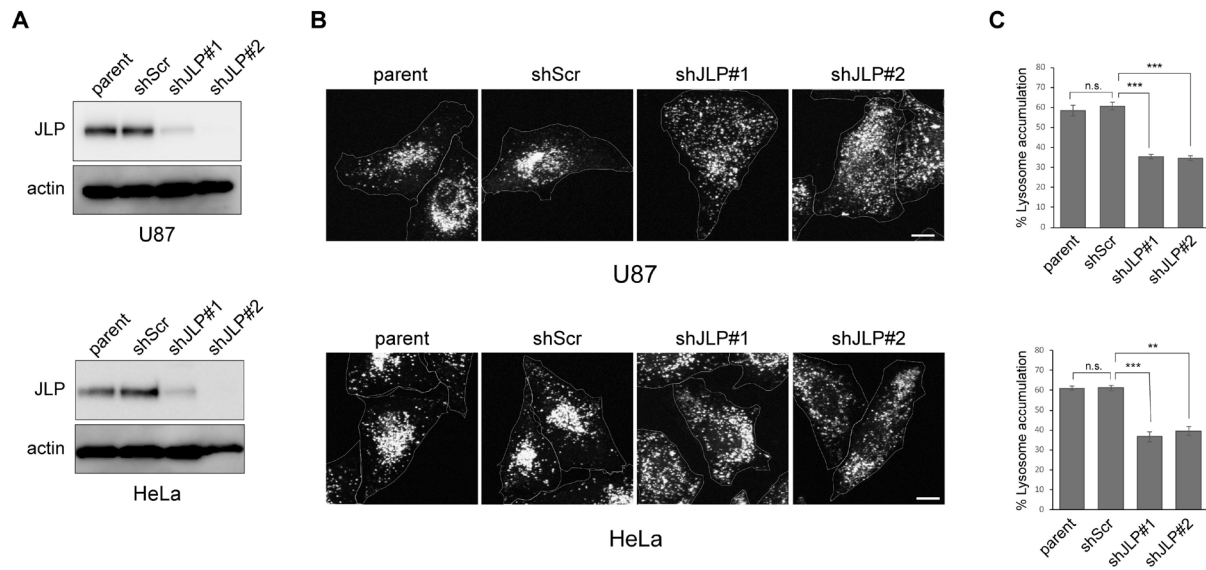


Figure 1. JLP knockdown impairs lysosomal accumulation around the perinuclear region. (A) U87 and HeLa cells were transduced or not (parent cells) with lentiviral vectors for shScr, shJLP#1, or shJLP#2, as indicated, and the expression levels of JLP were analyzed by western blotting with an anti-JLP antibody. Actin was utilized as the loading control. (B) U87 and HeLa cells expressing shScr, shJLP#1, shJLP#2, and their corresponding parent cells, as indicated, were immunostained with an anti-LAMP-1 antibody. Images were obtained by confocal microscopy. Scale bars, 10 μ m. (C) Quantification of the lysosome distribution imaged in (B). Quantitative data are expressed as mean \pm S.E.M. of three independent experiments. The perinuclear region was defined as 0–5 μ m from the nuclear rim. At least 20 cells per experiment condition were analyzed. ** $p < 0.01$; *** $p < 0.001$; n.s., not significant.

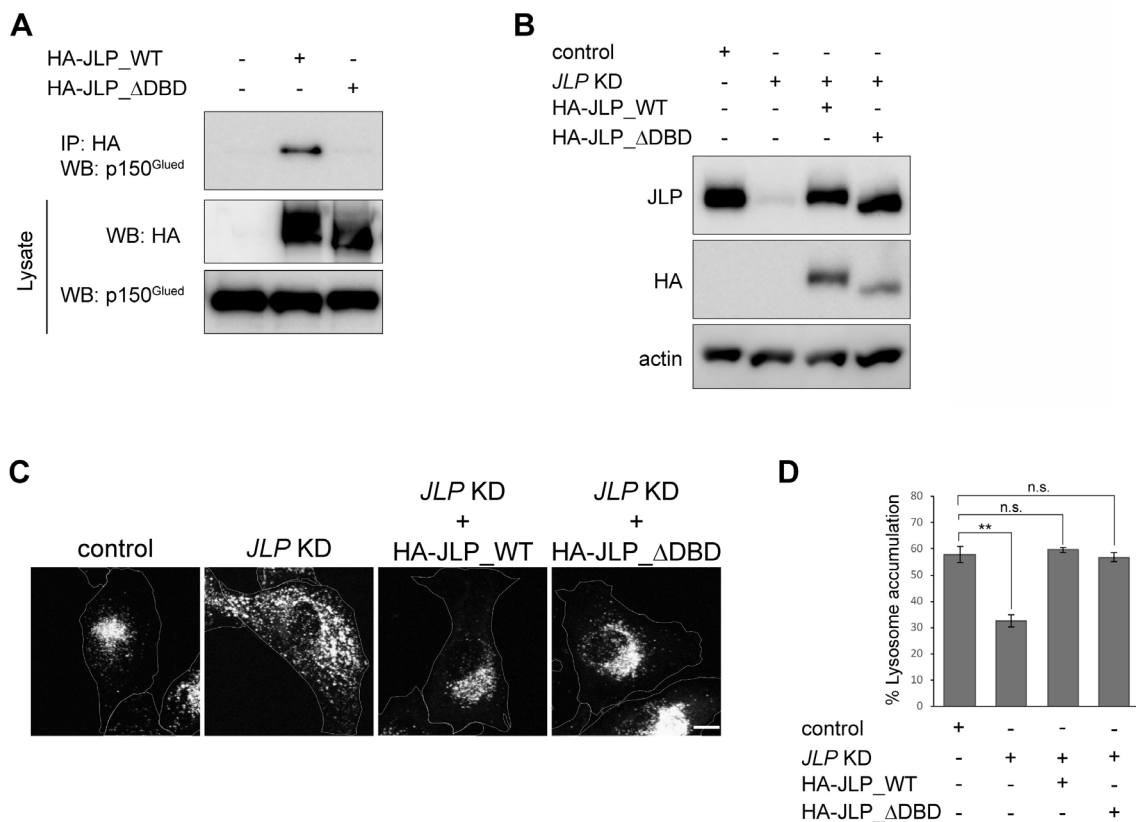


Figure 2. JLP is involved in lysosome localization independently from its interaction with dynactin p150^{Glued}. (A) HA-JLP-WT or HA-JLP- Δ DBD were transiently expressed in HEK293T cells as indicated, immunoprecipitated (IP) with anti-HA antibody beads and subjected to western blotting (WB) using an anti-p150^{Glued} antibody. The expression of HA-JLPs (middle panel) and of p150^{Glued} (lower panel) in total cell lysates is shown. (B) U87 cells expressing either shScr (control) or shJLP#2 (JLP KD), alone or together with HA-JLP_WT or HA-JLP_ Δ DBD as indicated, were analyzed by western blotting with anti-JLP and anti-HA antibodies. Actin was used as a loading control. (C) The U87 cells in (B) were immunostained with an anti-LAMP-1 antibody and observed by confocal microscopy. Scale bar, 10 μ m. (D) The results of lysosome distribution in (C) were quantified as in Figure 1C. ** $p < 0.01$; n.s., not significant.

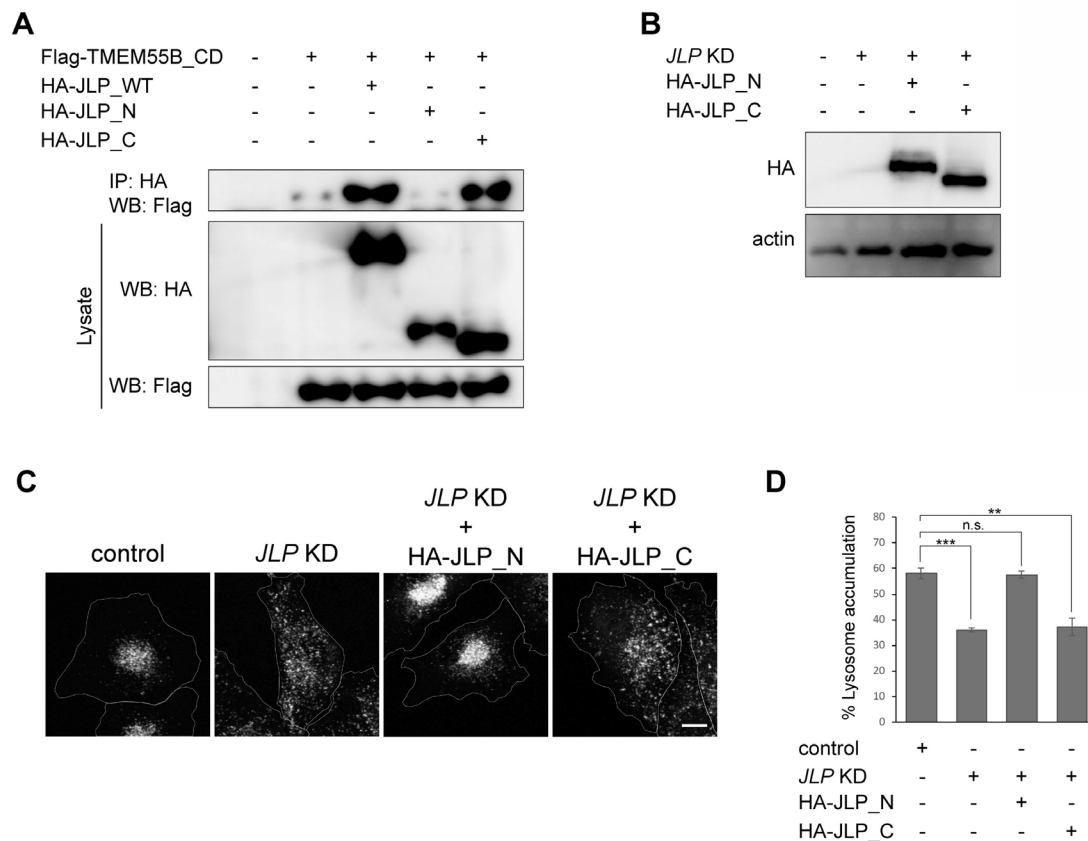


Figure 3. JLP-TMEM55B interaction is dispensable for lysosome localization. (A) Flag-TMEM55B_CD was transiently co-expressed with HA-JLP_WT, HA-JLP_N, or HA-JLP_C as indicated in HEK293T cells, immunoprecipitated (IP) with anti-HA antibody beads, and subjected to western blotting (WB) using an anti-Flag antibody. The expression of HA-JLPs (middle panel) and of Flag-TMEM55B_CD (lower panel) in total cell lysates is shown. HA-JLP_N and HA-JLP_C were expressed using the pCL20c-CMV vector. (B) U87 cells expressing shJLP#2 (*JLP* KD) alone or together with HA-JLP_N or HA-JLP_C as indicated were analyzed by western blotting with an anti-HA antibody. Actin was utilized as a loading control. (C, D) The U87 cells in (B) were immunostained with an anti-LAMP-1 antibody (C), and the results were quantified as in Figure 1C (D). ** $p < 0.01$; *** $p < 0.001$; n.s., not significant. Scale bar, 10 μ m.

transduced with lentiviral particles containing HA-tagged wild-type JLP (HA-JLP_WT) or its mutant lacking DBD (HA-JLP_ΔDBD), both of which are shJLP#2-resistant (Figure 2). We confirmed that HA-JLP_ΔDBD was unable to interact with dynactin p150^{Glued} (Figure 2A). However, as shown in Figure 2C and D, both HA-JLP_WT and HA-JLP_ΔDBD reversed the lysosome distribution in *JLP* knockdown cells. The expression levels of JLP were comparable among the U87 cells expressing shScr, HA-JLP_WT, and HA-JLP_ΔDBD (Figure 2B). In addition, the percent of HA-positive cells were over 90% in cells transduced with lentivirus for HA-JLP_WT or HA-JLP_ΔDBD (Figure S2A, <http://www.ddtjournal.com/action/getSupplementalData.php?ID=53>). Taken together, these results suggest that the role of JLP in lysosome localization is independent from its interaction with dynactin p150^{Glued}.

3.3. JLP mutants lacking the TMEM55B-binding domain, but not the N-terminal region, restore altered lysosome localization in *JLP* knockdown cells

As TMEM55B has been reported to recruit JLP to the

lysosomal surface, inducing retrograde transport of lysosomes (4), we asked whether the JLP-TMEM55B interaction is involved in lysosome localization. As a first step to examine this possibility, we generated expression plasmids for HA-tagged N- and C-terminal half deletion mutants of JLP (named HA-JLP_N and HA-JLP_C, respectively) in addition to HA-tagged full-length wild-type JLP, HA-JLP_WT. In HEK293T cells we transiently co-expressed one of the HA-JLPs together with Flag-tagged TMEM55B and performed immunoprecipitation-western blot analysis. Through this approach, we found that the C-terminal half, but not the N-terminal half, of JLP is responsible for interaction with TMEM55B (Figure 3A). We then performed rescue experiments using these JLP deletion mutants using the same approach detailed above for HA-JLP-ΔDBD. The expression levels of lentivirus-transduced HA-JLP_N and HA-JLP_C were comparable (Figure 3B), and the percent of HA-positive cells were over 90% in cells transduced with the respective lentivirus particles (Figure S2B, <http://www.ddtjournal.com/action/getSupplementalData.php?ID=53>). We observed that HA-JLP_N, but not HA-JLP_C, restored the localization of lysosomes in *JLP*

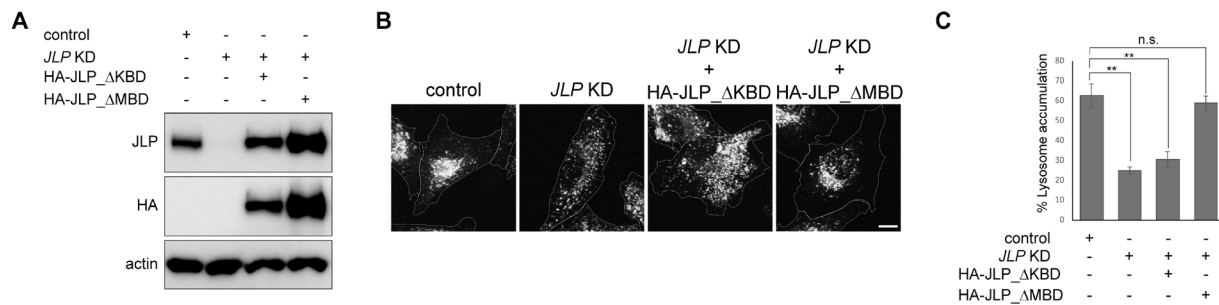


Figure 4. A JLP mutant lacking KBD, but not MBD, fails to reverse the altered lysosomal distribution in JLP knockdown cells. (A-C) U87 cells expressing either shScr (control) or shJLP#2 (*JLP* KD), alone or together with HA-JLP_ΔKBD or HA-JLP_ΔMBD as indicated were analyzed by western blotting with an anti-HA antibody (A). The cells in (A) were immunostained with an anti-LAMP-1 antibody (B), and the results were quantified as in Figure 1C (C). Actin was used as a loading control. ** $p < 0.01$; n.s., not significant. Scale bar, 10 μ m.

knockdown cells (Figures 3C and D). Collectively, these results suggest that the JLP-TMEM55B interaction is unrelated to lysosome localization and that the N-terminal half of JLP is necessary and sufficient for the regulation of lysosome localization.

3.4. JLP may play a role in retrograde movement of lysosomes through interaction with KHC

It is known that JLP contains two domains, KBD and MBD, in its N-terminal region (10,14). We, therefore, examined whether KBD and/or MBD are involved in lysosome localization using HA-tagged shJLP#2-resistant JLP mutants lacking KBD (HA-JLP_ΔKBD) or MBD (HA-JLP_ΔMBD). After confirming the expression levels of HA-JLP_ΔKBD and HA-JLP_ΔMBD (Figure 4A), and the transduction efficiency of the lentiviral particles in cells (Figure S2C, <http://www.ddtjournal.com/action/getSupplementalData.php?ID=53>), we carried out rescue experiments. Interestingly, HA-JLP_ΔMBD, but not HA-JLP_ΔKBD, restored the altered lysosomal distribution in *JLP* knockdown cells (Figure 4B and C), suggesting that the JLP-KHC interaction may play a role in the retrograde movement of lysosomes.

3.5. JLP knockdown impairs autophagosome-lysosome fusion

Because lysosome localization is important for autophagy (20), we examined whether *JLP* knockdown affects the induction of autophagy. We first assessed autophagy based on the level of LC3-II, which has been reported to closely reflect the number of autophagosomes (21). Control cells expressing shScr were placed under amino acid starvation to induce autophagy, then incubated in the presence or absence of chloroquine, an inhibitor of autophagosome-lysosome fusion. An increased amount of LC3-II was observed in chloroquine-treated control cells, which was further increased by treatment of the cells with both amino acid starvation and chloroquine (Figure 5A). A similar expression profile of LC3-II was observed in amino acid-starved *JLP* knockdown cells (Figure 5A),

suggesting that *JLP* knockdown has little or no effect on LC3-II generation in amino acid starvation-induced autophagy. We next asked whether JLP is involved in autophagosome-lysosome fusion, part of the maturation process of autophagosomes. To examine this possibility, we employed a unique, tandem fluorophore reporter, mRFP-GFP-LC3 (22). We expressed mRFP-GFP-LC3 by lentiviral transduction in the control and *JLP* knockdown cells, performed amino acid starvation, and immunostained cells with an antibody against LAMP-1. Control cells showed a good colocalization of mRFP puncta and LAMP-1 signals, and low colocalization of punctate signals of LAMP-1-positive mRFP with GFP (Figures 5B-5D). By contrast, in *JLP* knockdown cells we observed low colocalization of mRFP puncta and LAMP-1 signals, and good colocalization of punctate signals of LAMP-1-positive mRFP with GFP (Figures 5B-5D). The altered profile observed in the *JLP* knockdown was reversed by the expression of HA-JLP_WT or HA-JLP_N, but not HA-JLP_ΔKBD (Figures 5B-5D). Taken together, these results suggest that JLP plays an important role in autophagy by regulating lysosome localization.

4. Discussion

In the present study, we demonstrated that JLP plays an important role in lysosome localization and autophagy, as evidenced by the lysosome distribution and the impairment of autophagosome-lysosome fusion in *JLP* knockdown cells.

It is well known that lysosomes move toward the cell center using dynein motors (1,3). Additionally, JLP has been reported to interact with p150^{glued}, a key component of the dynactin complex (23). However, expression of a JLP mutant lacking the binding domain of dynactin p150^{glued} in *JLP* knockdown cells restored the altered lysosomal distribution (Figure 2). JLP has been suggested to interact with p50/dynamitin (23), a component of dynactin complex. Therefore, it is possible that other component(s) of the dynein-dynactin complex, including p50/dynamitin, are involved in lysosome

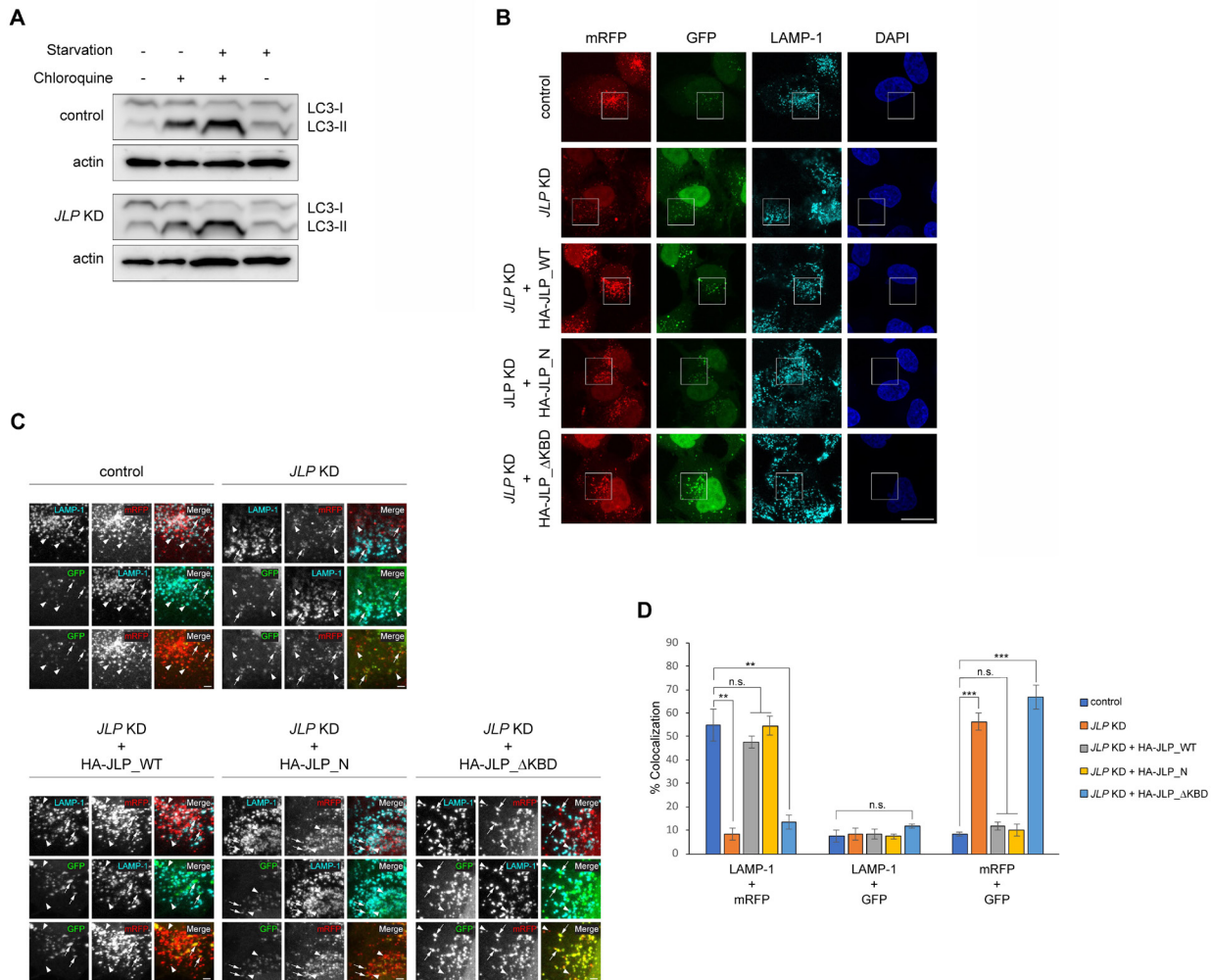


Figure 5. JLP mediates autophagy induction. (A) HeLa cells expressing shScr (control) or shJLP#2 (*JLP* KD) were amino acid starved for 4 hours in the absence or presence of chloroquine, as indicated, and subjected to western blotting with an anti-LC3 antibody. Actin was utilized as a loading control. (B) The control and *JLP* knockdown HeLa cells treated as in (A) were transduced with a lentivirus expressing the mRFP-GFP-LC3 fusion protein, amino acid starved for 4 hours, immunostained with an anti-LAMP-1 antibody, fixed, and analyzed by confocal microscopy. For rescue experiments, *JLP* knockdown HeLa cells were transduced with lentiviruses expressing HA-JLP_WT, HA-JLP_N, or HA-JLP_ΔKBD as indicated together with mRFP-GFP-LC3, amino acid starved for 4 hours, immunostained, fixed, and analyzed as described above. Nuclei were stained with DAPI. Areas in the boxes indicated by dotted-lines are shown at a higher magnification in (C). Scale bar, 20 μ m. (C) Arrowheads indicate typical examples of colocalization signals of LAMP-1 and mRFP. Arrows indicate typical examples of colocalization signals of mRFP and GFP. Scale bars, 2 μ m. (D) The results of the colocalization analyses in (B) and (C) were quantified. At least 20 cells per experimental condition were analyzed. ** $p < 0.01$; *** $p < 0.001$; n.s., not significant.

localization through interaction with JLP.

Willett *et al.* (4) identified the dynein adaptor JLP as a binding protein of the lysosomal transmembrane protein TMEM55B, and proposed that TMEM55B recruits JLP to the lysosomal surface and facilitates dynein-dependent transport of lysosomes under stress conditions, including starvation. In addition, they demonstrated a scattered distribution of lysosomes in cells depleted of TMEM55B or JLP (4). Here we found the

N-terminal half fragment of JLP is necessary and sufficient to rescue the dispersed distribution of lysosomes in *JLP* knockdown cells, although this N-terminal fragment is unable to bind with TMEM55B (Figure 3). It is therefore unlikely that the JLP-TMEM55B interaction is involved in the regulation of lysosome localization. However, we cannot rule out

the possibility that the JLP N-terminal region indirectly interacts with TMEM55B through unknown factor(s). Further studies are needed to clarify the mechanisms of JLP- and/or TMEM55B-mediated lysosome distribution.

We found in this study that a JLP mutant lacking the KBD was unable to reverse the altered distribution of lysosomes in *JLP* knockdown cells (Figure 4). This result might suggest that JLP mediates retrograde transport of lysosomes *via* interaction with kinesin-1. In support of this possibility, Arimoto *et al.* (24) reported that kinesin-1 and UNC-16, an ortholog of mammalian JLP and its family member JSAP1, are required for retrograde transport of various axonal proteins in *Caenorhabditis elegans*. It is also possible that the KBD may have another function, unrelated to kinesin-1, which is necessary for retrograde transport of lysosomes.

This study provides new insight into the regulatory mechanisms of lysosomal trafficking. Our findings contribute to the understanding of how lysosomes exert their multiple functions, potentially enabling the identification of molecular targets for diseases caused by lysosomal dysfunction.

Acknowledgements

This study was supported in part by JSPS KAKENHI Grant Numbers 16K08579 (to KY) and 19K16737 (to IKG).

References

- Pu J, Guardia CM, Keren-Kaplan T, Bonifacino JS. Mechanisms and functions of lysosome positioning. *J Cell Sci.* 2016; 129:4329-4339.
- Cabukusta B, Neefjes J. Mechanisms of lysosomal positioning and movement. *Traffic.* 2018; 19:761-769.
- Lawrence RE, Cho KF, Rappold R, Thrun A, Tofaute M, Kim DJ, Moldavski O, Hurley JH, Zoncu R. The lysosome as a cellular centre for signalling, metabolism and quality control. *Nat Cell Biol.* 2018; 20:1052-1063.
- Willett R, Martina JA, Zewe JP, Wills R, Hammond GRV, Puertollano R. TFEB regulates lysosomal positioning by modulating TMEM55B expression and JIP4 recruitment to lysosomes. *Nat Commun.* 2017; 8:1580.
- Lee CM, Onésime D, Reddy CD, Dhanasekaran N, Reddy EP. JLP: A scaffolding protein that tethers JNK/p38MAPK signaling modules and transcription factors. *Proc Natl Acad Sci U S A.* 2002; 99:14189-14194.
- Kelkar N, Standen CL, Davis RJ. Role of the JIP4 scaffold protein in the regulation of mitogen-activated protein kinase signaling pathways. *Mol Cell Biol.* 2005; 25:2733-2743.
- Verhey KJ, Meyer D, Deehan R, Blenis J, Schnapp BJ, Rapoport TA, Margolis B. Cargo of kinesin identified as JIP scaffolding proteins and associated signaling molecules. *J Cell Biol.* 2001; 152:959-970.
- Cavalli V, Kujala P, Klumperman J, Goldstein LS. Sunday Driver links axonal transport to damage signaling. *J Cell Biol.* 2005; 168:775-787.
- Sun F, Zhu C, Dixit R, Cavalli V. Sunday Driver/JIP3 binds kinesin heavy chain directly and enhances its motility. *EMBO J.* 2011; 30:3416-3429.
- Tuvshintugs B, Sato T, Enkhtuya R, Yamashita K, Yoshioka K. JSAP1 and JLP are required for ARF6 localization to the midbody in cytokinesis. *Genes Cells.* 2014; 19:692-703.
- Sato T, Ishikawa M, Yoshihara T, Nakazato R, Higashida H, Asano M, Yoshioka K. Critical role of JSAP1 and JLP in axonal transport in the cerebellar Purkinje cells of mice. *FEBS Lett.* 2015; 589(19 Pt B):2805-2811.
- Sato T, Ishikawa M, Mochizuki M, Ohta M, Ohkura M, Nakai J, Takamatsu N, Yoshioka K. JSAP1/JIP3 and JLP regulate kinesin-1-dependent axonal transport to prevent neuronal degeneration. *Cell Death Differ.* 2015; 22:1260-1274.
- Li R, Gunarta IK, Suzuki R, Boldbaatar J, Nakazato R, Yuliana D, Davaakhuu G, Oyunsuren T, Takamatsu N, Kobayashi M, Hirao A, Yoshioka K. JLP-JNK signaling protects cancer cells from reactive oxygen species-induced cell death. *Biochem Biophys Res Commun.* 2018; 501:724-730.
- Boldbaatar J, Gunarta IK, Suzuki R, Erdenebaatar P, Davaakhuu G, Hohjoh H, Yoshioka K. Protective role of c-Jun NH₂-terminal kinase-associated leucine zipper protein (JLP) in curcumin-induced cancer cell death. *Biochem Biophys Res Commun.* 2020; 522:697-703.
- Ito M, Yoshioka K, Akechi M, Yamashita S, Takamatsu N, Sugiyama K, Hibi M, Nakabeppu Y, Shiba T, Yamamoto KI. JSAP1, a novel jun N-terminal protein kinase (JNK)-binding protein that functions as a Scaffold factor in the JNK signaling pathway. *Mol Cell Biol.* 1999; 19:7539-7548.
- Sato T, Torashima T, Sugihara K, Hirai H, Asano M, Yoshioka K. The scaffold protein JSAP1 regulates proliferation and differentiation of cerebellar granule cell precursors by modulating JNK signaling. *Mol Cell Neurosci.* 2008; 39:569-578.
- Morita E, Arai J, Christensen D, Votteler J, Sundquist WI. Attenuated protein expression vectors for use in siRNA rescue experiments. *Biotechniques.* 2012; 0:1-5.
- Sato T, Enkhat A, Yoshioka K. Role of plasma membrane localization of the scaffold protein JSAP1 during differentiation of cerebellar granule cell precursors. *Genes Cells.* 2011; 16:58-68.
- Michelet X, Garg S, Wolf BJ, Tuli A, Ricciardi-Castagnoli P, Brenner MB. MHC class II presentation is controlled by the lysosomal small GTPase, Arl8b. *J Immunol.* 2015; 194:2079-2088.
- Korolchuk VI, Saiki S, Lichtenberg M, Siddiqi FH, Roberts EA, Imarisio S, Jahress L, Sarkar S, Futter M, Menzies FM, O'Kane CJ, Deretic V, Rubinsztein DC. Lysosomal positioning coordinates cellular nutrient responses. *Nat Cell Biol.* 2011; 13:453-60.
- Kabeya Y, Mizushima N, Ueno T, Yamamoto A, Kirisako T, Noda T, Kominami E, Ohsumi Y, Yoshimori T. LC3, a mammalian homologue of yeast Apg8p, is localized in autophagosome membranes after processing. *EMBO J.* 2000; 19:5720-5728.
- Kimura S, Noda T, Yoshimori T. Dissection of the autophagosome maturation process by a novel reporter protein, tandem fluorescent-tagged LC3. *Autophagy.* 2007; 3:452-460.
- Cavalli V, Kujala P, Klumperman J, Goldstein LS. Sunday Driver links axonal transport to damage signaling. *J Cell Biol.* 2005; 168:775-787.
- Arimoto M, Koushika SP, Choudhary BC, Li C, Matsumoto K, Hisamoto N. The Caenorhabditis elegans JIP3 protein UNC-16 functions as an adaptor to link kinesin-1 with cytoplasmic dynein. *J Neurosci.* 2011; 31:2216-2224.

Received January 7, 2020; Accepted January 9, 2020.

*Address correspondence to:

Katsuji Yoshioka, Division of Molecular Cell Signaling, Cancer Research Institute, Kanazawa University, Kakumachi, Kanazawa, Ishikawa 920-1192, Japan.
E-mail: katsuji@staff.kanazawa-u.ac.jp

Released online in J-STAGE as advance publication February 5, 2020.

Usefulness of next-generation DNA sequencing for the diagnosis of urinary tract infection

Toru Ishihara¹, Nobuo Watanabe², Shigeaki Inoue², Hiromichi Aoki², Tomoatsu Tsuji², Bunsei Yamamoto², Hidetaka Yanagi¹, Masayuki Oki¹, Kirill Kryukov³, So Nakagawa³, Sadaki Inokuchi², Hideki Ozawa¹, Tadashi Imanishi^{3,*}

¹ Department of General Internal Medicine, Tokai University School of Medicine, Isehara, Kanagawa, Japan;

² Department of Emergency and Critical Care Medicine, Tokai University School of Medicine, Isehara, Kanagawa, Japan;

³ Department of Molecular Life Science, Tokai University School of Medicine, Isehara, Kanagawa, Japan.

SUMMARY Acute urinary tract infection (UTI) is a highly common clinical condition. Although bacterial culture is the gold standard diagnostic test, false negative results may be possible, leading to the pathogen being unidentified. In recent years, bacterial DNA sequencing analysis has garnered much attention, but clinical studies are rare in Japan. In this study, we assessed the usefulness of next-generation DNA sequencing (NGS) analysis for acute UTI patients. We thus performed an observational, retrospective case series study. Urine and blood samples were collected from ten acute UTI patients, of whom four had also been diagnosed with urosepsis. Seven variable regions of bacterial 16S rRNA genes were amplified by PCR and then sequenced by IonPGM. The identified bacterial species were compared with those identified using the culture tests and the clinical parameters were analyzed. As a result, the NGS method effectively identified predominant culture-positive bacteria in urine samples. The urine NGS also detected several culture-negative species, which have been reported to be potentially pathogenic. Out of four urosepsis cases, three were pathogen-positive in blood NGS results, while two were pathogen-negative in blood culture. In one sepsis case, although blood culture was negative for *Escherichia coli*, this species was detected by blood NGS. For non-sepsis cases, however, blood NGS, as well as blood culture, was less effective in detecting bacterial signals. In conclusion, NGS is potentially useful for identifying pathogenic bacteria in urine from acute UTI patients but is less applicable in patients who do not meet clinical criteria for sepsis.

Keywords Next-generation DNA sequencing, 16S rRNA amplicon sequencing analysis, urinary tract infection

1. Introduction

Urinary tract infection (UTI) is a highly common condition diagnosed at emergency departments (ED) worldwide. The pathology of UTIs has various subdivisions, notably upper or lower, simple or complex, and minor or serious (1). Urosepsis has high morbidity and mortality rates, and as such, its early diagnosis and treatment are essential (2). Clinicians diagnose patients with UTIs comprehensively based on clinical conditions and their clinical parameters, collect urine and blood samples, and begin broad-spectrum antibiotic treatment experimentally (3). Later, when the UTI diagnosis is more definite based on the culture results, more targeted antibiotics are prescribed. However, if the culture test is negative, the pathogenic bacteria remains unidentified. This is potentially due to previous antibiotic exposure, error at the time of

sampling, an insufficient sample volume, and/or un-culturable bacteria (4). Unidentified pathogenic bacteria can cause many issues in the quality of diagnosis and treatment, such as the administration of less-effective antibiotics, and futile repeated antibiotic administration. These situations can escalate medical costs.

While the gold standard test for pathogenic bacteria is still the conventional culture test, bacterial DNA sequencing analysis tests are gaining attention in recent years (5,6). This is due to recent advances in next-generation DNA sequencing (NGS) technology. Nevertheless, there is a lack of clinical studies comparing conventional culture tests and bacterial DNA sequencing analysis, as well as medical case data. Furthermore, blood cultures in addition to urine cultures are recommended for complex pyelonephritis and urosepsis (7). Identifying the pathogenic bacteria in bacteremia patients is very important owing to its

potential impact on patient condition. However, few studies have examined both urine and blood samples by comparing cultures and NGS, and included clinical contexts. Here we investigated the advantages and limitations of using NGS as a method to identify pathogenic bacteria in ED patients with acute UTI. To our knowledge, this is the first report addressing these issues in Japan.

2. Materials and Methods

2.1. Definition of UTI

UTIs were diagnosed comprehensively through a combination of clinical condition, urinalysis, and imaging test findings after excluding other sources of infection. Acute cystitis included typical urinary symptoms such as urinary urgency, frequent urination, painful urination, abdominal pain, and suprapubic pain. Acute pyelonephritis included chills, fever, flank pain, costovertebral angle tenderness, nausea, and vomiting. Urosepsis and septic shock were also included, and diagnoses followed the definition of sepsis (sepsis-3) (8). Urinalysis included qualitative examination of urine sediment, white blood cell count ($400 \times$ magnification), nitrous acid level, Gram staining, and culture bacterial count. Non-contrast CT scans assessed hydronephrosis, ureteropelvic enlargement, ureteral calculus, and gas formation. Contrast CT scans were used to search for renal abscess and localized sparse pathological changes.

2.2. Ethics and study design

Here we performed an observational and retrospective case series study, which was approved by the Clinical Ethical Committee of Tokai University Medical School (14R220). This study also conforms to the Helsinki Declaration. We conducted this study at two hospitals of Tokai University in Japan between January 2017 and December 2017. The study subject group consisted of ED cases of acute UTI, including subgroups such as upper and lower, simple and complex, and mild and severe. Samples were only collected after explaining the details of the study to the patients and receiving their written consent or that of their families. A total of ten patients agreed to participate in the study and their urine and blood samples were collected in sterile containers and heparin-coated evacuated blood collection tubes, respectively, by experienced registered nurses or physicians operating in a standard disinfected and hygienic manner. Unless otherwise noted, blood and urine samples were collected before the initial administration of antibiotics and subjected to culture and NGS tests. All patients underwent antibiotic treatment based on conventional urine and blood culture. The results of the urine and blood NGS

tests were not revealed to patients or to their attending physicians, and thus these results did not influence their treatment. For all cases, after the patients were discharged from the hospital, a retrospective examination was conducted comparing the NGS and culture test results, taking into account the clinical contexts.

2.3. NGS Methodology (Bacterial 16S rRNA amplicon sequencing analysis)

Blood and urine samples were aliquoted and stored at -80°C until use. DNA in urine was isolated using a DNeasy Blood & Tissue Kit (Qiagen, Hilden, Germany) with some modifications to the manufacturer's protocol. Urine (~ 1 mL) was thawed and centrifuged at $10,000 \times g$ for 10 min, and particulate materials were collected. The particulates were suspended in 180 μL of a lysis buffer (1.2% Triton X-100, 20 mg/mL lysozyme, 2 mM EDTA, 20 mM Tris-HCl (pH 8.0)) and incubated at 37°C for 30 min. Next, 4 μL of RNase (100 mg/mL) was added and the reaction was allowed to stand for 2 min at room temperature (22 - 25°C). Proteinase K (25 μL) and buffer AL (200 μL), both supplied with the kit, were then added to the mixture, followed by incubation at 56°C for 30 min. After mixing with 200 μL ethanol, the mixture was applied to the column. Subsequent purification processes were carried out according to the manufacturer's instructions.

Bacterial DNA in blood was isolated as described previously (9). Bacterial 16S rRNA gene variable regions were amplified from both DNA samples and were sequenced by IonPGM followed by our in-house metagenomic data analysis pipeline, Genome Search Toolkit (GSTK, <http://kirill-kryukov.com/study/tools/gstk/>) with 5840 representative bacterial species' genomes (<http://genomesync.org>) as described previously (9).

In this study, we assumed that a bacterial species exists in a given sample if the number of sequence reads corresponding to the species exceed 10% of those corresponding to all bacterial species.

3. Results and Discussion

3.1. Characteristics of patients with acute UTI

A total of ten acute UTI patients (three male and seven female, median age: 85 years) were included in this study. The patients' characteristics are summarized in Table 1. Of the ten cases, two were lower- and eight were upper-UTIs. Three were uncomplicated and seven were complicated. Cases 1-6 were diagnosed as non-sepsis and cases 7-10 as urosepsis. The range of sequential organ failure assessment (SOFA) scores among the urosepsis cases was 3-17, indicating mild to severe organ failure. Initial antibiotics were selected

Table 1 Characteristics of 10 patients with acute urinary tract infection

Case	Age/sex	Onset of UTI	Type of UTI (cause)	Sepsis(SOFA)	Septic shock	Initial laboratory data	Initial Antibiotics	Definitive Antibiotics	ICU stay	Hospital stay	Outcome
1	89, M	Community	Complicated acute cystitis (prostate cancer)	No	No	WBC 9300/ μ L CRP 1 mg/dL	ABPC/SBT	Same	No	34 days	Improved
2	89, F	Community	Uncomplicated acute cystitis	No	No	WBC 17800/ μ L CRP 16 mg/dL	ABPC/SBT	CTR _X	No	14 days	Improved
3	86, F	Community	Uncomplicated acute pyelonephritis	No	No	WBC 9300/ μ L CRP 3 mg/dL	CTR _X	Same	No	12 days	Improved
4	74, F	Medical facility	Complicated UTI (neurogenic bladder)	No	No	WBC 13600/ μ L CRP 7 mg/dL	CTR _X	Same	No	1 days	Unknown
5	68, F	Community	Complicated UTI (ureteral calculi)	No	No	WBC 13600/ μ L CRP 51 mg/dL	LVFX	Same	No	18 days	Improved
6	84, M	Medical facility	Complicated acute pyelonephritis (neurogenic bladder)	No	No	WBC 8300/ μ L CRP 21 mg/dL	CTR _X	Same	No	6 days	Improved
7	86, F	Medical facility	Uncomplicated acute pyelonephritis	Yes (3)	No	WBC 9300/ μ L CRP 4 mg/dL	CTR _X	Same	No	34 days	Improved
8	66, F	Community	Complicated UTI (ureteral calculi)	Yes (8)	Yes	WBC 24300/ μ L CRP 22 mg/dL	CFPM TOB VCM	CTR _X	3 days	11 days	Improved
9	86, M	Medical facility	Complicated UTI (renal abscess)	Yes (11)	Yes	WBC 30200/ μ L CRP 12 mg/dL	CFPM CPFX VCM	CTR _X	10 days	95 days	Improved
10	82, F	Community	Complicated UTI (ureteral calculi)	Yes (17)	Yes	WBC 27200/ μ L CRP 46 mg/dL	CTR _X VCM	Same	2 days	2 days	Death

ABPC/SBT, Ampicillin/sulbactam; CFPM, Cefepime; CPFX, Ciprofloxacin; CRP, C reactive protein (normal < 0.3 mg/dL); CTR_X, Ceftriaxone; ICU, intensive care unit; LVFX, Levofloxacin; SOFA, sequential organ failure assessment; TOB, Tobramycin; UTI, urinary tract infection; VCM, Vancomycin; WBC, white blood cell.

empirically with reference to the clinical background, severity, and Gram stain test results. Three patients were admitted to the intensive care unit. Nine patients improved, but one died.

3.2. Comparison of culture and NGS results

Table 2 summarizes our comparison of culture and NGS results from the patients' urine and blood samples. Nine out of ten cases were pathogen-positive in urine culture results, whereas all ten were pathogen-positive in urine NGS results. In most cases, the pathogenic species identified in the urine culture were also predominant in the urine NGS data. However, urinary NGS detected many additional bacteria that were negative in urine culture. Two out of the four urosepsis cases (Case 7-10) were pathogen-positive in blood culture results, and three were pathogen-positive in blood NGS results. In case 7, only contamination was detectable, in culture and NGS analysis of blood. In non-sepsis cases (Cases 1-6), blood culture and NGS testing detected some bacteria that were different from those detected by culture and NGS analysis of urine.

3.3. Usefulness of NGS for the diagnosis of acute UTI

In this study, we evaluated an NGS analysis of 16S rRNA gene amplicons as a new method of detecting pathogenic bacteria in acute UTI patients by studying a group of cases. The study revealed the advantages and limitations of NGS testing in comparison with conventional culture testing of urine and blood. The following three points were demonstrated as clinically important for utilizing NGS testing. Firstly, our results imply that urine NGS testing is not only a potential substitute for urine culture testing but is also useful for detecting other dangerous unculturable bacteria. Secondly, blood NGS testing may be useful for detecting severely spreading pathogenic bacteria in severe urosepsis cases. Lastly, it seems likely that our data from non-severe, non-sepsis cases reflect the potential of NGS for detecting false-positive bacteria due to contaminants or noise, as a result of low abundance of infecting bacteria in the blood.

3.4. Advantages of urine NGS in acute UTI patients

In support of the usefulness of urine NGS testing, we found that in most cases, urine culture-positive pathogenic bacteria showed the highest occupancy rates in urine NGS. Furthermore, urine NGS detected many additional bacteria that were negative in the urine culture. As discussed below, we found some evidence supporting the contention that this result reflected more sensitive detection of pathogenic bacteria by urine NGS, rather than contamination.

The pathogenic bacteria detected in urine culture

NGS tests are shown in Figure 1. In this study, the pathogenic bacteria detected in both the urine culture and NGS tests were *Escherichia coli*, *Klebsiella pneumoniae*, *Proteus mirabilis*, *Enterococcus faecalis*, and *Aerococcus urinae*, which are all common UTI pathogenic bacteria (10,11). In addition, many other bacteria detected in the urine NGS tests were negative in the urine culture tests. The NGS-detectable, unculturable bacteria included some pathogenic bacteria occasionally found in UTIs by previous studies (10-14). Possibly owing to prior antibiotic administration, Case 6 tested negative for *Aerococcus urinae* in a urine culture test, but positive in a urine NGS test. This could have been the causative bacteria, whose DNA was detected by NGS from its dead remnants. Therefore, urine NGS tests may be able to detect bacteria even after antibiotic administration (15). For Case 7, the urine culture test showed *Streptococcus species*, but the urine NGS test showed *Aerococcus urinae*, which previous evidence suggests is likely to be the true causative bacterium. *Aerococcus urinae* are often difficult to isolate by urine culture and are therefore suitable for diagnosis by genome analysis (16).

A recent study comparing urine culture and NGS testing reported that in acute cystitis cases, urine NGS testing demonstrates good diagnostic performance and is helpful in medical treatment (17). However, this study was limited to acute cystitis cases, and did not examine detailed information about the pathogenic bacteria detected, nor did it perform blood NGS tests simultaneously.

3.5. Advantages of blood NGS in urosepsis patients

Our second main finding was evidence supporting the usefulness of blood NGS testing for detecting pathogenic bacteria in very severe cases of urosepsis. Two out of four urosepsis cases (Cases 7-10) were pathogen-positive in blood culture results, and three were pathogen-positive in blood NGS results. Therefore, blood NGS may be able to detect pathogenic bacteria more sensitively than (or at a comparable level to) blood culture.

Figure 2 shows the occupation ratios of bacteria based on urine and blood NGS tests of urosepsis cases. Notably, the blood culture test of Case8 was negative for *Escherichia coli*, but this species was detected in both blood and urine by the NGS tests. *Escherichia coli* was also detected in both blood culture and blood NGS tests in Case 10, coinciding with the results of the upper urinary tract culture from ureteral calculus. Ureteral calculus UTIs are highly likely affected by pathogenic bacteria from the upper area rather than the obstruction area, and the bacteria can differ from those in the urine of the lower area (18). In urosepsis cases, the causative bacterium commonly detected by both blood culture tests and blood NGS tests was *Escherichia*

Table 2 Comparison of urine culture and urine NGS, blood culture and blood NGS

Case	Antibiotics before sampling	Urine culture (colony forming units/mL)	Urine NGS	Blood culture	Blood NGS
1	No	<i>Enterococcus faecalis</i> (10^4 cfu/mL)	<i>Enterococcus faecalis</i> 49%	Negative	No bacteria (more than 10%)
2	No	<i>Proteus mirabilis</i> (10^7 cfu/mL) <i>Lactobacillus species</i> (10^7 cfu/mL)	<i>Proteus mirabilis</i> 58% <i>Actinotignum schaalii</i> 14%	Negative	<i>Bacteroides vulgatus</i> 16%
3	No	<i>Klebsiella pneumoniae</i> (10^6 cfu/mL)	<i>Klebsiella pneumoniae</i> 18% <i>Salmonella enterica</i> 13% <i>Enterobacter lignolyticus</i> 10%	Negative	No bacteria (more than 10%)
4	Yes	ESBL <i>Escherichia coli</i> (10^6 cfu/mL)	<i>Escherichia coli</i> 65%	Negative	No bacteria (more than 10%)
5	No	<i>Escherichia coli</i> (10^6 cfu/mL)	<i>Escherichia coli</i> 55%	<i>Staphylococcus epidermidis</i>	<i>Staphylococcus capitis</i> 20% <i>Staphylococcus epidermidis</i> 18% <i>Comamonas kerstersii</i> 12% <i>Corynebacterium aurimucosum</i> 10%
6	Yes	Negative	<i>Aerococcus urinae</i> 20%	<i>Bacillus species</i>	No bacteria (more than 10%)
7	No	<i>Streptococcus species</i> (10^7 cfu/mL) <i>Escherichia coli</i> (10^6 cfu/mL)	<i>Aerococcus urinae</i> 51% <i>Escherichia coli</i> 19%	<i>Staphylococcus epidermidis</i>	<i>Corynebacterium glucuronolyticum</i> 12%
8	No	<i>Escherichia coli</i> (10^2 cfu/mL)	<i>Escherichia coli</i> 57%	Negative	<i>Escherichia coli</i> 28%
9	No	<i>Escherichia coli</i> (10^7 cfu/mL)	<i>Escherichia coli</i> 48% <i>Streptococcus dysgalactiae</i> 14%	<i>Escherichia coli</i>	<i>Escherichia coli</i> 52%
10	No	*Lower urine <i>Aerococcus urinae</i> (10^5 cfu/mL) <i>Lactobacillus species</i> (10^5 cfu/mL) <i>Enterobacteria</i> (10^3 cfu/mL) *Upper urine <i>Escherichia coli</i> (10^6 cfu/mL)	*Lower urine <i>Aerococcus urinae</i> 25% <i>Lactobacillus gasseri</i> 14% <i>Escherichia coli</i> 12% *Upper urine Not tested	<i>Escherichia coli</i>	<i>Escherichia coli</i> 11%

coli, which was considered to be the likely causative bacteria because it is the most common pathogenic bacterium in urosepsis (19). Blood NGS testing is therefore useful for identifying the pathogenic bacteria that are clinically most important and influential. This requirement is also present for blood culture testing in febrile UTIs (20).

A recent study of ICU patients with suspected sepsis reported that, in comparison with blood culture testing, blood NGS testing had the advantage of detecting multiple pathogenic bacteria. Furthermore, diagnostic sensitivity was significantly higher in blood NGS than blood culture (21).

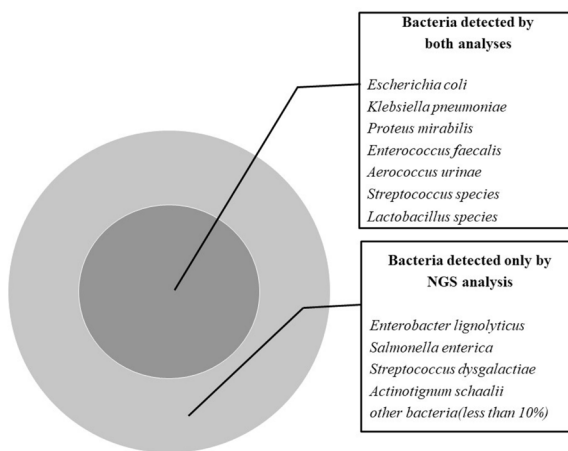


Figure 1. Venn diagram of urine culture and urine NGS results for all UTI cases. The pathogenic bacteria detected in both the urine culture and NGS tests were *Escherichia coli*, *Klebsiella pneumoniae*, *Proteus mirabilis*, *Enterococcus faecalis*, and *Aerococcus urinae*, which are all common UTI pathogenic bacteria. In addition, many other bacteria detected in the urine NGS tests were negative in the urine culture tests.

3.6. Disadvantages of blood NGS in non-sepsis patients

Our third major finding was that, in less-severe, non-sepsis UTI cases (Cases 1-6), blood NGS testing requires increased caution regarding the possibility of false-positives due to contamination. In Cases 1, 3, 4, and 6, although no bacterial species exceeded the threshold occupancy rate of 10% in the blood NGS test, a large number of bacterial species with extremely low occupancy rates were detected. In Case 5, some bacteria with occupancy rates over 10% were detected with the blood NGS test, but the bacteria detected by the urine and blood NGS tests were different, suggesting that they may have been false-positives. Generally, in UTI-induced bacteremia, the same bacterial species are detected in urine and blood (22). Previous studies have addressed the question of whether bacteria cultured from blood are true bloodstream infections or contaminant bacteria. In light of these reports, we suspect that the blood NGS results of Case 5 may represent contaminations (23).

The primary cause of false positives is live bacterial contamination, but another cause is DNA contamination from dead bacteria after sterilization. It is difficult to completely remove contamination, and its most frequent source is the patient's skin at the time of drawing blood (24). Furthermore, because NGS testing involves several steps, contamination can occur from the environment or the experimental materials used in testing (21). The second cause of false positives is related to the fact that NGS testing displays the relative abundance of bacteria, rather than their absolute quantities. That is, even if no pathogenic bacteria are present in the blood from healthy donors, the blood NGS test inevitably amplifies small quantities of contaminants.

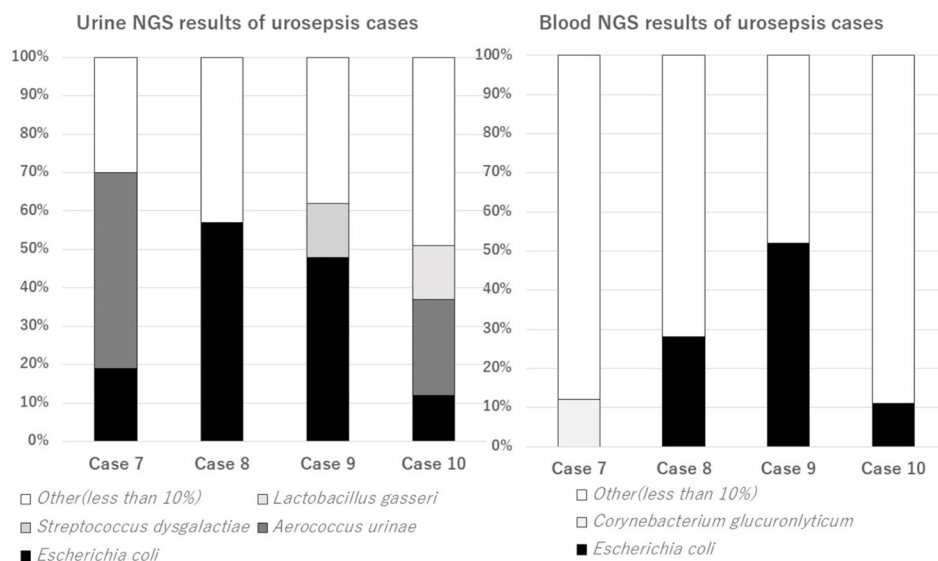


Figure 2. Bacterial occupancy rate based on urine and blood NGS in urosepsis cases. In cases 8-10, both urine and blood NGS results are positive for *Escherichia coli*, which is the most important causative bacteria of urosepsis cases.

Furthermore, a recent study reported that many anaerobic bacteria can be detected in the blood of healthy people by NGS, suggesting the presence of asymptomatic bacteremia (25). The detection of bacteria with little or no pathogenicity in the blood of healthy people can cause confusion in clinical diagnosis and treatment. Thus, the results of blood NGS tests for low-severity non-sepsis UTI cases are not reliable.

We propose the following two practices to overcome these limitations of blood NGS testing. First, NGS tests should be conducted on both urine and blood. We also suggest conducting separate NGS tests of blood taken from two or more different sites, before any antibiotics are administered to the patient. This would be useful for distinguishing true infection from contamination and is a standard method in blood culture tests (26). The second proposal is to use blood NGS testing for cases that are highly likely to be bacteremia. As predictors for true bacteremia, fevers and increased white blood cell counts are not sufficient; it has been reported that shaking chills are a more useful indicator (27). Additionally, there is a strong relationship between having quick SOFA ≥ 2 and bacteremia (28). In fact, this study also used quick SOFA ≥ 2 as a criterion of diagnosing urosepsis, in line with the guideline for sepsis-3.

3.7. Limitations of this study

This study has several notable limitations. Firstly, it was confined to retrospective observational analysis of a group of cases, and no statistical analysis was carried out. Furthermore, before the practical application of NGS testing, practical limitations including turnaround time and cost have to be addressed. It takes nearly one week to complete the entire process, from preparing the library, to using the GSTK program, and to analyzing data. For us, the material cost of an NGS test is around \$100 (USD). To use NGS testing practically, these issues will need to be overcome (9).

4. Conclusion

The results of this study suggest that as a method of identifying pathogenic bacteria in acute UTI patients, urine NGS testing is highly accurate and useful. For sepsis patients, conducting blood NGS testing in parallel may increase the likelihood of detecting the most clinically important pathogenic bacteria. On the other hand, NGS testing involves some limitations that need to be overcome, such as the need to optimize the criteria for applying this method, the qualitative nature of the results, contamination, and the time and expense of the tests. Nevertheless, for cases in which the pathogenic bacteria are unculturable, this method deserves attention as a new and highly sensitive diagnostic technique. To refine this method, it will be important to accumulate more clinical data.

Acknowledgements

This work was financially supported by AMED J-GRID (Grant Number JP17fm0108023) and a research grant from Takeda Science Foundation. We would like to thank Editage (<http://www.editage.jp>) for English language editing. We acknowledge Ms. Keiko Yokoyama of the Support Center for Medical Research and Education of Tokai University for her excellent technical supports.

References

1. Long B, Koyfman A. The emergency department diagnosis and management of urinary tract infection. *Emerg Med Clin North Am.* 2018; 36:685-710.
2. Wagenlehner FM, Tandogdu Z, Bjerklund Johansen TE. An update on classification and management of urosepsis. *Curr Opin Urol.* 2017; 27:133-137.
3. Gupta K, Grigoryan L, Trautner B. Urinary tract infection. *Ann Intern Med.* 2017; 167:ITC49-ITC64.
4. Lever A, Mackenzie I. Sepsis: definition, epidemiology, and diagnosis. *BMJ.* 2007; 335:879-883.
5. Smelov V, Naber K, Bjerklund Johansen TE. Letter to the Editor: Diagnostic criteria in urological diseases do not always match with findings by extended culture techniques and metagenomic sequencing of 16S rDNA. *Open Microbiol J.* 2016; 10:23-26.
6. Smelov V, Naber K, Bjerklund Johansen TE. Improved classification of urinary tract infection: future consideration. *Eur Urol Suppl.* 2016; 15:71-80.
7. Long B, Koyfman A. Best clinical practice: blood culture utility in the emergency department. *J Emerg Med.* 2016; 51:529-539.
8. Seymour CW, Liu VX, Iwashyna TJ, Brunkhorst FM, Rea TD, Scherag A, Rubenfeld G, Kahn JM, Shankar-Hari M, Singer M, Deutschman CS, Escobar GJ, Angus DC. Assessment of clinical criteria for sepsis: For the third international consensus definitions for sepsis and septic shock (Sepsis-3). *JAMA.* 2016; 315:762-774.
9. Watanabe N, Kryukov K, Nakagawa S, Takeuchi JS, Takeshita M, Kirimura Y, Mitsuhashi S, Ishihara T, Aoki H, Inokuchi S, Imanishi T, Inoue S. Detection of pathogenic bacteria in the blood from sepsis patients using 16S rRNA gene amplicon sequencing analysis. *PLoS One.* 2018; 13:e0202049.
10. Czaja CA, Scholes D, Hooton TM, Stamm WE. Population-based epidemiologic analysis of acute pyelonephritis. *Clin Infect Dis.* 2007; 45:273-280.
11. Echols RM, Tosiello RL, Haverstock DC, Tice AD. Demographic, clinical, and treatment parameters influencing the outcome of acute cystitis. *Clin Infect Dis.* 1999; 29:113-119.
12. Horton LE, Mehta SR, Aganovic L, Fierer J. *Actinotignum schaalii* infection: A clandestine cause of sterile pyuria? *Open Forum Infect Dis.* 2018; 5:ofy015.
13. Mellon G, Delanoe C, Roux AL, Heym B, Dubourg O, Hardy P, Chevallier B, Perronne C, Rouveix E, Salomon J. Non-typhi *Salmonella enterica* urinary tract infections. *Med Mal Infect.* 2017; 47:389-393.
14. Takahashi T, Asami R, Tanabe K, Hirono Y, Nozawa Y, Chiba N, Ubukata K. Clinical aspects of invasive infection with *Streptococcus dysgalactiae* subsp. *equisimilis* in elderly patients. *J Infect Chemother.* 2010; 16:68-71.

15. Budding AE, Hoogewerf M, Vandembroucke-Grauls CM, Savelkoul PH. Automated broad-range molecular detection of bacteria in clinical samples. *J Clin Microbiol.* 2016; 54:934-943.
16. Rasmussen M. Aerococci and aerococcal infections. *J Infect.* 2013; 66:467-474.
17. McDonald M, Kameh D, Johnson ME, Johansen TEB, Albala D, Mouraviev V. A head-to-head comparative phase II study of standard urine culture and sensitivity versus DNA next-generation sequencing testing for urinary tract infections. *Rev Urol.* 2017; 19:213-220.
18. Korets R, Graverson JA, Kates M, Mues AC, Gupta M. Post-percutaneous nephrolithotomy systemic inflammatory response: a prospective analysis of preoperative urine, renal pelvic urine and stone cultures. *J Urol.* 2011; 186:1899-1903.
19. Dreger NM, Degener S, Ahmad-Nejad P, Wöbker G, Roth S. Urosepsis – etiology, diagnosis, and treatment. *Dtsch Arztebl Int.* 2015; 112:837-847; quiz 848.
20. Karakonstantis S, Kalemaki D. Blood culture useful only in selected patients with urinary tract infections - a literature review. *Infect Dis (Lond).* 2018; 50:584-592.
21. Long Y, Zhang Y, Gong Y, Sun R, Su L, Lin X, Shen A, Zhou J, Caiji Z, Wang X, Li D, Wu H, Tan H. Diagnosis of sepsis with gell-free DNA by next-generation sequencing technology in ICU patients. *Arch Med Res.* 2016; 47:365-371.
22. Thanassi M. Utility of urine and blood cultures in pyelonephritis. *Acad Emerg Med.* 1997; 4:797-800.
23. Pien BC, Sundaram P, Raof N, Costa SF, Mirrett S, Woods CW, Reller LB, Weinstein MP. The clinical and prognostic importance of positive blood cultures in adults. *Am J Med.* 2010; 123:819-828.
24. Hall KK, Lyman JA. Updated review of blood culture contamination. *Clin Microbiol Rev.* 2006; 19:788-802.
25. Gosiewski T, Ludwig-Galezowska AH, Huminska K, Sroka-Oleksiak A, Radkowski P, Salamon D, Wojciechowicz J, Kus-Slowinska M, Bulanda M, Wolkow PP. Comprehensive detection and identification of bacterial DNA in the blood of patients with sepsis and healthy volunteers using next-generation sequencing method - the observation of DNAemia. *Eur J Clin Microbiol Infect Dis.* 2017; 36:329-336.
26. Lee A, Mirrett S, Reller LB, Weinstein MP. Detection of bloodstream infections in adults: how many blood cultures are needed? *J Clin Microbiol.* 2007; 45:3546-3548.
27. Coburn B, Morris AM, Tomlinson G, Detsky AS. Does this adult patient with suspected bacteremia require blood cultures? *JAMA.* 2012; 308:502-511.
28. Ramos JGR, da Hora Passos R, Teixeira MB, Gobatto ALN, Coutinho RVDS, Caldas JR, da Guarda SF, Ribeiro MP, Batista PBP. Prognostic ability of quick-SOFA across different age groups of patients with suspected infection outside the intensive care unit: A cohort study. *J Crit Care.* 2018; 47:178-184.

Received January 2, 2020; Revised February 17, 2020;
Accepted February 22, 2020

**Address correspondence to:*

Tadashi Imanishi, Department of Molecular Life Science,
Tokai University School of Medicine, Shimokasuya 143,
Isehara, Kanagawa 259-1193, Japan.
E-mail: imanishi@tokai.ac.jp

Released online in J-STAGE as advance publication February
27, 2020.

Association of moderately abnormal behavior and administered neuraminidase inhibitors

Tamie Sugawara¹, Yasushi Ohkusa^{1,*}, Kiyosu Taniguchi², Chiaki Miyazaki³, Mariko Y. Momoi⁴, Nobuhiko Okabe⁵

¹Infectious Disease Surveillance Center, National Institute of Infectious Diseases, Tokyo, Japan;

²National Hospital Organization Mie National Hospital, Mie, Japan;

³Fukuoka Welfare Center for the Disabled, Fukuoka, Japan;

⁴Ryoumou Seishi Ryogoen for the Severely Disabled, Gunma, Japan;

⁵Kawasaki City Institute for Public Health, Kawasaki, Japan.

SUMMARY Our earlier study investigated the incidence of severe abnormal behavior associated with neuraminidase inhibitors (NIs), but some studies have specifically examined the association of oseltamivir use and moderately abnormal behavior. Therefore, this study was undertaken to assess associations between moderately abnormal behavior and administered drugs. All cases of patients with influenza who exhibited moderately abnormal behavior were reported to us by physicians of all sentinel clinics and hospitals for influenza throughout Japan. Open Data of the National Database of Electronic Medical Claims include the numbers of patients diagnosed as having influenza who were prescribed NI. Incidence by NI was tested using Fisher's exact test. We received 518 moderately abnormal cases in 5-9-year-olds and 207 moderately abnormal behavior cases in 10-19-year-olds. The incidence among NI ranged from 193 per one million influenza patients in laninamivir among 10-19-year-olds to 1021 for peramivir among 5-9-year-olds. Estimation results revealed the order of risk among NIs as peramivir, oseltamivir, zanamivir and laninamivir in moderate abnormal behavior. Because of data limitations, risk among patients with and without NI cannot be compared.

Keywords Moderately abnormal behavior, neuraminidase inhibitors, influenza, relative risk, incidence

1. Introduction

Since February 2007, when two influenza-infected Japanese junior high students jumped from a great height and died, abnormal behavior in influenza patients, especially in 10-19-year-olds, has been a public health concern in Japan and throughout the world (1-9). Although the Ministry of Health, Labour and Welfare abolished the Yellow Letter restricting the issuance of oseltamivir prescriptions to 10-19-year-old influenza patients on August 21, 2018 (10), abnormal behavior has persisted as an important public health concern.

Our earlier study (8) to assess the incidence of severely abnormal behavior, which was defined as active motion that can be life-threatening if given no intervention, including behaviors such as sudden running away, jumping from a high place, or rampaging involving self-injury. Results showed that no significant difference in the incidence rates of abnormal behavior by the type of neuraminidase inhibitor (NI).

By contrast, some studies have specifically examined the association of oseltamivir use with abnormal behavior and with adverse neuropsychiatric events (11). Nevertheless, because they used comparison of a small sample with nationwide data, these studies might specifically examine moderately abnormal behavior that might not be life-threatening even if given no intervention (12,13). We also collect information about moderately abnormal behavior along with that of severely abnormal behavior. However, the incidence of moderately abnormal behavior has not been evaluated in the earlier investigations, yet (8).

The National Database of Electronic Medical Claims (NDBEMC), which includes all electronic medical claims, accounting for about 98.4% of all medical claims throughout Japan as of May 2015. However, use of the data takes more than one year because an application must be filed to obtain permission to use data for analyses. Therefore, analysis using NDBEMC might be unrealistic. Instead, the NDBEMC open data are data of NDBEMC that are available for general

use. The data include the amounts of prescribed drugs, but do not include information related to diagnosis. Because the earlier study specifically addressed only the severe abnormal behavior, the object of the present study specifically examines association between moderate abnormal behavior and administered NI.

2. Materials and Methods

2.1. Data

All cases of patients with influenza who presented moderately abnormal behavior were reported to us by physicians of all sentinel clinics and hospitals for influenza throughout Japan. Of the 5,000 sentinels for influenza, 3,000 were pediatric medical facilities; 2,000 were of internal medicine. These accounted for almost 10% of pediatric and internal medicine facilities nationwide. In Japan, almost all influenza-like illness cases are assessed using rapid tests, reporting results confirmed as positive for influenza virus infection. We defined the moderately abnormal behaviors as non-life-threatening abnormal behaviors, even if no intervention was given. We have continued to survey abnormal behaviors since the 2006/2007 season.

The influenza season is defined as the period from the 36th epidemiological week to the 35th week of the following year. We extracted data from NDBEMC open data for the amounts with NI by age class and transformed the data to the number of patients using standard formulation by age or body weight evaluated at average weight in an age class.

2.2. Study period and subjects

The study period was limited to September 2014 through March 2018. Subjects were grouped into two age groups: 5-9 and 10-19-year-olds.

2.3. Analysis

We evaluated differences in incidence rates among patients administered types of NI as relative risks using Fisher's exact test. Incidence was defined as the number of influenza patients of moderately abnormal behavior multiplied by 10 and dividing the estimated number of patients with each NI. We adopted 5% as the significance level.

2.4. Ethical consideration

This study was approved by the Committee for Ethical Consideration, National Institution of Infectious Diseases, Japan: approval numbers were 261, 312, 375, and 462. Approval by the Kawasaki City Institution for Health and Safety, Committee for Ethical Consideration was 27-5.

3. Results and Discussion

Table 1 presents the number of influenza patients of the 5-9 and 10-19-year-olds with moderate abnormal behavior according to the administered drug: oseltamivir, zanamivir, peramivir, or laninamivir. It also shows the incidence per million patients by age group according to the administered drug. Moderately abnormal behavior was reported from the sentinels of influenza, as described above.

Results show that, for 5-9-year-olds, 518 moderately abnormal cases were reported. For 10-19-year-olds, 207 moderately abnormal behavior cases were reported. The highest incidence among NI was 1,021 per one million influenza patients for peramivir among 5-9-year-olds. The lowest was 193 in laninamivir among 10-19-year-olds.

Table 2 presents the relative risks and *p*-values of the exact test. The relative risk is defined as the incidence in the first column over the incidence in the second column. Almost all results were found to be statistically significant except for relative risk among zanamivir and laninamivir, which were not significant among 10-19-year-olds. In both of age classes, peramivir was found to have the highest incidence, followed by oseltamivir and zanamivir. The lowest incidence was that of laninamivir.

The cases of moderately abnormal behavior were 2-10 times greater than cases of severely abnormal behavior (8). Moderately abnormal behaviors were reported only from the influenza sentinels. Therefore, the implied incidence of moderately abnormal behavior was 20-100 times higher than the reported incidence of severely abnormal behavior. Even though almost all relative risks were significant because of the large number of cases, the characteristics of the results were similar to those obtained for severely abnormal behavior.

Another study conducted in Japan (7) found 28 cases of A-type abnormal behavior among the 10,000 cohort. That is the most severely abnormal behavior in their definition: "Abnormal behavior potentially leading to an accident or harm to another person." Consequently, their inferred incidence was 2,800 per million patients. Our obtained results were 193-1,021 per million patients in the two age classes. Therefore, incidence found in the earlier study was approximately 2-14 times higher than our estimate.

The incidence with oseltamivir was at least 777 for 5-9-year-olds and 414 for 10-19-year-olds. An earlier study (7) found 24 cases of A-type abnormal behavior, implying incidence of 2,400 per million patients. That figure is 3-6 times greater than our estimates. The A-type abnormal behavior found in that earlier study (7) apparently occurs more often than the moderately abnormal behavior found in the present study. One must bear in mind that data used for the earlier study

Table 1. Number of moderately abnormal behavior cases and incidence per million patients by age group and administered drug

Administered drug/ Age class	No. of moderately abnormal behavior cases reported		Incidence per million patients	
	5-9	10-19	5-9	10-19
Oseltamivir	240	20	777.1	414.7
Zanamivir	55	57	502.8	277.9
Peramivir	8	4	1021	328.9
Laninamivir	88	97	445	193.0
None	127	43		

Notes: "Incidence per million patients" is defined as the "Number of moderately abnormal behavior cases reported" multiplied by 10 and divided by the estimated number of patients with each neuraminidase inhibitor (NI). "None" in the administered drug column denotes patients who were not administered any NI.

Table 2. Relative risk and *p*-values

Age class		5-9		10-19	
Numerator	Denominator	relative risk	<i>p</i> -value	relative risk	<i>p</i> -value
Zanamivir	Zanamivir	1.545	0.000	1.492	0.000
Oseltamivir	Peramivir	0.070	0.000	0.052	0.000
Oseltamivir	Laninamivir	19.181	0.000	52.084	0.000
Zanamivir	Peramivir	0.492	0.000	0.845	0.303
Zanamivir	Laninamivir	1.129	0.025	1.440	0.000
Peramivir	Laninamivir	2.294	0.000	1.704	0.001

Notes: Relative risk is the incidence of the first column divided by the incidence of the second column.

were collected in 2007. Our data period was after 2007, when public health concern had emerged and abnormal behavior had continued. This difference of data might account for the greater size gap. Therefore, we conclude that A-type abnormal behavior reported from the earlier study (7) might be comparable to less severely abnormal behavior than the moderate behavior examined in the present study.

Comparison of our results with those of an earlier study (8) indicated no significant difference in the incidence rates of severe abnormal behavior by the type of NI. We found that almost all relative risks among NI were significant. This difference might derive from the definition of abnormal behavior. We specifically examined moderate abnormal behavior, but the earlier study was limited to severe behavior, which was defined as life-threatening if given no intervention. Therefore, the numbers of cases of the two definitions were much different. These differences might clarify the present result among NI. However, it is notable that the risk order among NI, which was peramivir, oseltamivir, zanamivir, and laninamivir in moderate abnormal behavior, might not hold in severe abnormal behavior even though data of severe abnormal behavior will be accumulated comparably to the moderate abnormal behavior found in the present study.

The present study is constrained by some limitations. The most potentially important limitation is that related to the sampling fraction of sentinels for influenza able to report moderately abnormal behavior. We assumed that sampling fraction to be 10% for both age classes. However, as described above, some differences might

arise in the fraction rates for pediatric and internal medicine facilities. The fraction rate might actually be higher for pediatric facilities than for internal medicine facilities. Some 15-19-year-old influenza patients might visit internal medicine rather than pediatric facilities. Therefore, the sampling fraction for 15-19-year-olds might be smaller than others. That point has not been well investigated. Therefore, we do not consider that point for adjustment. It remains as a challenge for future research.

Secondly, because we used NDBEMC open data as the number of patients with NI, we cannot analyze patients without NI. The NDBEMC open data which we used did not include information about diagnosis, although NDBEMC data include it. It takes a long time, actually several years, as described above, to use NDBEMC itself to analyze abnormal behavior without NI.

4. Conclusion

Results show that the order of risk among NI was peramivir, oseltamivir, zanamivir, and laninamivir in moderate abnormal behavior with an exception. Comparison with moderate abnormal behavior without NI persists as the next challenge for research on this subject.

Acknowledgements

This research was supported financially by Health and Labor Sciences Research Grants from the Ministry of

Health, Labour and Welfare (H22-Pharmaceuticals and Medical Devices-Assignment-023 in 2010, H23-Global Health-Assignment-005 in 2011, H24-Global Health-Assignment-001 in 2012, H25-Global Health-Assignment-002 in 2013, and H26-Medical B-Assignment -009 in 2014) and by the Japan Agency for Medical Research and Development (15mk0101045h0101 in 2015, 16mk0101059j0102 in 2016, 17mk0101059j0102 in 2017, 18mk0101059j0103 in 2018, and 19mk010114h0001 in 2019).

References

1. Kashiwagi S, Yoshida S, Yamaguchi H, Niwa S, Mitsui N, Tanigawa M, Shiosakai K, Yamanouchi N, Shiozawa T, Yamaguchi F. Safety of the long-acting neuraminidase inhibitor laninamivir octanoate hydrate in post-marketing surveillance. *Int J Antimicrob Agents*. 2012; 40:381-388.
2. Nakano T, Okumura A, Tanabe T, Niwa S, Fukushima M, Yonemochi R, Eda H, Tsutsumi H. Safety evaluation of laninamivir octanoate hydrate through analysis of adverse events reported during early post-marketing phase vigilance. *Scand J Infect Dis*. 2013; 45:469-477.
3. Nakamura Y, Sugawara T, Ohkusa Y, Taniguchi K, Miyazaki C, Momoi M, Okabe N. Abnormal behavior during influenza in Japan during the last seven seasons: 2006-2007 to 2012-2013. *J Infect Chemother*. 2014; 20:789-793.
4. Toovey S, Prinssen EP, Rayner CR, Thakrar BT, Dutkowski R, Koerner A, Chu T, Sirzen-Zelenskaya A, Britschgi M, Bansod S, Donner B. Post-marketing assessment of neuropsychiatric adverse events in influenza patients treated with oseltamivir: An updated review. *Adv Ther*. 2012; 29:826-848.
5. Hoffman KB, Demakas A, Erdman CB, Dimbil M, Doraiswamy PM. Neuropsychiatric adverse effects of oseltamivir in the FDA Adverse Event Reporting System, 1999-2012. *BMJ*. 2013; 347:f4656.
6. Jefferson T, Jones M, Doshi P, Spencer EA, Onakpoya I, Heneghan CJ. Oseltamivir for influenza in adults and children: Systematic review of clinical study reports and summary of regulatory comments. *BMJ*. 2014; 348:g2545.
7. Fukushima W, Ozasa K, Okumura A, *et al*. Oseltamivir use and severe abnormal behavior in Japanese children and adolescents with influenza: Is a self-controlled case series study applicable? *Vaccine*. 2017; 35:4817-4824.
8. Nakamura Y, Sugawara T, Ohkusa Y, *et al*. Life-threatening abnormal behavior incidence in 10-19 year old patients administered neuraminidase inhibitors. *PLoS One*. 2015; 10:e0129712.
9. Shimizu E, Kawahara K. Assessment of Medical Information Databases to Estimate Patient Numbers. *Jpn J Pharmacoepidemiol*. 2014; 19:1-11.
10. Japan's Ministry of Health, Labour and Welfare. <http://www.pmda.go.jp/safety/info-services/drugs/calling-attention/revision-of-precautions/0337.html#2> (accessed 7 March 2019) (in Japanese).
11. Kang HR, Lee EK, Kim WJ, Shin JY. Risk of neuropsychiatric adverse events associated with the use of oseltamivir: A nationwide population-based case-crossover study. *J Antimicrob Chemother*. 2019; 74:453-461.
12. Ohkusa Y, Sugawara T, Taniguchi K, Miyazaki C, Momoi YM, Okabe N. Inquiry into some gap among oseltamivir use and severe abnormal behavior in Japanese children and adolescents with influenza. *Drug Discov Ther*. 2018; 12:381-383.
13. Ohkusa Y, Sugawara T, Taniguchi K, Miyazaki C, Momoi MY, Okabe N. Comment on: Risk of neuropsychiatric adverse events associated with the use of oseltamivir: a nationwide population-based case-crossover study. *J Antimicrob Chemother*. 2019; 74:1762-1764.
14. Takeuchi S, Tetsuhashi M, Sato D. Oseltamivir phosphate-Lifting the restriction on its use to treat teenagers with influenza in Japan. *Pharmacoepidemiol Drug Saf*. 2019; 28:434-436.

Received December 4, 2019; Revised December 20, 2019; Accepted February 12, 2020

*Address correspondence to:

Dr. Yasushi Ohkusa, Infectious Disease Surveillance Center, National Institute of Infectious Diseases, 1-23-1 Toyama, Shinjuku-ku, Tokyo 162-8640, Japan.
E-mail: ohkusa@nih.go.jp

Released online in J-STAGE as advance publication February 26, 2020.

Efficacy of Chinese prescription Kangen-karyu for patient with metabolic syndrome

Tsutomu Kitazawa¹, Chan Hum Park^{2,*}, Kazuyuki Hiratani¹, Jae Sue Choi³, Takako Yokozawa^{4,*}

¹ Shinseikai Toyama Hospital, Toyama, Japan;

² Department of Medicinal Crop Research, National Institute of Horticultural and Herbal Science, Rural Development Administration, Eumseong, Republic of Korea;

³ Department of Food and Life Science, Pukyong National University, Busan, Republic of Korea;

⁴ Graduate School of Science and Engineering for Research, University of Toyama, Toyama, Japan.

SUMMARY Metabolic syndrome is a cluster of risk factors for cardiovascular disease and type 2 diabetes mellitus. The risk factors include hypertension, dyslipidemia, hyperglycemia, and central obesity. Various diagnostic criteria have been proposed by different organizations over the past decade. The utilization of traditional Chinese medicine to treat metabolic syndrome has received increasing attention due to its wide availability. In this paper, we report the case of a 68-year-old patient with hypertension, hypercholesterolemia, borderline diabetes, and obesity, who showed an improvement in metabolic syndrome on the administration of 7.5 g of Kangen-karyu extract per day. After 6 months, the levels of serum total cholesterol, low-density lipoprotein-cholesterol, triglycerides, hemoglobin A1c were decreased. The abdominal circumference and body weight were decreased following administration. At that time, the somatic and subjective symptoms had partially disappeared. Herein, we present and discuss the evidence supporting the use of Kangen-karyu extract against metabolic syndrome.

Keywords Metabolic syndrome, traditional Chinese medicine, Kangen-karyu, case report

1. Introduction

Metabolic syndrome is a complex of interrelated risk factors for cardiovascular disease and diabetes. These factors include dysglycemia, hypertension, hypertriglyceridemia, low high-density lipoprotein cholesterol levels, and obesity (particularly central adiposity). Metabolic syndrome is now both a public health and clinical problem. In the public health arena, more attention must be given to modification of lifestyles of the general public of all nations to reduce obesity and increase physical activity. Although therapeutic lifestyle modification is first-line therapy for the metabolic syndrome and thus deserves initial attention, drug therapy may be necessary in many patients to achieve recommended goals (1-3).

Major pharmacological interventions include management of dyslipidemia with statins, decreasing prothrombotic risk with antiplatelet drugs, and the use of insulin sensitizers to decrease the risk of diabetes. There is no single drug therapy for metabolic syndrome and currently available pharmacotherapy and associated comorbidities necessitate prolonged use of multiple medications, which is challenging for patients due to

polypharmacy and reduced compliance (2). Thus, there is growing interest in the use of natural products to reduce the risk and progression of metabolic syndrome.

Kangen-karyu (Guan-Yuan-Ke-Li), a crude drug developed from a traditional Chinese prescription consisting of six herbs (*Salviae Miltiorrhizae Radix*, *Cnidii Rhizoma*, *Paeoniae Radix*, *Carthami Flos*, *Aucklandiae Radix*, and *Cyperi Rhizoma*, shown in Table 1), has been clinically used as a treatment for cardiovascular diseases, such as angina pectoris and cerebrovascular diseases. Kangen-karyu shows biological activity, such as an anti-aging effect, the inhibition of platelet aggregation, hypotensive effect, and the recovery of learning and memory impairment induced by senescence (4-7). In our previous studies, Kangen-karyu showed favorable ameliorative effects on signs of fructose-induced metabolic syndrome, such as hyperglycemia, hyperlipidemia, and hypertension, through the reduction of triglyceride and cholesterol levels with the regulation of hepatic sterol regulatory element-binding protein-1 (SREBP-1) expression, and also exhibited protective effects against diet-induced hypercholesterolemia in rats (8,9). We also reported the beneficial effect of Kangen-karyu on dyslipidemia in

Table 1. Composition of Kangen-karyu

Common name	Botanical name	Family name
Salviae Miltiorrhizae Radix	<i>Salvia miltiorrhiza</i> BUNGE	Labiatae
Cnidii Rhizoma	<i>Cnidium officinale</i> MAKINO	Umbelliferae
Paeoniae Radix	<i>Paeonia lactiflora</i> PALLAS	Paeoniaceae
Carthami Flos	<i>Carthamus tinctorius</i> L.	Compositae
Aucklandiae Radix	<i>Aucklandia lappa</i> DCNE.	Compositae
Cyperi Rhizoma	<i>Cyperus rotundus</i> L.	Cyperaceae

a mouse model of type 2 diabetes (10). These results suggest that Kangen-karyu can ameliorate metabolic syndrome.

On the basis of the findings obtained from these fundamental studies, we administered Kangen-karyu to a metabolic syndrome patient, and evaluated its treatment-based usefulness.

2. Case report

This study was conducted according to the ethical guidelines for epidemiological research set by the Japanese Ministry of Education, Culture, Sports, Science and Technology and Ministry of Health, Labour, and Welfare. Ethical approval was obtained from the Clinical Research Ethics Committees of Shinseikai Toyama Hospital. Written informed consent was obtained from the patient at the time of enrollment for the collection of clinical information and biosamples for archival and research purposes. A 68-year-old man with hypertension, hypercholesterolemia, and borderline diabetes was previously diagnosed with metabolic syndrome at Shinseikai Toyama Hospital (Toyama, Japan). From December 2017, the patient subsequently modified his lifestyle and continued to receive existing treatments: antihypertensive agents (amlodin: 5 mg/day, azilva: 20 mg/day), an antilipidemic agent (lipitor: 5 mg/day), and agents for reflux esophagitis (takepron: 30 mg/day, gasmotin: 15 mg/day). However, he presented to our hospital on February 13, 2019, seeking to recover his functional level with herbal medicine. Kangen-karyu extract (7.5 g/day) was administered three times a day until August 30, 2019.

Before Kangen-karyu extract administration, his initial anthropometric measurements included a body weight of 82.6 kg with a height of 165 cm, a body mass index (BMI) of 30.3 kg/m², and an abdominal circumference of 105.8 cm which classified him as obese. His systolic/diastolic blood pressure was 133/85 mmHg (Table 2). Hemoglobin A1c (HbA1c) was 7.3%, showing poorly controlled blood glucose. The levels of serum lipids were as follows: total cholesterol: 230 mg/dL, low-density lipoprotein (LDL)-cholesterol: 142 mg/dL, LDL-cholesterol/high-density lipoprotein (HDL)-cholesterol: 2.3, and triglycerides: 353 mg/dL, indicating metabolic syndrome (Table 3).

Assessment of somatic and subjective symptoms

involved completing a series of questionnaires at the beginning and end of the study. The symptom checklist included the following symptoms: dizziness and palpitation, stiff shoulders and headache, coldness of the limbs and fatigability, mental stress, sleeping disorder, tension of the stomach and abdomen, pain, numbness of the waist and body, dark circles around eyes and lip symptoms, stains on face, mottled skin, and tongue symptoms. The change in each symptom was assessed with a 3-point rating scale: "marked improvement" was 5 points, "improvement" was 4 points, and "slight improvement" was 2 points. The assessment of global improvement rating of subjective symptoms simply involved the addition of points. At the same time, the tongue was evaluated based on factors such as the color, coating, and sublingual vein.

The patient continued to receive antihypertensive agents, the antilipidemic agent, and agents for reflux esophagitis. In addition, Kangen-karyu extract (7.5 g/day) was administered three times a day until August 30, 2019.

During the administration of Kangen-karyu extract, physical tests were performed to assess its effect on metabolic syndrome. As shown in Table 2, BMI and abdominal circumference showed slight decreases on treatment with Kangen-karyu extract. The total cholesterol level decreased from 230 to 178 mg/dL at the 6-month follow-up. The elevated level of LDL-cholesterol also reduced from 142 to 91 mg/dL. In addition, oral administration of Kangen-karyu extract reduced the increased serum triglyceride and HbA1c levels. Other parameters such as hepatic and renal function parameters [aspartate aminotransferase (AST), alanine aminotransferase (ALT), urea nitrogen, and creatinine] were not affected by the administration of Kangen-karyu extract, as shown in Table 3. At that time, the somatic and subjective symptoms such as stiff shoulders, headache, feeling heavy in the head, and mottled skin had improved. After 6 months, the score using the questionnaire had decreased from 51 to 41 at follow-up. There was a slight improvement in the tongue coating on the administration of Kangen-karyu.

3. Discussion

The first formalized definition of metabolic syndrome was proposed in 1998 by a consultation group on the

Table 2. Physical characteristics on administration of Kangen-karyu for 6 months

Parameter	Pre	Post
Body weight (kg)	82.6	80.6
Height (cm)	165	165
BMI (kg/m ²)	30.3	29.6
Abdominal circumference (cm)	105.8	101.8
Systolic blood pressure (mmHg)	133	131
Diastolic blood pressure (mmHg)	85	83

Table 3. Laboratory data on administration of Kangen-karyu for 6 months

Parameter	Pre	Post
HbA1c (%)	7.3	6.6
Total cholesterol (mg/dL)	230	178
LDL-cholesterol (mg/dL)	142	91
LDL-cholesterol/HDL-cholesterol	2.3	1.7
Triglycerides (mg/dL)	353	269
AST (U/L)	15	12
ALT (U/L)	19	18
Urea nitrogen (mg/dL)	13.5	14.7
Creatinine (mg/dL)	0.54	0.60

definition of diabetes for the World Health Organization (WHO) (11). This group emphasized insulin resistance as the major underlying risk factor and the necessity of evidence of insulin resistance for diagnosis. A diagnosis of the syndrome based on the WHO could thus be made on the basis of several markers of insulin resistance plus 2 additional risk factors, including obesity, hypertension, a high triglyceride level, reduced high-density lipoprotein cholesterol level, or microalbuminuria. Subsequently, various criteria have been put forward by the International Diabetes Federation, WHO, and other diabetic societies throughout the world (12). Japanese criteria of metabolic syndrome were established in 2005, and the definition is as follows: if a man has a waist circumference > 85 cm (in the case of a woman, > 90 cm) in addition to two or more of the following: lipid abnormality [high triglyceride level (> 150 mg/dL) and/or HDL-cholesterol level (< 40 mg/dL)], elevated blood pressure [systolic blood pressure (> 130 mmHg) and/or diastolic blood pressure (> 85 mmHg)], and elevated blood glucose [fasting blood glucose (> 110 mg/dL)] (13). In the present case, the patient fulfilled the criteria for metabolic syndrome. In spite of favorable blood lipid and blood pressure management, there was no improvement in the disease status. Therefore, the patient gave his consent to experimentally receive herbal medication to improve his condition.

We chose Kangen-karyu extract for the following reasons. Kangen-karyu was developed by the modification of herbal constituents of Kan-shin No. 2 in Japan (14). It has been clinically used as a treatment for cardiovascular diseases. Kangen-karyu has received much attention as a source of new therapeutic agents

based on pre-clinical animal experiments related to various human diseases (4-6,8-10,15-17). To add to these findings, we reported evidence supporting its preventive and/or therapeutic potential against metabolic syndrome (9). The administration of Kangen-karyu significantly improved high-fructose-induced metabolic syndrome such as hyperglycemia, hyperlipidemia, and hypertension through the reductions of triglyceride and cholesterol contents with the regulation of hepatic SREBP-1 and the nuclear factor-kappa B signaling pathway. The results of our previous study suggest that Kangen-karyu may play a protective role against metabolic syndrome.

In the present case, there was an improvement in metabolic syndrome following the administration of Kangen-karyu extract for 6 months. Most notably, the levels of serum total cholesterol, LDL-cholesterol, triglycerides, and HbA1c improved following the administration of Kangen-karyu extract. The abdominal circumference and body weight decreased compared with non-administration (from 105.8 to 101.8 cm; from 82.6 to 80.6 kg, respectively). In addition, the score using the questionnaire was decreased during the follow-up. Herein, we present a therapeutic option of Kangen-karyu based on metabolic parameters.

Treatment for metabolic syndrome involves the management of a cluster of chronic diseases such as diabetes mellitus, hypertension, dyslipidemia, and obesity. There is no single treatment for patients with metabolic syndrome. However, traditional Chinese medicine has received much attention as a source of multi-target strategies due to their multiple beneficial effects and absence of toxic and/or side effects. We have been investigating the multi-target therapeutic effects of Kangen-karyu, one of our major interests among traditional Chinese medicine agents, on patients with metabolic disease. The present case provides strong evidence to support the administration of Kangen-karyu extract as a therapeutic agent to prevent the progression of metabolic syndrome.

We report evidence to support the use of Kangen-karyu as an adjunctive therapy for a patient with metabolic syndrome. Kangen-karyu exhibits good efficacy in the treatment of metabolic syndrome.

References

1. Grundy SM, Hansen B, Smith Jr SC, Cleeman JI, Kahn RA, for Conference Participants. Clinical management of metabolic syndrome: report of the American Heart Association/National Heart, Lung, and Blood Institute/American Diabetes Association conference on scientific issues related to management. *Circulation*. 2004; 109:551-556.
2. Rochlani Y, Pothineni NV, Kovelamudi S, Mehta JL. Metabolic syndrome: pathophysiology, management, and modulation by natural compounds. *Ther Adv Cardiovasc Dis*. 2017; 11:215-225.

3. Saklayen MG. The global epidemic of the metabolic syndrome. *Curr Hypertens Rep.* 2018; 20:12.
4. Takahashi M, Sugaya K, Kubota K. Kangenkaryu prevents the decrease of cholinergic markers following the nucleus basalis magnocellularis lesion. *Jpn J Pharmacol.* 1992; 60:307-310.
5. Gao M, Ikeda K, Noguchi T, Mori K, Yamori Y. Studies on preventive effect of 'Kangenkaryu', Chinese herbal medicine, on stroke in SHR-SP. *J Trad Med.* 2001; 18:245-250.
6. Makino T, Wakushima H, Okamoto T, Okukubo Y, Saito K, Kano Y. Effects of Kangen-karyu on coagulation system and platelet aggregation in mice. *Biol Pharm Bull.* 2002; 25:523-525.
7. Cho EJ, Okamoto T, Yokozawa T. Therapeutic efficacy of Kangen-karyu against H₂O₂-induced premature senescence. *J Pharm Pharmacol.* 2008; 60:1537-1544.
8. Yokozawa T, Cho EJ, Sasaki S, Satoh A, Okamoto T, Sei Y. The protective role of Chinese prescription Kangen-karyu extract on diet-induced hypercholesterolemia in rats. *Biol Pharm Bull.* 2006; 29:760-765.
9. Yokozawa T, Kim HJ, Yamabe N, Okamoto T, Cho EJ. The protective role of Kangen-karyu against fructose-induced metabolic syndrome in a rat model. *J Pharm Pharmacol.* 2007; 59:1271-1278.
10. Noh JS, Park CH, Kim HY, Zhao Q, Yamabe N, Matsumoto K, Yokozawa T. Chinese prescription Kangen-karyu prevents dyslipidaemia and oxidative stress in mouse model of type 2 diabetes. *J Pharm Pharmacol.* 2011; 63:111-119.
11. Alberti KG, Zimmet PZ. Definition, diagnosis and classification of diabetes mellitus and its complications. Part 1: Diagnosis and classification of diabetes mellitus provisional report of a WHO consultation. *Diabet Med.* 1998; 15:539-553.
12. Alberti KG, Zimmet P, Shaw J, IDF Epidemiology Task Force Consensus Group. The metabolic syndrome – a new worldwide definition. *Lancet.* 2005; 366:1059-1062.
13. Committee for the Diagnostic Criteria of Metabolic Syndrome. Definition and criteria of metabolic syndrome. *J Jpn Soc Int Med.* 2005; 94:794-809.
14. Makino T, Wakushima H, Okamoto T, Okukubo Y, Deguchi Y, Kano Y. Pharmacokinetic and pharmacological interactions between ticlopidine hydrochloride and Kangen-karyu – Chinese traditional herbal medicine. *Phytother Res.* 2003; 17:1021-1024.
15. Pu F, Kaneko T, Enoki M, Irie K, Okamoto T, Sei Y, Egashira N, Oishi R, Mishima K, Kamimura H, Iwasaki K, Fujiwara M. Ameliorating effects of Kangen-karyu on neuronal damage in rats subjected to repeated cerebral ischemia. *J Nat Med.* 2010; 64:167-174.
16. Yamabe N, Kim HY, Kang KS, Zhao Q, Matsumoto K, Yokozawa T. Effect of Chinese prescription Kangen-karyu on lipid metabolism in type 2 diabetic *db/db* mice. *J Ethnopharmacol.* 2010; 129:299-305.
17. Zhao Q, Yokozawa T, Yamabe N, Tsuneyama K, Li X, Matsumoto K. Kangen-karyu improves memory deficit caused by aging through normalization of neuro-plasticity-related signaling system and VEGF system in the brain. *J Ethnopharmacol.* 2010; 131:377-385.

Received January 10, 2020; Revised February 20, 2020;
Accepted February 22, 2020

**Address correspondence to:*

Dr. Takako Yokozawa, Graduate School of Science and Engineering for Research, University of Toyama, 3190 Gofuku, Toyama 930-8555, Japan.
E-mail: yokozawa@inm.u-toyama.ac.jp

Dr. Chan Hum Park, Department of Medicinal Crop Research, National Institute of Horticultural and Herbal Science, Rural Development Administration, Eumseong 369-873, Republic of Korea.
E-mail: ptman123@korea.kr

Released online in J-STAGE as advance publication February 28, 2020.

Discovering drugs to treat coronavirus disease 2019 (COVID-19)

Liying Dong¹, Shasha Hu², Jianjun Gao^{1,*}

¹ Department of Pharmacology, School of Pharmacy, Qingdao University, Qingdao, Shandong, China;

² Department of Pathology, the Affiliated Hospital of Qingdao University, Qingdao, Shandong, China.

SUMMARY The SARS-CoV-2 virus emerged in December 2019 and then spread rapidly worldwide, particularly to China, Japan, and South Korea. Scientists are endeavoring to find antivirals specific to the virus. Several drugs such as chloroquine, arbidol, remdesivir, and favipiravir are currently undergoing clinical studies to test their efficacy and safety in the treatment of coronavirus disease 2019 (COVID-19) in China; some promising results have been achieved thus far. This article summarizes agents with potential efficacy against SARS-CoV-2.

Keywords novel coronavirus, pneumonia, COVID-19, 2019-nCoV, SARS-CoV-2

The virus SARS-CoV-2 (formerly designated 2019-nCoV) emerged in December 2019 and then spread rapidly worldwide, particularly to China, Japan, and South Korea. As of February 21, 2020, a total of 76,288 confirmed cases of coronavirus disease 2019 (COVID-19) and 2,345 deaths have been reported in mainland China (1). Scientists are endeavoring to find drugs to treat this disease. Research thus far has revealed more than 30 agents including Western medicines, natural products, and traditional Chinese medicines that may have potential efficacy against COVID-19. Some of these agents have been quickly tested in clinical studies and demonstrated preliminary efficacy against COVID-19. Antivirals including interferon α (IFN- α), lopinavir/ritonavir, chloroquine phosphate, ribavirin, and arbidol have been included in the latest version of the Guidelines for the Prevention, Diagnosis, and Treatment of Novel Coronavirus-induced Pneumonia issued by the National Health Commission (NHC) of the People's Republic of China for tentative treatment of COVID-19 (Table 1) (2).

The Guidelines have been revised 5 times since first being issued on January 15, 2020; the latest edition (the 6th edition) was issued on February 18, 2020. The fifth edition of the Guidelines recommends antivirals including IFN- α , lopinavir/ritonavir, and ribavirin for treatment of COVID-19 (3). Chloroquine phosphate and arbidol are included in the sixth edition of the Guidelines based on the preliminary outcomes of clinical studies (2). The specific method for administration of IFN- α is vapor inhalation at a dose of 5 million U (and 2 mL of sterile water for injection) for adults, 2 times/day. The dosage of lopinavir/ritonavir is 400 mg/100 mg for adults, 2 times/

day. Ribavirin should be administered *via* intravenous infusion at a dose of 500 mg for adults, 2 to 3 times/day in combination with IFN- α or lopinavir/ritonavir. Chloroquine phosphate is orally administered at a dose of 500 mg (300 mg for chloroquine) for adults, 2 times/day. Arbidol is orally administered at a dose of 200 mg for adults, 3 times/day. The duration of treatment is no more than 10 days.

IFN- α is a broad-spectrum antiviral that is usually used to treat hepatitis, though it is reported to inhibit SARS-CoV reproduction *in vitro* (4). Lopinavir/ritonavir is a medication for the human immunodeficiency virus (HIV) used in combination with other medications to treat adults and children over 14 days of age who are infected with HIV-1 (5). Chu *et al.* found that lopinavir/ritonavir has anti-SARS-CoV activity *in vitro* and in clinical studies (6). Ribavirin is a nucleoside analogue with a broad-spectrum of antiviral effects. A study compared 111 patients with severe acute respiratory syndrome (SARS) treated with ribavirin monotherapy and 41 patients with SARS treated with lopinavir/ritonavir and ribavirin; patients treated with the combined therapy had a lower risk of acute respiratory distress syndrome (ARDS) and death (6). Chloroquine is a widely used antimalarial that was found to be a potential broad-spectrum antiviral in 2006 (7). Chloroquine was found to block SARS-CoV-2 infection at low-micromolar concentration, with a half-maximal effective concentration (EC₅₀) of 1.13 μ M and a half-cytotoxic concentration (CC₅₀) greater than 100 μ M (8). Arbidol is an antiviral that can be used to treat influenza virus. A study has revealed that arbidol can effectively inhibit SARS-CoV-2 infection at a concentration of 10-30 μ M

Table 1. Antivirals included in the Guidelines (version 6) for treatment of COVID-19

Drug	Dosage	Method of administration	Duration of treatment
IFN- α	5 million U or equivalent dose each time, 2 times/day	Vapor inhalation	No more than 10 days
Lopinavir/ritonavir	200 mg/50 mg/capsule, 2 capsules each time, 2 times/day	Oral	No more than 10 days
Ribavirin	500 mg each time, 2 to 3 times/day in combination with IFN- α or lopinavir/ritonavir	Intravenous infusion	No more than 10 days
Chloroquine phosphate	500 mg (300 mg for chloroquine) each time, 2 times/day	Oral	No more than 10 days
Arbidol	200 mg each time, 3 times/day	Oral	No more than 10 days

in vitro (9).

Besides the drugs above that have been included in the Guidelines, favipiravir is a drug that warrants attention. Favipiravir was approved for treatment of novel influenza on February 15, 2020 in China. This drug is currently undergoing clinic trials in treating COVID-19. Favipiravir is a new type of RNA-dependent RNA polymerase (RdRp) inhibitor. In addition to its anti-influenza virus activity, favipiravir is capable of blocking the replication of flavi-, alpha-, filo-, bunya-, arena-, noro-, and other RNA viruses (10). Favipiravir is converted into an active phosphoribosylated form (favipiravir-RTP) in cells and is recognized as a substrate by viral RNA polymerase, thus inhibiting RNA polymerase activity (11). Therefore, favipiravir may have potential antiviral action on SARS-CoV-2, which is a RNA virus. On February 14, a clinical trial on favipiravir for the treatment of COVID-19 initiated by the Clinical Medical Research Center of the National Infectious Diseases and the Third People's Hospital of Shenzhen achieved promising results. The preliminary results from a total of 80 patients (including the experimental group and the control group) indicated that favipiravir had more potent antiviral action than that of lopinavir/ritonavir (12). No significant adverse reactions were noted in the favipiravir treatment group, and it had significantly fewer adverse effects than the lopinavir/ritonavir group (12).

Remdesivir is another potential drug for treatment of COVID-19. Remdesivir is a nucleoside analogue and a broad-spectrum antiviral. Animal experiments (13) indicated that remdesivir can effectively reduce the viral load in lung tissue of mice infected with MERS-CoV, improve lung function, and alleviate pathological damage to lung tissue. Wang *et al.* found that remdesivir potently blocks SARS-CoV-2 infection at low-micromolar concentrations and has a high selectivity index (half-maximal effective concentration (EC_{50}), 0.77 μ M; half-cytotoxic concentration (CC_{50}) > 100 μ M; SI > 129.87) (8). Holshue *et al.* reported that remdesivir yielded promising results in the treatment of a patient with COVID-19 in the United States (14). In order to evaluate the efficacy and safety of the drug in patients with COVID-19, a randomized, placebo-controlled, double-blind, multicenter, phase III clinical trial was

launched on February 5, 2020 in China (15,16). Patients in the experimental group received a initial dose of 200 mg of remdesivir and a subsequent dose of 100 mg for 9 consecutive days *via* intravenous infusion in addition to routine treatment. Patients in the control group received routine treatment and the same dose of a placebo. The trial is expected to conclude by the end of April 2020.

Studies have also revealed some other drugs may have potential efficacy in treating COVID-19. One is darunavir, which is a second-generation of HIV-1 protease inhibitor. On February 4, 2020, researchers in China announced that darunavir inhibited SARS-CoV-2 infection *in vitro* (9). Cell experiments indicated that darunavir significantly inhibited viral replication at a concentration of 300 μ M *in vitro* and that its inhibition efficiency was 280-fold that in the untreated group (9). Other potential drugs include type II transmembrane serine protease (TMSPSS2) inhibitors and BCR-ABL kinase inhibitor imatinib. Hoffmann *et al.* indicated that SARS-CoV-2 uses the SARS-CoV receptor, ACE2, and the cellular protease TMPRSS2 to enter target cells. A TMPRSS2 inhibitor would block entry and thus constitute a treatment option (17). Imatinib has anti-coronal activity primarily because it inhibits the fusion of virions with the endosomal membrane (18).

A joint research team of the Shanghai Institute of Materia Medica and Shanghai Tech University performed drug screening in silicon and an enzyme activity test, and they reported 30 agents with potential antiviral activity against SARS-CoV-2 on January 25, 2020 (19). These agents are indinavir, saquinavir, lopinavir, carfilzomib, ritonavir, remdesivir, atazanavir, darunavir, tipranavir, fosamprenavir, enzaplatovir, presatovir, abacavir, bortezomib, elvitegravir, maribavir, raltegravir, montelukast, deoxyrhapontin, polydatin, chalcone, disulfiram, carmofur, shikonin, ebselen, tideglusib, PX-12, TDZD-8, cyclosporin A, and cinanserin. The same study also found that Chinese herbal medicines such as *Rhizoma Polygoni Cuspidati* and *Radix Sophorae Tonkinensis* may contain active ingredients against SARS-CoV-2 (19).

As the epidemic spreads, scientists around the world are actively exploring drugs that would be potentially effective in combating COVID-19. Generally, there are

no finally verified antivirals specific to COVID-19 at present. The efficacy and safety of these candidate drugs in the treatment of COVID-19 need to be confirmed in further preclinical and clinical trials.

References

- Update on the prevalence and control of novel coronavirus-induced pneumonia as of 24:00 on February 21. <http://www.nhc.gov.cn/xcs/yqtb/202002/543cc508978a48d2b9322bdc83daa6fd.shtml> (accessed February 23, 2020). (in Chinese).
- Guidelines for the Prevention, Diagnosis, and Treatment of Novel Coronavirus-induced Pneumonia, The 6th ed. <http://www.nhc.gov.cn/yzygj/s7653p/202002/8334a8326dd94d329df351d7da8aefc2/files/b218cfcb1bc54639af227f922bf6b817.pdf> (accessed February 23, 2020). (in Chinese).
- Guidelines for the Prevention, Diagnosis, and Treatment of Novel Coronavirus-induced Pneumonia, The 5th ed. <http://www.nhc.gov.cn/yzygj/s7653p/202002/d4b895337e19445f8d728fcaf1e3e13a/files/ab6bec7f93e64e7f998d802991203cd6.pdf> (accessed February 18, 2020). (in Chinese).
- Stockman LJ, Bellamy R, Garner P. SARS: Systematic review of treatment effects. *PLoS Med.* 2006; 3:e343.
- Su B, Wang Y, Zhou R, Jiang T, Zhang H, Li Z, Liu A, Shao Y, Hua W, Zhang T, Wu H, He S, Dai L, Sun L. Efficacy and tolerability of lopinavir/ritonavir- and efavirenz-based initial antiretroviral therapy in HIV-1-infected patients in a tertiary care hospital in Beijing, China. *Front Pharmacol.* 2019; 10:1472.
- Chu CM, Cheng VCC, Hung IFN, Wong MML, Chan KH, Chan KS, Kao RYT, Poon LLM, Wong CLP, Guan Y, Peiris JSM, Yuen KY. Role of lopinavir/ritonavir in the treatment of SARS: Initial virological and clinical findings. *Thorax.* 2004; 59:252-256.
- Savarino A, Di Trani L, Donatelli I, Cauda R, Cassone A. New insights into the antiviral effects of chloroquine. *Lancet Infect Dis.* 2006; 6:67-69.
- Wang M, Cao R, Zhang L, Yang X, Liu J, Xu M, Shi Z, Hu Z, Zhong W, Xiao G. Remdesivir and chloroquine effectively inhibit the recently emerged novel coronavirus (2019-nCoV) *in vitro*. *Cell Res.* 2020.
- News: Abidol and darunavir can effectively inhibit coronavirus <http://www.sd.chinanews.com/2/2020/0205/70145.html> (accessed February 21, 2020). (in Chinese).
- Delang L, Abdelnabi R, Neyts J. Favipiravir as a potential countermeasure against neglected and emerging RNA viruses. *Antiviral Res.* 2018; 153:85-94.
- Furuta Y, Komeno T, Nakamura T. Favipiravir (T-705), a broad spectrum inhibitor of viral RNA polymerase. *Proc Jpn Acad, Ser B, Phys Biol Sci.* 2017; 93:449-463.
- News. <http://www.szdsyy.com/News/0a6c1e58-e3d0-4cd1-867a-d5524bc59cd6.html> (accessed February 22, 2020). (in Chinese).
- Sheahan TP, Sims AC, Leist SR, *et al.* Comparative therapeutic efficacy of remdesivir and combination lopinavir, ritonavir, and interferon beta against MERS-CoV. *Nat Commun.* 2020; 11:222.
- Holshue ML, DeBolt C, Lindquist S, *et al.* First case of 2019 novel coronavirus in the United States. *N Engl J Med.* 2020.
- Mild/Moderate 2019-nCoV Remdesivir RCT. <https://clinicaltrials.gov/ct2/show/NCT04252664> (accessed February 22, 2020). (in Chinese).
- Severe 2019-nCoV Remdesivir RCT. <https://clinicaltrials.gov/ct2/show/NCT04257656> (accessed February 22, 2020). (in Chinese).
- Hoffmann M, Kleine-Weber H, Krüger N, Müller M, Drosten C, Pöhlmann S. The novel coronavirus 2019 (2019-nCoV) uses the SARS-coronavirus receptor ACE2 and the cellular protease TMPRSS2 for entry into target cells. *bioRxiv.* 2020.2001.2031.929042.
- Coleman CM, Sisk JM, Mingo RM, Nelson EA, White JM, Frieman MB. Abelson kinase inhibitors are potent inhibitors of severe acute respiratory syndrome coronavirus and Middle East respiratory syndrome coronavirus fusion. *J Virol.* 2016; 90:8924-8933.
- Shanghai Institute of Materia Medica website, Chinese Academy of Sciences. A joint research team of the Shanghai Institute of Materia Medica and Shanghai Tech University discover a group of old and traditional Chinese medicines that may be efficacious in treating the novel form of pneumonia. http://www.simm.ac.cn/xwzx/kydt/202001/t20200125_5494417.html (accessed February 22, 2020). (in Chinese).

Received February 23, 2020; Revised February 27, 2020; Accepted February 28, 2020.

*Address correspondence to:

Jianjun Gao, Department of Pharmacology, School of Pharmacy, Qingdao University, Qingdao, China.

E-mail: gaojj@qdu.edu.cn

Guide for Authors

1. Scope of Articles

Drug Discoveries & Therapeutics welcomes contributions in all fields of pharmaceutical and therapeutic research such as medicinal chemistry, pharmacology, pharmaceutical analysis, pharmaceuticals, pharmaceutical administration, and experimental and clinical studies of effects, mechanisms, or uses of various treatments. Studies in drug-related fields such as biology, biochemistry, physiology, microbiology, and immunology are also within the scope of this journal.

2. Submission Types

Original Articles should be well-documented, novel, and significant to the field as a whole. An Original Article should be arranged into the following sections: Title page, Abstract, Introduction, Materials and Methods, Results, Discussion, Acknowledgments, and References. Original articles should not exceed 5,000 words in length (excluding references) and should be limited to a maximum of 50 references. Articles may contain a maximum of 10 figures and/or tables.

Brief Reports definitively documenting either experimental results or informative clinical observations will be considered for publication in this category. Brief Reports are not intended for publication of incomplete or preliminary findings. Brief Reports should not exceed 3,000 words in length (excluding references) and should be limited to a maximum of 4 figures and/or tables and 30 references. A Brief Report contains the same sections as an Original Article, but the Results and Discussion sections should be combined.

Reviews should present a full and up-to-date account of recent developments within an area of research. Normally, reviews should not exceed 8,000 words in length (excluding references) and should be limited to a maximum of 100 references. Mini reviews are also accepted.

Policy Forum articles discuss research and policy issues in areas related to life science such as public health, the medical care system, and social science and may address governmental issues at district, national, and international levels of discourse. Policy Forum articles should not exceed 2,000 words in length (excluding references).

Case Reports should be detailed reports of the symptoms, signs, diagnosis, treatment, and follow-up of an individual patient. Case reports may contain a demographic profile of the patient but usually describe an unusual or novel occurrence. Unreported or unusual side effects or adverse interactions involving medications will also be considered. Case

Reports should not exceed 3,000 words in length (excluding references).

News articles should report the latest events in health sciences and medical research from around the world. News should not exceed 500 words in length.

Letters should present considered opinions in response to articles published in Drug Discoveries & Therapeutics in the last 6 months or issues of general interest. Letters should not exceed 800 words in length and may contain a maximum of 10 references.

3. Editorial Policies

Ethics: Drug Discoveries & Therapeutics requires that authors of reports of investigations in humans or animals indicate that those studies were formally approved by a relevant ethics committee or review board.

Conflict of Interest: All authors are required to disclose any actual or potential conflict of interest including financial interests or relationships with other people or organizations that might raise questions of bias in the work reported. If no conflict of interest exists for each author, please state "There is no conflict of interest to disclose".

Submission Declaration: When a manuscript is considered for submission to Drug Discoveries & Therapeutics, the authors should confirm that 1) no part of this manuscript is currently under consideration for publication elsewhere; 2) this manuscript does not contain the same information in whole or in part as manuscripts that have been published, accepted, or are under review elsewhere, except in the form of an abstract, a letter to the editor, or part of a published lecture or academic thesis; 3) authorization for publication has been obtained from the authors' employer or institution; and 4) all contributing authors have agreed to submit this manuscript.

Cover Letter: The manuscript must be accompanied by a cover letter signed by the corresponding author on behalf of all authors. The letter should indicate the basic findings of the work and their significance. The letter should also include a statement affirming that all authors concur with the submission and that the material submitted for publication has not been published previously or is not under consideration for publication elsewhere. The cover letter should be submitted in PDF format. For example of Cover Letter, please visit <http://www.ddtjournal.com/downloadcentre.php> (Download Centre).

Copyright: A signed JOURNAL PUBLISHING AGREEMENT (JPA) must be provided by post, fax, or as a scanned file before acceptance of the article. Only forms with a hand-written signature are accepted. This copyright will ensure the widest possible dissemination of information. A form facilitating transfer of copyright can be downloaded by clicking the appropriate link and can be returned to the e-mail address or fax number noted on the form (Please visit

Download Centre). Please note that your manuscript will not proceed to the next step in publication until the JPA form is received. In addition, if excerpts from other copyrighted works are included, the author(s) must obtain written permission from the copyright owners and credit the source(s) in the article.

Suggested Reviewers: A list of up to 3 reviewers who are qualified to assess the scientific merit of the study is welcomed. Reviewer information including names, affiliations, addresses, and e-mail should be provided at the same time the manuscript is submitted online. Please do not suggest reviewers with known conflicts of interest, including participants or anyone with a stake in the proposed research; anyone from the same institution; former students, advisors, or research collaborators (within the last three years); or close personal contacts. Please note that the Editor-in-Chief may accept one or more of the proposed reviewers or may request a review by other qualified persons.

Language Editing: Manuscripts prepared by authors whose native language is not English should have their work proofread by a native English speaker before submission. If not, this might delay the publication of your manuscript in Drug Discoveries & Therapeutics.

The Editing Support Organization can provide English proofreading, Japanese-English translation, and Chinese-English translation services to authors who want to publish in Drug Discoveries & Therapeutics and need assistance before submitting a manuscript. Authors can visit this organization directly at <http://www.iacmhr.com/iac-eso/support.php?lang=en>. IAC-ESO was established to facilitate manuscript preparation by researchers whose native language is not English and to help edit works intended for international academic journals.

4. Manuscript Preparation

Manuscripts should be written in clear, grammatically correct English and submitted as a Microsoft Word file in a single-column format. Manuscripts must be paginated and typed in 12-point Times New Roman font with 24-point line spacing. Please do not embed figures in the text. Abbreviations should be used as little as possible and should be explained at first mention unless the term is a well-known abbreviation (e.g. DNA). Single words should not be abbreviated.

Title page: The title page must include 1) the title of the paper (Please note the title should be short, informative, and contain the major key words); 2) full name(s) and affiliation(s) of the author(s); 3) abbreviated names of the author(s); 4) full name, mailing address, telephone/fax numbers, and e-mail address of the corresponding author; and 5) conflicts of interest (if you have an actual or potential conflict of interest to disclose, it must be included as a footnote on the title page of the manuscript; if no conflict of interest exists for each author, please state "There is no conflict of interest to disclose"). Please visit [Download Centre](#) and refer to the title page of the manuscript sample.

Abstract: The abstract should briefly state the purpose of the study, methods, main findings, and conclusions. For article types including Original Article, Brief Report, Review, Policy Forum, and Case Report, a one-paragraph abstract consisting of no more than 250 words must be included in the manuscript. For News and Letters, a brief summary of main content in 150 words or fewer should be included in the manuscript. Abbreviations must be kept to a minimum and non-standard abbreviations explained in brackets at first mention. References should be avoided in the abstract. Key words or phrases that do not occur in the title should be included in the Abstract page.

Introduction: The introduction should be a concise statement of the basis for the study and its scientific context.

Materials and Methods: The description should be brief but with sufficient detail to enable others to reproduce the experiments. Procedures that have been published previously should not be described in detail but appropriate references should simply be cited. Only new and significant modifications of previously published procedures require complete description. Names of products and manufacturers with their locations (city and state/country) should be given and sources of animals and cell lines should always be indicated. All clinical investigations must have been conducted in accordance with Declaration of Helsinki principles. All human and animal studies must have been approved by the appropriate institutional review board(s) and a specific declaration of approval must be made within this section.

Results: The description of the experimental results should be succinct but in sufficient detail to allow the experiments to be analyzed and interpreted by an independent reader. If necessary, subheadings may be used for an orderly presentation. All figures and tables must be referred to in the text.

Discussion: The data should be interpreted concisely without repeating material already presented in the Results section. Speculation is permissible, but it must be well-founded, and discussion of the wider implications of the findings is encouraged. Conclusions derived from the study should be included in this section.

Acknowledgments: All funding sources should be credited in the Acknowledgments section. In addition, people who contributed to the work but who do not meet the criteria for authors should be listed along with their contributions.

References: References should be numbered in the order in which they appear in the text. Citing of unpublished results, personal communications, conference abstracts, and theses in the reference list is not recommended but these sources may be mentioned in the text. In the reference list, cite the names of all authors when there are fifteen or fewer authors; if there are sixteen or more authors, list the first three followed by *et al.* Names of journals should

be abbreviated in the style used in PubMed. Authors are responsible for the accuracy of the references. Examples are given below:

Example 1 (Sample journal reference):
Nakata M, Tang W. Japan-China Joint Medical Workshop on Drug Discoveries and Therapeutics 2008: The need of Asian pharmaceutical researchers' cooperation. *Drug Discov Ther.* 2008; 2:262-263.

Example 2 (Sample journal reference with more than 15 authors):
Darby S, Hill D, Auvinen A, *et al.* Radon in homes and risk of lung cancer: Collaborative analysis of individual data from 13 European case-control studies. *BMJ.* 2005; 330:223.

Example 3 (Sample book reference):
Shalev AY. Post-traumatic stress disorder: Diagnosis, history and life course. In: *Post-traumatic Stress Disorder, Diagnosis, Management and Treatment* (Nutt DJ, Davidson JR, Zohar J, eds.). Martin Dunitz, London, UK, 2000; pp. 1-15.

Example 4 (Sample web page reference):
World Health Organization. The World Health Report 2008 – primary health care: Now more than ever. http://www.who.int/whr/2008/whr08_en.pdf (accessed September 23, 2010).

Tables: All tables should be prepared in Microsoft Word or Excel and should be arranged at the end of the manuscript after the References section. Please note that tables should not in image format. All tables should have a concise title and should be numbered consecutively with Arabic numerals. If necessary, additional information should be given below the table.

Figure Legend: The figure legend should be typed on a separate page of the main manuscript and should include a short title and explanation. The legend should be concise but comprehensive and should be understood without referring to the text. Symbols used in figures must be explained.

Figure Preparation: All figures should be clear and cited in numerical order in the text. Figures must fit a one- or two-column format on the journal page: 8.3 cm (3.3 in.) wide for a single column, 17.3 cm (6.8 in.) wide for a double column; maximum height: 24.0 cm (9.5 in.). Please make sure that artwork files are in an acceptable format (TIFF or JPEG) at minimum resolution (600 dpi for illustrations, graphs, and annotated artwork, and 300 dpi for micrographs and photographs). Please provide all figures as separate files. Please note that low-resolution images are one of the leading causes of article resubmission and schedule delays. All color figures will be reproduced in full color in the online edition of the journal at no cost to authors.

Units and Symbols: Units and symbols conforming to the International System of Units (SI) should be used for physicochemical quantities. Solidus notation (*e.g.* mg/kg, mg/mL, mol/mm²/min) should be used. Please refer to the SI Guide www.bipm.org/en/si/ for standard units.

Supplemental data: Supplemental data might be useful for supporting and enhancing your scientific research and Drug Discoveries & Therapeutics accepts the submission of these materials which will be only published online alongside the electronic version of your article. Supplemental files (figures, tables, and other text materials) should be prepared according to the above guidelines, numbered in Arabic numerals (*e.g.*, Figure S1, Figure S2, and Table S1, Table S2) and referred to in the text. All figures and tables should have titles and legends. All figure legends, tables and supplemental text materials should be placed at the end of the paper. Please note all of these supplemental data should be provided at the time of initial submission and note that the editors reserve the right to limit the size and length of Supplemental Data.

5. Submission Checklist

The Submission Checklist will be useful during the final checking of a manuscript prior to sending it to Drug Discoveries & Therapeutics for review. Please visit [Download Centre](#) and download the Submission Checklist file.

6. Online submission

Manuscripts should be submitted to Drug Discoveries & Therapeutics online at <http://www.ddtjournal.com>. The manuscript file should be smaller than 5 MB in size. If for any reason you are unable to submit a file online, please contact the Editorial Office by e-mail at office@ddtjournal.com

7. Accepted manuscripts

Proofs: Galley proofs in PDF format will be sent to the corresponding author *via* e-mail. Corrections must be returned to the editor (proof-editing@ddtjournal.com) within 3 working days.

Offprints: Authors will be provided with electronic offprints of their article. Paper offprints can be ordered at prices quoted on the order form that accompanies the proofs.

Page Charge: A page charge of \$140 will be assessed for each printed page of an accepted manuscript. The charge for printing color figures is \$340 for each page. Under exceptional circumstances, the author(s) may apply to the editorial office for a waiver of the publication charges at the time of submission.

(Revised February 2013)

Editorial and Head Office:

Pearl City Koishikawa 603
2-4-5 Kasuga, Bunkyo-ku
Tokyo 112-0003
Japan
Tel: +81-3-5840-9697
Fax: +81-3-5840-9698
E-mail: office@ddtjournal.com

